



UNIVERSITY OF TM
KWAZULU-NATAL

INYUVESI
YAKWAZULU-NATALI

**HIV cell-to-cell spread leads to a
differential transcriptional response and
slows evolution of drug resistance relative
to cell-free infection**

Jessica Hunter

*Submitted in fulfilment of the requirements for the degree of
Doctor of Philosophy (Medicine) in the School of Laboratory
Medicine and Medical Sciences, College of Health Sciences,
University of KwaZulu-Natal*

November 2020

DECLARATION

I, **Ms Jessica Hunter**, declare as follows:

- i) The research proposed in this dissertation, except where otherwise indicated, is my original work.
- ii) The work contained in this thesis, except for the sections indicated below, has not been submitted for any degree or examination at any other university.

The paper submitted in chapter 2 of this thesis titled “*Incomplete inhibition of HIV infection results in more HIV infected lymph node cells by reducing cell death*” published in eLife in 2018, was submitted by Dr Laurelle Jackson as part of the fulfilment of her Doctor of Philosophy (Medicine) thesis titled “*Increase in live infected cell number with drug and generation of a quasispecies are consequences of multiply HIV infected cells*” submitted in 2018. On this paper, myself and Dr Jackson are the primary co-authors and we contributed equally to this work. While Dr Jackson and I have shared research interests, the focus of our theses differs substantially. The results of this co-authored paper support both of our research questions.

- iii) This thesis does not contain other persons’ data, pictures, graphs or other information, unless specifically acknowledged as being sourced from other persons.
- iv) This thesis does not contain other persons’ writing, unless specifically acknowledged as being sourced from other researchers. Where other written sources have been quoted, then:
 - a.) their words have been re-written, but the general information attributed to them has been referenced.
 - b.) where their exact words have been used, their writing has been placed inside quotation marks, and referenced.
- v) Parts of this thesis have been published in a publication titled “*Incomplete inhibition of HIV infection results in more HIV infected lymph node cells by reducing cell death*”
- vi) This dissertation does not contain text, graphics or tables copied and pasted from the internet, unless specifically acknowledged, and the source being detailed in the thesis and in the References sections.

Signed: _____  _____

Jessica Hunter (student)

Date: 30/11/2020

Signed: _____  _____

Dr. Alex Sigal (supervisor)

Date: 30/11/2020

LIST OF PUBLICATIONS

1. Laurelle Jackson*, **Jessica Hunter***, Sandile Cele, Isabella Markham Ferreira, Andrew C Young, Farina Karim, Rajhmun Madansein, Kaylesh J Dullabh, Chih-Yuan Chen, Noel J Buckels, Yashica Ganga, Khadija Khan, Mikael Boullé, Gila Lustig, Richard A Neher, Alex Sigal (2018) Incomplete inhibition of HIV infection results in more HIV infected lymph node cells by reducing cell death. *eLife*. 7:e30134 DOI: [10.7554/eLife.30134](https://doi.org/10.7554/eLife.30134)
2. **Jessica Hunter**, Sandile Cele, Laurelle Jackson, Jennifer Giandhari, Tulio de Oliveira, Gila Lustig, Alex Sigal (2020) HIV cell-to-cell spread slows evolution of drug resistance. *bioRxiv*. DOI: <https://doi.org/10.1101/2020.09.04.283192>
3. Deeqa Mahamed, Mikael Boule, Yashica Ganga, Chanelle Mc Arthur, Steven Skroch, Lance Oom, Ooana Catinas, Kelly Pillay, Myshnee Naiker, Sanisha Rampersad, Colisile Mathonsi, **Jessica Hunter**, Emily B Wong, Moosa Suleman, Gopalkishna Sreejit, Alexander S Pym, Gila Lustig, Alex Sigal. (2017) Intracellular growth of Mycobacterium tuberculosis after macrophage cell death leads to serial killing of host cells. *eLife*. 2017;6:e22028 DOI: [10.7554/eLife.22028](https://doi.org/10.7554/eLife.22028)

ACKNOWLEDGMENTS

The work detailed in this thesis would not have been possible without the incredible contributions of several individuals whom I would like to acknowledge:

My supervisor, Dr Alex Sigal, for his guidance and mentoring throughout the course of my masters and PhD studentships in his lab. His time and expertise were key to the success of this work as well as shaping me into the scientist I am today.

All the members of the Sigal lab, both past and present. It was a pleasure to work with a group of energizing and talented scientists who motivated me produce good research. I would like to give a special mention to Dr Laurelle Jackson for her support, advise, and significant input she made throughout my PhD. I would also like to thank Sandile Cele for his technical contributions and Dr Gila Lustig and Vivienne Clarence for their administrative support and management of the lab.

The AHRI clinical core and biorepository team, led by Farina Karim and Khadija Khan, for their contributions in both obtaining and managing the clinical samples required for this research. I would also like to acknowledge the cardiothoracic surgeons, Rajhmun Madansein, Kaylesh J Dullabh, Chih-Yuan Chen and Noel J Buckels who saw the value in this research and agreed to partner with us by providing lymph nodes obtained from participants undergoing surgery for diagnostic purposes and/or complications of inflammatory lung disease.

Our collaborators, which includes, Prof. Alex Shalek (Massachusetts Institute of Technology, Boston, USA) and members of his lab, Carly Ziegler and Marko Vukovic, and Prof. Tulio de Oliveira (KwaZulu-Natal Research and Innovation Sequencing Platform, UKZN, Durban, South Africa) for their expertise and input into this research.

The National Research Foundation (NRF) in South Africa for funding the first two years of this degree.

I would also like to acknowledge members of my family. My parents, Terry and Rosemary Hunter, for always believing in me and through personal sacrifices afforded me the foundation required to pursue a PhD. My husband, Byron, for all the support and encouragement he gave me to complete this degree. And finally, I would like to thank my Lord and Saviour, for His faithfulness and goodness in my life.

TABLE OF CONTENTS

DECLARATION	1
LIST OF PUBLICATIONS	3
ACKNOWLEDGMENTS	4
LIST OF FIGURES AND TABLES	6
ACRONYMS	9
ABSTRACT	11
INTRODUCTION	12
CHAPTER 1:	15
Literature Review.....	15
REFERENCES	32
CHAPTER 2:	40
Incomplete inhibition of HIV infection results in more HIV infected lymph node cell by reducing cell death.....	40
CHAPTER 3:	66
HIV cell-to-cell spread slows evolution of drug resistance	66
CHAPTER 4:	84
Increased interferon response in HIV cell-to-cell spread.....	84
GENERAL DISCUSSION:	87
FUTURE RESEARCH:	103
REFERENCES:	104

LIST OF FIGURES AND TABLES

Chapter 1: Literature Review

Figure 1:

HIV genome structure.....17

Figure 2:

Schematic of HIV virion.....17

Figure 3:

HIV replication cycle.....18

Figure 4:

Modes of HIV infection.....20

Figure 5:

Multiple infections per cell occurring in cell-to-cell spread decrease sensitivity to drug.....21

Figure 6:

Multiple proviral copies of HIV per cell.....23

Figure 7:

In vivo infected splenocytes show multiple HIV infections.....24

Figure 8:

Mode of HIV spread determines the outcome cell death pathway.....26

Figure 9:

Drug concentration determines fitness of drug sensitive wildtype and drug resistant mutant virus.....27

Figure 10:

Schematic showing how spatiotemporal heterogeneity can create conditions conducive to the evolution of drug resistance.....27

Figure 11:

Model of stepwise evolution of multidrug resistance.....28

Figure 12:

Summary of key findings per cell population type.....29

Figure 13:

Model of CD4⁺ T cell differentiation.....30

Chapter 2: Incomplete inhibition of HIV infection results in more HIV infected lymph node cell by reducing cell death

Figure 1:	
Probability for a cell to be infected and live as a function of inhibitor.....	42
Figure 2:	
Partial inhibition increases the number of live infected cells.....	44
Figure 3:	
Partial inhibition of the EFV-resistant L100I mutant shifts the peak of live infected cells to higher EFV concentrations.....	46
Figure 4:	
Partial inhibition of coculture infection with neutralizing antibody results in higher numbers of live infected cells.....	47
Figure 5:	
Infection optimum with EFV in lymph node cells.....	48
Figure 6:	
Infection with the K103N mutant shows an infection optimum at clinically observed lymph node EFV concentrations.....	50
 Chapter 3: HIV cell-to-cell spread slows evolution of drug resistance	
Figure 1:	
Wild-type virus is predicted to be more rapidly supplanted by the drug resistant mutant with cell-free infection relative to cell-to-cell spread.....	65
Figure 2:	
Frequencies of L100I and K103N EFV resistance mutations rise more rapidly with a cell-free infection step.....	66
Figure 3:	
HIV infection with a cell-free infection cycle evolves multidrug resistance.....	67
Figure 4:	
Increasing drug concentration in coculture infection increases the rate of drug resistance evolution.....	68
Figure 5:	
Frequency of resistance mutations with a cell-free infection cycle under increased selective pressure.....	69
SFigure 1:	
Mutant frequencies measured at start of evolution experiments after two cycles of infection in the absence of drug.....	73
SFigure 2:	
Frequencies of single and linked multidrug resistant mutations.....	73

Chapter 4: Increased interferon response in HIV cell-to-cell spread

Figure 1:

Gating strategy and transcriptional patterns in HIV cell-to-cell spread versus cell-free infection.....76

Figure 2:

Differentially regulated gene sets in cell-to-cell spread versus cell-free infection in lymph node cells.....77

Figure 3:

Gene sets differentially regulated in HIV infected relative to uninfected lymph node cells.....78

Figure 4:

Interferon induced genes upregulated in HIV cell-to-cell spread versus cell-free infection.....79

Figure 5:

Differentially expressed genes within the most enriched genes sets in HIV cell-to-cell spread.....80

Stable 1:

Participant information for the lymph node cells used to infect in vitro to determine whether there are differences in transcriptional responses from different infection modes.....84

SFigure 1:

GSEA reports for our three condition comparisons for the top 5 most enriched gene sets in cell-to-cell infected relative to the cell-free infected.....85

ACRONYMS

HIV - Human Immunodeficiency Virus

ARV - Antiretroviral drugs

ART - Antiretroviral therapy

DNA - Deoxyribonucleic acid

RNA - Ribonucleic acid

AIDS - Acquired immunodeficiency syndrome

LTR - Long terminal repeats

MA - Matrix

CA - Capsid

NC - Nucleocapsid

VS - Virologic synapse

LFA-1 - Lymphocyte function antigen-1

IFI16 - Interferon- γ -Inducible Protein 16

DC - Dendritic cell

DC-SIGN - Dendritic cell- specific C-type lectin

MOI - Multiplicity of infection

VL - Viral Load

NNRTI - Non-nucleoside reverse transcriptase

EFV - Efavirenz

FTC - Emtricitabine

MSW - Mutant selection window

CNS - Central nervous system

CFS - Cerebral spinal fluid

DEG - Differentially expressed genes

ISG - Interferon Stimulated Gene

PBMC - Peripheral blood mononuclear cells

GFP – Green Fluorescent Protein

YFP – Yellow Fluorescent Protein

PCR – Polymerase Chain Reaction

PID – Participant Identification Number

CTFR – Cell Trace Far Red

PCA – Principle Component Analysis

GSEA – Gene Set Enrichment Analysis

1 **ABSTRACT**

2
3
4
5
6
7
8
9
10
11
12
13
14
15
16
17
18
19
20
21
22
23
24
25
26
27
28

HIV transmits between hosts but also transmits between cells in the same host. How this latter, cellular transmission occurs has been the subject of extensive study. Yet why HIV transmits between cells using two different infection modes: cell-to-cell spread and cell-free infection, is not clearly understood. This is because cell-to-cell spread is a more efficient mode of infection, where the virus is able to be successfully transmitted between cells despite natural inhibitors such as antibodies. Here, using in vitro experimentation, I have determined some of the implications of cell-to-cell spread of HIV for cell death, evolution, and inflammation. I have discovered potential costs to this infection mode, such as increased cell death, slowed evolution of resistance, and an increased interferon response which may interfere with viral replication. Hence, costs associated with cell-to-cell spread may prevent it being the dominant infection mode in cellular transmission.

29 INTRODUCTION

30

31 HIV is known to infect by two general mechanisms: cell-free infection and cell-to-cell spread. Cell-free
32 infection involves the non-targeted dissemination of the virus, where the virus does not use the cellular
33 machinery available to it in the infected cell to infect a new cell.

34 In contrast, cell-to-cell spread is a set of mechanisms where the machinery of the already infected cell
35 is used for directed transmission of the virus. This increases transmission efficiency. The known
36 mechanisms include the formation of a virological synapse [1-3] where there is directional secretion of
37 the virus in the direction of the yet uninfected cell. This greatly shortens the distance that virus must
38 cover to reach a new cell to infect and therefore greatly increases the efficiency of infection.

39 In addition to transmission by the manipulation of cellular pathways in the infected cell, cell-to-cell
40 spread can occur from an uninfected cell (cell-to-cell in *trans*) [4-6] using binding of HIV to DC-SIGN
41 of dendritic and other cells. This binding enables the virus to be in close proximity to infectable cells
42 when these cells interact with dendritic cells.

43 Cell-to-cell spread has decreased sensitivity to infection inhibitors, such as antiretroviral drugs (ARVs)
44 [7-10] and antibodies [11, 12], due to the transfer of multiple virions increasing the probability of at
45 least one successful infection despite the presence of an inhibitor [8].

46 In the event where some HIV replication occurs during antiretroviral therapy (ART) due to treatment
47 interruption, the HIV reservoir may consist of actively replicating virus. In addition, some evidence
48 exists for possible ongoing HIV replication in the face of suppressive antiretroviral therapy at least in
49 some individuals [13-16]. The evolution of drug resistance and virologic failure is clear evidence for
50 HIV replication at some levels of antiretroviral therapy since the presence of antiretroviral drugs is
51 required to provide selective pressure for drug resistance mutations to arise. Because of its insensitivity
52 to ARVs, cell-to-cell spread may contribute to the establishment and persistence of the HIV reservoir
53 through ongoing replication during ART [8]. In addition, cell-to-cell spread is well suited for
54 transmission within lymphoid tissue, a known anatomical reservoir compartment [13, 17]. This site is
55 ideal for cell-to-cell spread as there are high numbers of infectable cells CD4⁺ T cells [18, 19] in close
56 proximity to each other [3, 20-23] with little lymphatic flow to disturb cellular contacts [24, 25].

57 Despite the higher efficiency of cell-to-cell spread, just under half of HIV infection occurs by cell-free
58 infection [24, 26, 27]. It is possible that different infection modes yield different outcomes, which may
59 be advantageous in propagating the virus in a dynamic environment. Little is known regarding the
60 degree to which the different infection modes determine outcomes such as infected cell survival, drug
61 resistance evolution and host gene regulation.

62 Cell-to-cell spread leads to increased CD4⁺ T cell death [28, 29]. Several mechanisms for HIV induced
63 cell death have been described. Cell death can occur in productively infected cells in response to HIV
64 infection through caspase-3-mediated apoptosis [29]. Alternatively, cell death can occur in bystander
65 cells, through the accumulation of incomplete HIV reverse transcripts [30], which are sensed by
66 interferon- γ -inducible protein 16 (IFI16) [31], triggering cell death by caspase-1-dependent pyroptosis
67 [29]. Another mechanism involves double stranded DNA breaks in the host genome caused by viral
68 integration attempts which results in cell death via the DNA-PK activation of the p53 response [32].
69 Additionally, viral proteins such as Tat and Env have been found to induce cell death through CD95-
70 mediated apoptosis following T cell activation [33-35]. The above studies suggest that, increases of cell
71 death in cell-to-cell spread could be the result of multiple HIV infection attempts associated with this
72 mode of infection [36, 37].

73 While HIV mediated cell death has been previously investigated, the effect of infection mode is not yet
74 clear. One possibility is that with cell-to-cell spread, sub-optimal drug concentrations may reduce the
75 number of infection attempts per cell, thereby increasing cell survival if the cell is successfully infected
76 with the reduced transmitted dose. In contrast, in cell-free infection where few virions reach the infected
77 cell, the effect of the drug is expected to be binary: either a cell is infected, or it is not. Furthermore,
78 cell death would be minimized since the number of infections attempts per cell is low. This may have
79 implications regarding the establishment of the viral reservoir, in tissues where drug levels may not be
80 fully suppressive [38], as persistence relies on long term survival of infected cells.

81 Cell-to-cell spread, is a mechanism of drug resistance which does not require the evolution of drug
82 resistant mutations. Instead it relies on multiple infection attempts to increase the probability of
83 infection despite drug [8]. However, HIV also has capacity to rapidly evolve, owing to its high mutation
84 rate [39, 40], the large population size of HIV within the body, the chronic nature of infection, the short
85 generation time, and the strong selection pressures imposed by the immune response or ART. Virologic
86 failure in ART treated patients, due to the evolution of drug resistance, is therefore a concern. If low
87 levels of viral replication occur following treatment interruptions [41-49] and in anatomical sites where
88 drug penetration is poor [38, 50-53] it may result in the selection of drug resistant mutants. The effect
89 of reduced drug sensitivity observed in cell-to-cell spread on the evolution of drug resistance mutations
90 has yet to be determined. Here we hypothesize that cell-to-cell spread may experience weaker selective
91 pressure relative to cell-free infection and the resulting outcome is reduced rate of fixation of drug
92 resistance mutants when transmitted by cell-to-cell spread. In contrast, cell-free infection would result
93 in a more rapid rate of selection of drug resistant mutations under drug pressure compared to cell-to-
94 cell spread. Transmitting by both cell-free infection as well as cell-to-cell spread may therefore benefit
95 the virus as the infection modes both contributes strengths that the other lack.

96 HIV infection dramatically influences the host gene regulation relating to innate immune pathways.
97 Upregulation of genes relating to the interferon response and cell cycle regulation has been
98 demonstrated in CD4⁺ T cells from HIV infected individuals [54-58]. Furthermore, interferon
99 upregulation has been reported in cells from HIV infected lymph nodes [59, 60]. However, it has not
100 yet been determined whether there are different outcomes in terms of the host transcriptional response
101 to HIV infection between cell-to-cell spread and cell-free infection. Differential gene regulation specific
102 to cell-to-cell spread or cell-free infection, could offer insight into the HIV pathogenesis as well as
103 highlight important considerations for novel therapies.

104 Here we compared cell-to-cell spread to cell-free HIV infection to test the hypothesis that there are
105 costs associated with cell-to-cell spread which may prevent it from being the dominant cellular
106 transmission mode. The potential costs tested where: cell-death, rate of evolution, and the interferon
107 response.

108 **The below studies investigate the outcomes of HIV infection modes: cell-free infection and cell-**
109 **to-cell spread.**

110 **Aim 1:** Determine the impact of infection mode on infected cell survival in the absence and presence
111 of ART

112 **Aim 2:** Determine the impact of infection mode on evolution of drug resistance

113 **Aim 3:** Determine whether mode of infection changes the transcriptional profile of the infected cell

CHAPTER 1:
Literature Review

114 **1.1 HIV background**

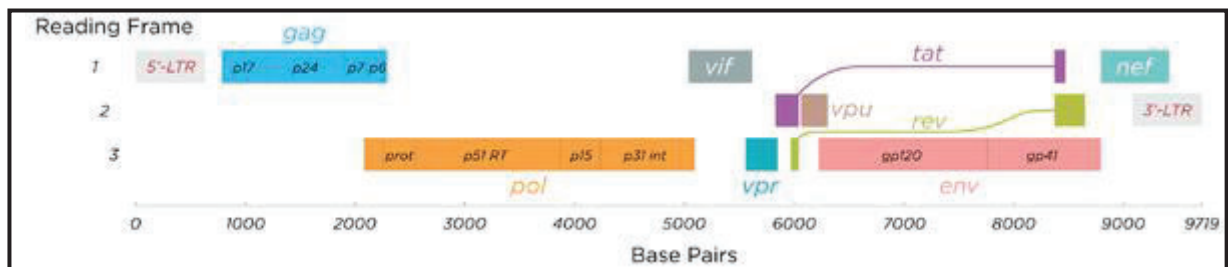
115 HIV is a retrovirus belonging to the lentivirus genus and is the causative agent of acquired
116 immunodeficiency syndrome (AIDS) [61, 62]. The virus primarily infects CD4⁺ T lymphocytes. Over
117 the course of the disease CD4⁺ T cells are depleted resulting in the patient developing AIDS. HIV is
118 transmitted from person to person via contact with infected bodily fluids, such as blood, semen, rectal
119 fluids, vaginal fluids, or breast milk.

120 Globally 38 million people are infected with HIV, with 23.4 million of those individuals on
121 antiretroviral therapy (ART) [63]. Whilst ART effectively suppresses HIV replication, it does not
122 eliminate the virus as HIV persists in viral reservoirs and viral rebound occurs when ART is
123 discontinued. A viral reservoir is defined as a cell type or anatomical site where replication competent
124 virus can stably persist for longer than the main pool of actively replicating virus. Proposed mechanisms
125 of HIV persistence are: long lived latently infected cells or ongoing replication in the face of ART [6,
126 64, 65]. Ongoing replication may include replication in anatomical compartments where drug
127 penetration is poor or infection by drug insensitive cell-to-cell spread.

128 An effective strategy for the eradication of the HIV reservoir has yet to be determined. Efforts to
129 prevent, control or cure HIV infection requires the study of the pathogenesis of the virus as well as the
130 interactions between the virus and the host cell.

131 **1.2 HIV structure and replication cycle**

132 The genome of HIV is 9.8 kb in length [66] and is made up of 9 genes; *gag*, *pol*, *env*, *tat*, *rev*, *nef*, *vif*,
133 *vpr* and *vpu* encoded on a positive sense, single stranded RNA molecule (Figure 1). On either ends of
134 these genes are long terminal repeats (LTR) [67]. Structural proteins and enzymes, required for HIV
135 replication are encoded for on the *gag*, *pol* and *env* genes. The Gag gene encodes a polyprotein
136 precursor, Pr55^{Gag}, which is cleaved into structural proteins, namely; matrix (MA or p17), capsid (CA
137 or p24), nucleocapsid (NC or p7) and p6 [66-69]. *Pol* encodes the three viral enzymes, protease, reverse
138 transcriptase and integrase [67, 69]. *Env* encodes the envelope glycoproteins, gp120 and gp41 which
139 are generated post-cleavage of the gp160 precursor [66-70]. Regulatory and accessory proteins Nef,
140 Rev, Tat, Vif, Vpu and Vpr play regulatory roles mediating viral replication [69].



141

Figure 1: HIV genome structure. The HIV genome is 9.8 kb in length and consists of 9 genes; *gag*, *pol*, *env*, *vif*, *tat*, *rev*, *nef*, *vpr* and *vpu*. The genes are flanked by 5' and 3' LTR. Structural proteins and enzymes are encoded on the *gag*, *pol* and *env* gene. Regulatory and accessory genes *tat*, *rev*, *nef*, *vif*, *vpr* and *vpu* are responsible for processes such as, regulation of transcription and transportation of viral components during the infection cycle (image by Thomas Spletstoeser, (www.scistyle.com)).

142 The mature HIV virion, as shown in Figure 2, is comprised of two single stranded RNA genomes bound
 143 to the nucleocapsid and then encased by a conical shaped capsid [66, 68]. Also contained within the
 144 capsid are the three viral enzymes: protease, reverse transcriptase and integrase as well as accessory
 145 proteins: Nef, Vif and Vpr [68, 71]. The capsid is surrounded by matrix protein which is then enclosed
 146 by the envelope [68]. The HIV envelope consists of a lipid bilayer which is derived from the membrane
 147 of the host cell but also contains viral Env-glycoproteins (gp120 and gp41) which facilitate entry into
 148 the host cell [68].

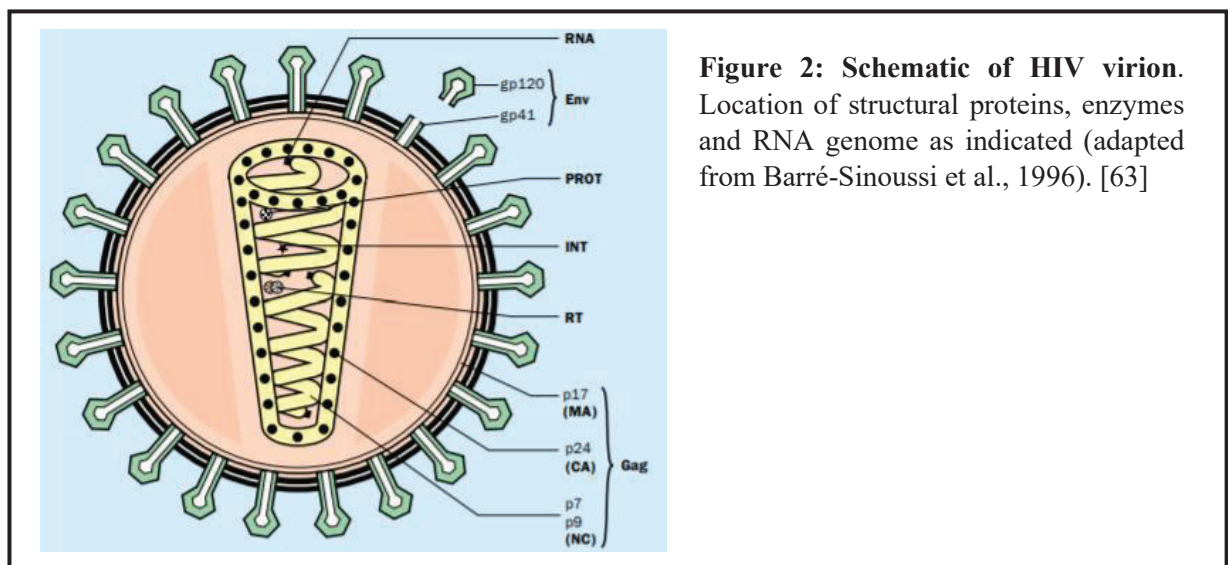


Figure 2: Schematic of HIV virion. Location of structural proteins, enzymes and RNA genome as indicated (adapted from Barré-Sinoussi et al., 1996). [63]

149

150 The early phase HIV replication cycle begins with the binding of viral envelope glycoprotein gp120 to
 151 the CD4 receptor on the surface of the host cell [70-72]. Subsequent conformational changes to the
 152 gp120 allows for the binding of one of the co-receptors, CCR5 and CXCR4, which is required for
 153 membrane fusion [71, 72]. This is followed by uncoating of the capsid, which releases the viral enzymes
 154 and two copies of the RNA genome into the cytoplasm. The single stranded RNA genome is then
 155 reverse transcribed to double stranded DNA in the cytosol by the reverse transcriptase enzyme [71, 72].
 156 The viral DNA along with other components of the preintegration complex; integrase, reverse

157 transcriptase, matrix and Vpr are transported to the nucleus [71]. This nuclear localization appears to
 158 be mediated by the accessory protein Vpr [73]. Following this transportation, the viral DNA is
 159 integrated into the host genome by the integrase enzyme [72].

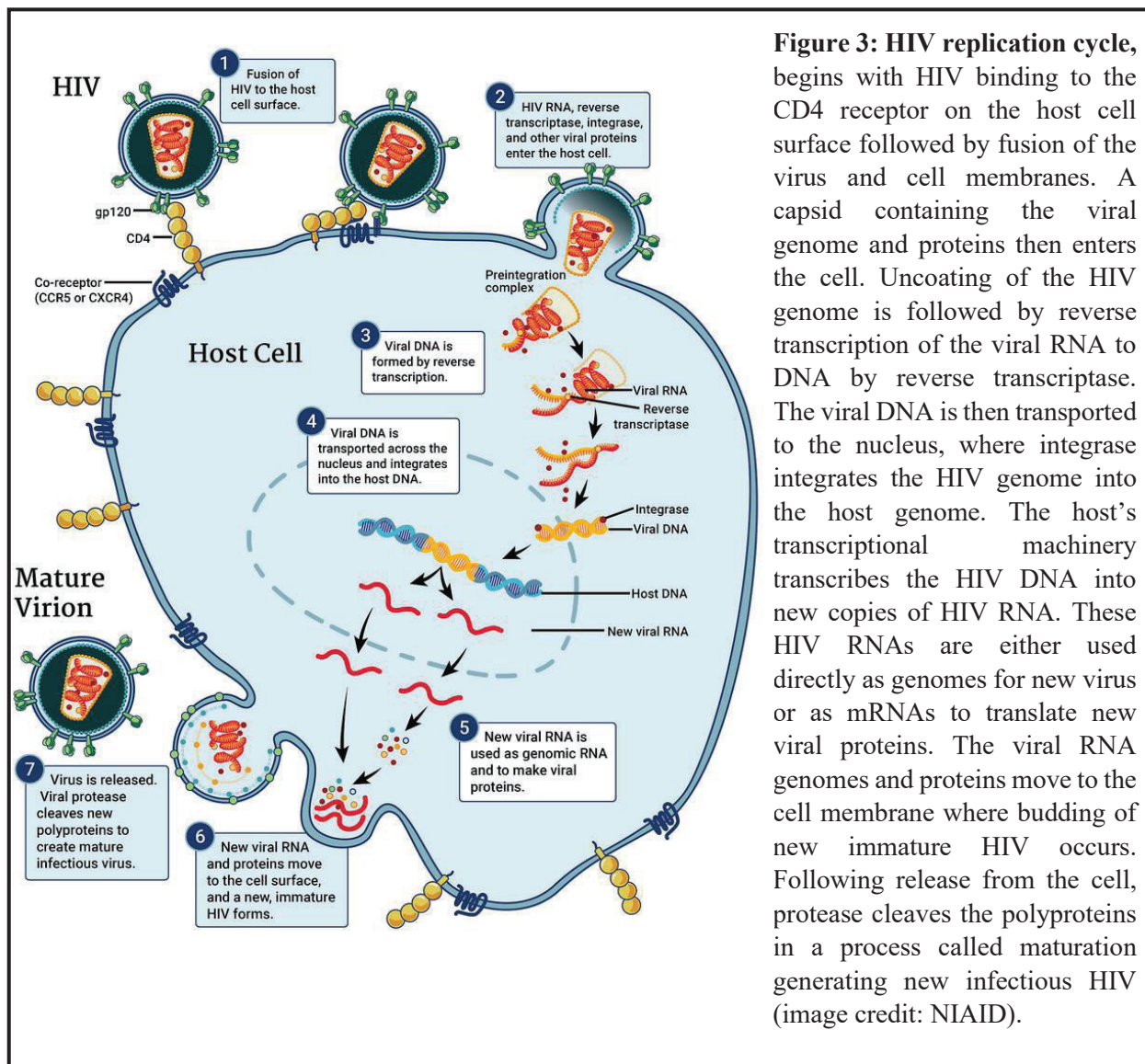


Figure 3: HIV replication cycle, begins with HIV binding to the CD4 receptor on the host cell surface followed by fusion of the virus and cell membranes. A capsid containing the viral genome and proteins then enters the cell. Uncoating of the HIV genome is followed by reverse transcription of the viral RNA to DNA by reverse transcriptase. The viral DNA is then transported to the nucleus, where integrase integrates the HIV genome into the host genome. The host's transcriptional machinery transcribes the HIV DNA into new copies of HIV RNA. These HIV RNAs are either used directly as genomes for new virus or as mRNAs to translate new viral proteins. The viral RNA genomes and proteins move to the cell membrane where budding of new immature HIV occurs. Following release from the cell, protease cleaves the polyproteins in a process called maturation generating new infectious HIV (image credit: NIAID).

160

161

162 Once integrated the viral genome, now referred to as a provirus, may lead to a transcriptionally active
 163 infection or transcriptionally dormant latent infection. Should the integrated viral genome lead to a
 164 transcriptionally active infection, mRNA transcripts are synthesised and transported out of the nucleus
 165 for translation. Initially, short multiply spliced transcripts which encode regulatory proteins Tat, Rev
 166 and Nef are synthesized [71, 72]. Tat upregulates HIV replication whilst Rev is responsible for the
 167 export of unspliced and partially spliced viral RNA by binding to the rev response element (RRE) [66,
 168 71, 72]. A portion of the unspliced full length viral RNAs are packaged directly into the new viral
 169 particles as new copies of the viral genome. The remaining unspliced viral RNAs and partially spliced
 170 viral RNAs are translated to generate polyprotein precursors such as gp160, Gag and Gag-Pol. gp160
 171 is cleaved in the endoplasmic reticulum and Golgi apparatus to form gp120 and gp41 which are then

172 transported to the plasma membrane to prepare for viral assembly [71, 72]. Gag and Gag-Pol also
173 localize at the plasma membrane binding to the cellular membrane and gp41. Budding packages
174 approximately 100 Gag-Pol and 1500 Gag molecules as well as two RNA genomes into the immature
175 viral particle [71].

176 Following budding from the host cell, Gag and Gag-Pol polyprotein precursors are cleaved by protease
177 to generate the viral enzymes and structural proteins [71, 74]. The various viral components then
178 rearrange in a process called maturation to form a viral particle capable of infecting a new cell. The
179 modes by which HIV infects new host cells are described below.

180 **1.3 Modes of HIV infection**

181 HIV, and other enveloped viruses, have evolved to transmit between cells by two modes of infection:
182 cell-free infection and cell-to-cell spread [1, 3, 75, 76] (Figure 4). Cell-free infection is non-directed
183 and relies on chance encounters between virion and an infectable cell. Cell-to-cell spread is directed
184 transfer of virion between cells and relies on close contact between an infected donor cell and uninfected
185 target cell, generally through a virological synapse (VS) [1, 3, 76-79] or infectious synapse [79, 80].
186 Both modes of infection have distinct advantages and disadvantages [1, 75, 81] and therefore it may be
187 beneficial for HIV that it transmits by both.

188 In cell-free infection, because the virion are released from an infected cell and disseminates through
189 extracellular fluids (Figure 4A), it is likely that the cell-free virus will encounter many biophysical,
190 kinetic and immunological obstacles along its journey to the new host cell [1]. This has the potential to
191 result in a great loss of virion and relatively few cells becoming infected [1]. Because the diffusion of
192 the virion is random, encountering an infectable target cell may require a significant length of time.
193 This may be problematic for the virus as the infectivity of cell-free HIV decreases with time as its Env
194 glycoprotein is prone to dissociate into non-functioning pieces [82]. This means that after the release
195 from a cell, virions have a limited time window to reach and infect a new cell. Mucus membranes,
196 antibodies, complement, chemokines, defensins, and cellular immune defenses such as macrophages all
197 represent potential barriers cell-free virus may encounter before it reaches a new target cell [1, 75] .
198 However, it is possible that despite the various barriers, cell-free infection is the best route of infection
199 for long distance dissemination, either between hosts or between distant anatomical compartments
200 within the host [1, 75, 81]. Transmission by cell-free virus may also have the advantage of not being
201 restricted to cell-cell contacts [75].

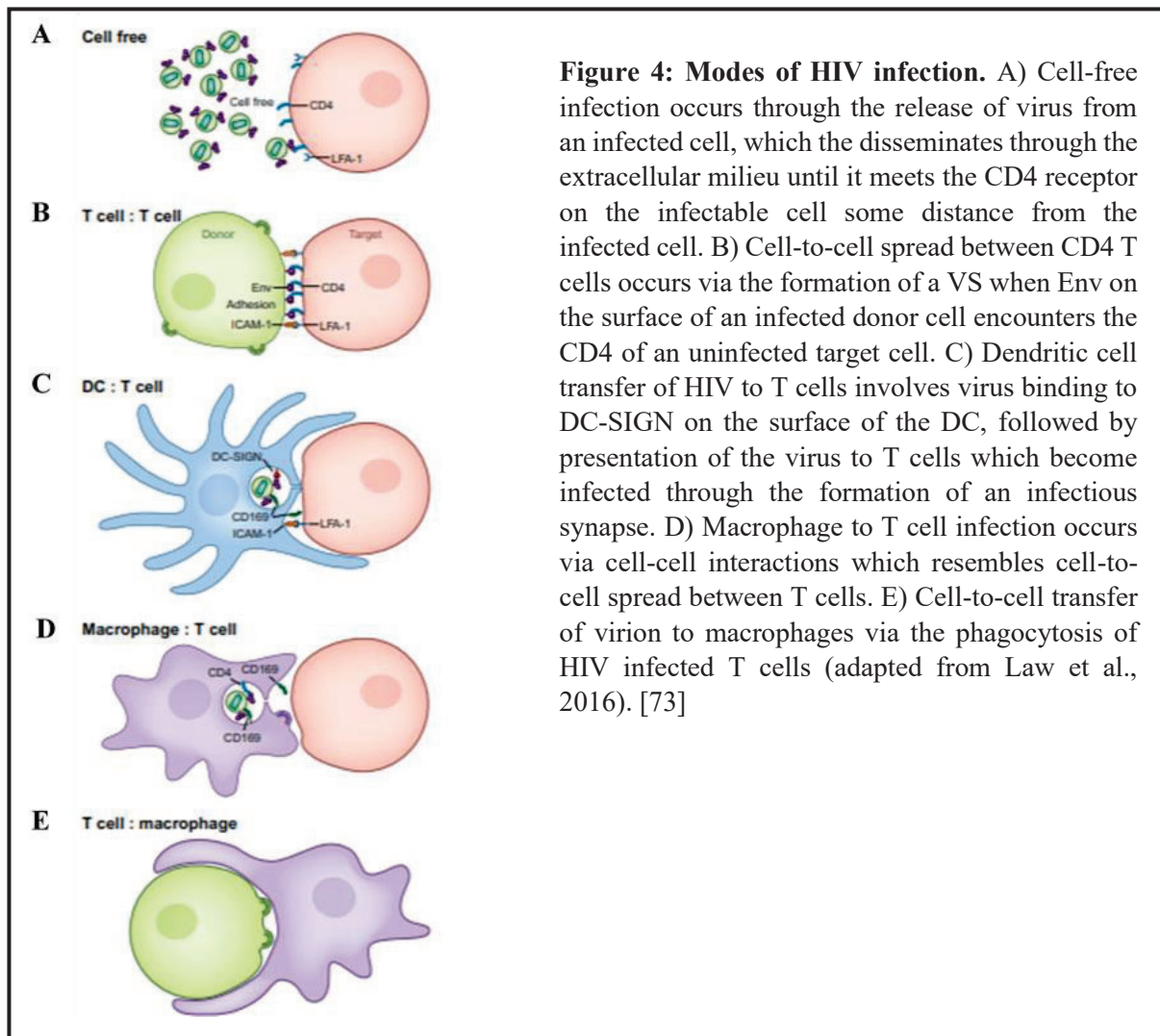


Figure 4: Modes of HIV infection. A) Cell-free infection occurs through the release of virus from an infected cell, which disseminates through the extracellular milieu until it meets the CD4 receptor on the infectable cell some distance from the infected cell. B) Cell-to-cell spread between CD4 T cells occurs via the formation of a VS when Env on the surface of an infected donor cell encounters the CD4 of an uninfected target cell. C) Dendritic cell transfer of HIV to T cells involves virus binding to DC-SIGN on the surface of the DC, followed by presentation of the virus to T cells which become infected through the formation of an infectious synapse. D) Macrophage to T cell infection occurs via cell-cell interactions which resembles cell-to-cell spread between T cells. E) Cell-to-cell transfer of virion to macrophages via the phagocytosis of HIV infected T cells (adapted from Law et al., 2016). [73]

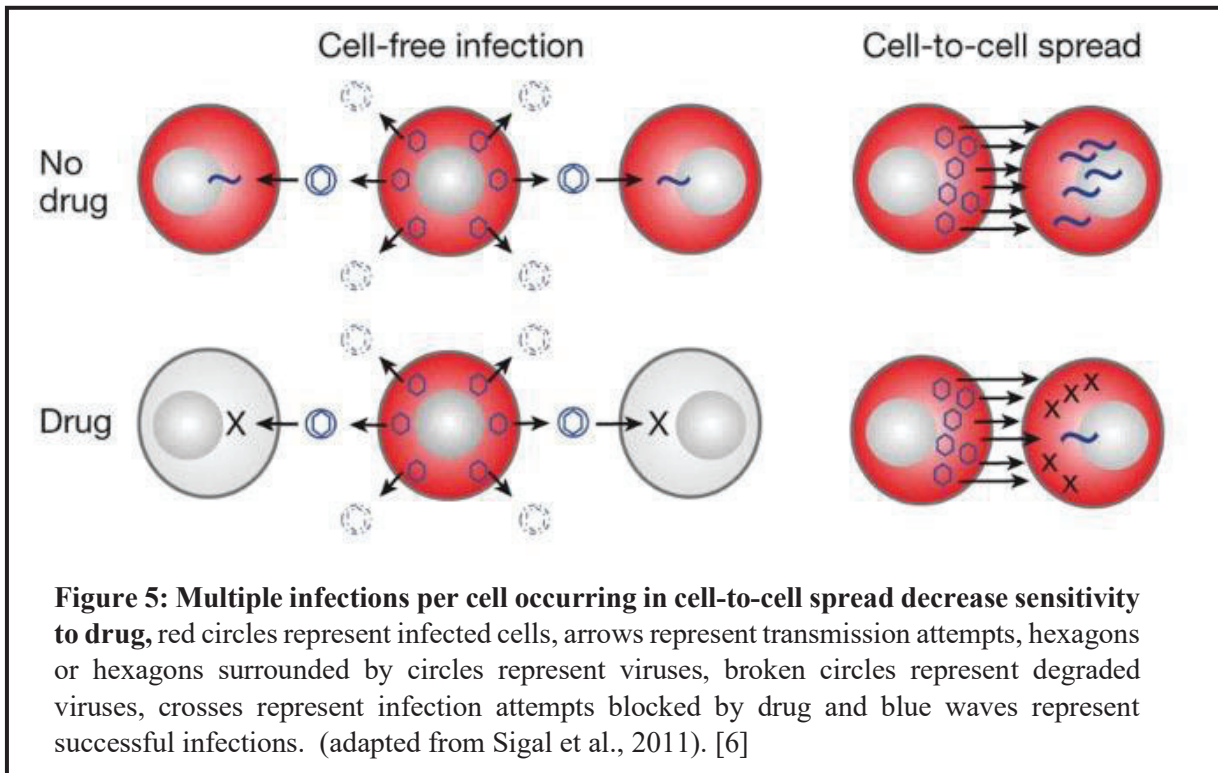
202

203 Cell-to-cell spread is a robust mode of infection as its directed approach and close contact between cells
 204 avoids many barriers experienced by cell-free virus [1, 83-85] (Figure 4B). There is strong evidence to
 205 indicate cell-to-cell spread of HIV may be several times more efficient than cell-free infection [2, 9,
 206 24]. An important feature of cell-to-cell spread, which accounts for its higher efficiency, is that it allows
 207 for the transfer of many virions at once thus increasing the probability of at least one successful
 208 transmission [8] (Figure 5). Because of these characteristics, cell-to-cell spread is linked to decreased
 209 sensitivity to ARVs [8-10, 76, 83] (Figure 5) and neutralising antibodies [2, 11, 12, 21, 76, 84, 86]. It
 210 also allows for the infection of cell types with low probability of infection such as, resting T cells, which
 211 are estimated to be 10-fold less infectable than activated T cells [7], and macrophages, in which the
 212 expression of viral entry receptors is low [23]. Furthermore, cell-to-cell spread is a more rapid method
 213 of viral infection of cells [87] which may be important in quickly establishing the HIV reservoir.

214 Contact dependent transfer of virus between infected T cells and uninfected target cells relies on the
 215 formation of a VS [3]. This formation is initiated by the binding of cell membrane-bound Env, on the
 216 infected donor cell, to the CD4 receptor on the uninfected target cell [21]. This, stable adhesion, is
 217 followed by the concentration of viral proteins, Env and Gag, as well as CD4, CXCR4 and lymphocyte

218 function-associated antigen-1 (LFA-1) at the site of the cellular contact [2, 3]. The relocation of these
 219 proteins to the cell-cell interface is dependent on actin and tubulin cytoskeleton after which the virus
 220 buds into the synaptic cleft between the cells where it is transferred to the target cell [3, 88]. By
 221 polarizing the proteins required for virus packaging and entry into the target cell, the VS facilitates
 222 efficient viral transmission. *In vitro* studies show the accumulation of fluorescent Gag at the site of the
 223 VS and in the target cell during and subsequent to contact with infected donor cells [2, 3], indicating
 224 the transfer of HIV to the target cells.

225



226 Other contact dependent transfer of HIV occurring between different cell types includes, dendritic cells
 227 (DCs) to T cell [5, 76, 80, 89, 90], macrophage to T cells [20, 76, 91] and T cells to macrophages [23,
 228 76]. DC mediated cell-to-cell spread involves the capture HIV on the surface of the DC, using the highly
 229 expressed DC-specific C-type lectin (DC-SIGN) [5] (Figure 4C). The DC then transports the virus to
 230 lymphoid tissue where it is presented to CD4⁺ T cells facilitating a contact driven infection of the CD4⁺
 231 T cells through an infectious synapse [80, 89, 90]. Productive infection of DCs is not required for this
 232 type of cell-to-cell spread [89] and so it is often referred to as *trans* infection. Infection via dendritic
 233 cells has been demonstrated to be more efficient than cell-free infection [89]. Infected macrophages
 234 transfer HIV, at a high multiplicity of infection (MOI), to CD4⁺ T cells in a contact dependent manner
 235 which, like the transfer of virion mediated by virologic synapses between T cells, is resistant to drug
 236 and antibody inhibition [9, 12, 20, 91-93] (Figure 4D). HIV infection of macrophages by cell-free
 237 infection is highly inefficient due to the low expression of viral receptors on the surface of macrophages

238 [94]. The virus can overcome this barrier of macrophage infection through a contact dependent
239 mechanism when macrophage phagocytose an infected CD4⁺ T cell [23, 93] (Figure 4E).

240 Despite the perceived superiority of cell-to-cell spread over cell-free infection, viruses like HIV transmit
241 by both modes of infection. The contribution of each mode of infection *in vivo* is unknown; however,
242 *in vitro* experiments indicate that cell-to-cell spread is the predominant mode of HIV infection [24],
243 with an estimated 60% of the infection occurring by cell-to-cell spread and the remainder by cell-free
244 infection [26]. Mathematical modelling predicts that cell-to-cell spread and cell-free infection
245 contribute equally to virus spread [27]. Moreover, fluorescence imaging shows that most but not all
246 Gag congregates at the VS and transmission electron microscopy reveals that a small but considerable
247 number of virus buds off the cell not situated at the VS [21] indicating that a portion of HIV infection
248 comes from a cell-free route. The predominant mode of HIV infection may be determined by specific
249 conditions such that, if all steps in the viral life cycle occur efficiently, cell-free infection appears to
250 happens *in vitro* at similar rates to cell-to-cell spread however when viral gene expression in or release
251 from the donor cell is low, neutralizing antibodies are present or when target cell susceptibility to
252 infection is low cell-to-cell spread outperforms cell-free. [84]. Given these *in vitro* observations, it
253 seems probable that cell-to-cell spread would be favoured in sites where there are many close cellular
254 contacts like the lymphoid organs, which are also the site thought to contribute majority of HIV
255 infection. Whereas at sites where cell-cell contacts are few, like in the blood, HIV might rely mainly on
256 cell-free infection for viral dissemination.

257 **1.3 Multiple infections and their impact on the HIV reservoir and evolution**

258 Cell-to-cell spread of HIV enables multiple copies of HIV to transfer from infected donor to uninfected
259 target cell. As previously mentioned, this is an important feature as it increases the probability of at
260 least one successful transmission in unfavourable conditions for infection [8]. This may result in
261 ongoing replication in the face of ART and therefore instrumental in maintaining the HIV reservoir and
262 preventing a functional cure. Multiple infection by cell-free infection is expected to be rare as 1) HIV
263 infected cells down-regulate the CD4 receptor used for viral entry [95] preventing subsequent infection;
264 2) The probability that two virions reach and successfully infect one cell in non-directed infection may
265 be small [36]. Multiple infection is therefore likely to mainly occur by cell-to-cell infection.

266 Infection with multiple copies of HIV may play a significant role in viral evolution by generating and
267 maintaining genetic diversity, further complicating treatment regimens. When multiple virions infect
268 a single cell, they will compete for cellular resources selecting virus better adapted for this [39]. In
269 addition, when multiple genetically different virions infect a single cell, the genetic material, viral
270 proteins and enzymes mix within the cell resulting in complementation, where by virion is packaged
271 containing a combination of the genotype from one parental virus and the structural proteins and
272 enzymes from a different parental virus [39, 96]. Complementation leads to the genotype and phenotype

273 of the virus being no longer linked which allows genetically less fit virus to persist at higher than
 274 expected frequencies because they are shielded from selective pressures by the help of more fit virus
 275 phenotype. This helps to maintain the quasispecies [96, 97].

276 Another phenomenon which occurs when multiple genetically different virions infect a single cell is
 277 recombination which contributes to the genetic diversity of the quasispecies. Like other retroviruses,
 278 HIV-1 packages two copies of viral RNA into one virion. If two different RNA genomes can be
 279 packages into one virion, in the subsequent infection the genomes may recombine as the reverse
 280 transcriptase switches between the two packaged RNA templates in the infecting virion and uses
 281 information from both to create a hybrid viral DNA. Together, these properties of co-infection influence
 282 viral evolution which contributes to the rate of immune escape and promotes or hinders drug resistance.

283 1.3a *In vitro* Evidence of multiple infections

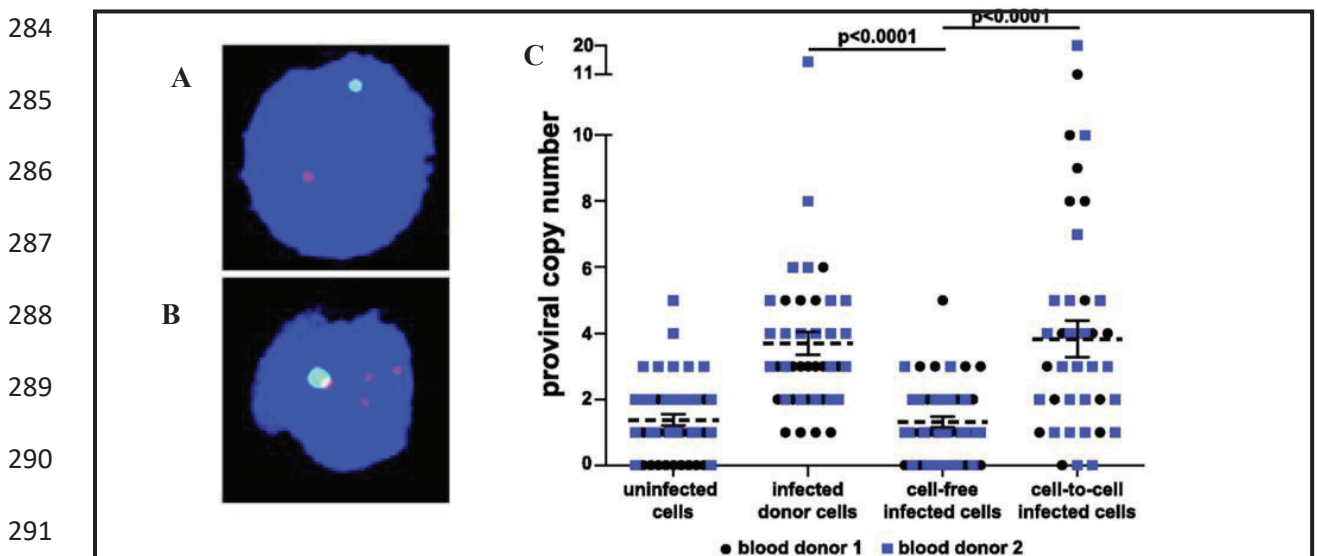


Figure 6: Multiple proviral copies of HIV per cell following *in vitro* cell-to-cell spread. Fluorescent *in situ* hybridization, where blue indicates staining of cellular DNA with DAPI, red dots indicates proviral copies of HIV and green dots indicates centromeric control probe. A) Cells infected by cell-free infection with a single provirus B) Cell infected by cell-to-cell spread with multiple proviral copies C) Distribution of proviral copies per cell for two donors. Combined means \pm SEM are shown. Blood donor 1: cell-free mean = 1.11, n = 26; cell-to-cell mean = 3.72, n = 25, P = 0.0003. Blood donor 2: cell-free mean = 1.55, n = 20; cell-to-cell mean = 3.95, n = 20, P = 0.0138. Combined blood donors: donor cell mean = 3.71, n = 45, cell-free mean = 1.30, n = 46, cell-to-cell mean = 3.82, n = 45; P values are displayed. Significance was tested using the two-tailed Mann-Whitney U test with an alpha level of 0.05 (adapted from Del Portillo et al., 2002). [30]

292 Multiple infections have been demonstrated to occur at high frequencies *in vitro* [9, 10, 36, 37, 98, 99].
 293 There is evidence of multiply infected cells (with on average 3.5 infections per cell) following cell-to-
 294 cell HIV spread [36, 37] (Figure 6). Moreover, Zhong et al. reported an MOI of as high as 10 provirus
 295 per cell after infection by co-culture compared to an average of 1 provirus in the cells infected by cell-

296 free infection [84]. Multicopy infection has also been demonstrated for dendritic cell mediated infection
 297 and for both CCR5- as well as CXCR4-trophic virus [98, 99]. Overwhelmingly, all of the before
 298 mentioned studies found cells infected by cell-free infection are mostly infected with a single copy of
 299 HIV [36]. The results of the above studies demonstrates that cell-to-cell spread can result in cells
 300 infected with multiple copies of HIV whereas cell-free infection mostly results in cells infected with a
 301 single copy of HIV.

302 1.3.b *In vivo* Evidence of multiple infections and debate

303 Humanized mice studies, suggest that multicopy infection by cell-to-cell transmission occurs in
 304 lymphoid tissue *in vivo* [100]. Furthermore *in vivo* infected cells in the spleens of HIV infected
 305 individuals were revealed to harbour multiple copies of HIV in as many as 75% of the cells analysed
 306 [101-103] (Figure 7). Moreover, sequencing of these cell revealed that they were infected with
 307 genetically distinct viral copies [101-103]. These results were taken as evidence of the viability of viral
 308 recombination which requires cells to be infected which more than one genetically distinct virus. Given
 309 these observations, two possible scenarios were mathematically modelled to explain how the cells
 310 became multiply infected, either by sequential singular infection events or simultaneous multiple
 311 infection by cell-to-cell spread [104]. Sequential infection seems unlikely as HIV-1 down-regulates the
 312 CD4 receptor used for viral entry preventing subsequent infection after the first [95]. It is more probable
 313 that simultaneous infection by cell-to-cell spread is responsible for multiply infected cells. However, if
 314 the susceptibility to infection differs substantially between target cells, the number of infection events
 315 per cell during cell-free HIV-1 infection may follow a negative-binomial distribution with multiple
 316 infection in the more infectable fraction of cells [105].

317

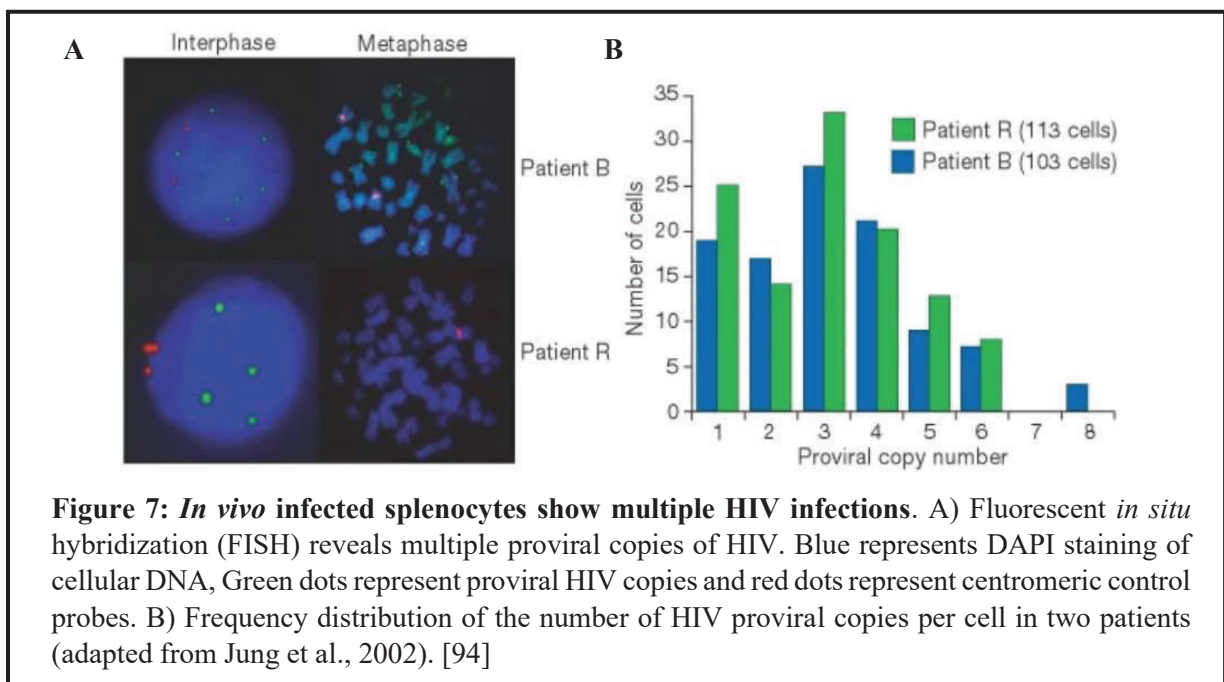


Figure 7: *In vivo* infected splenocytes show multiple HIV infections. A) Fluorescent *in situ* hybridization (FISH) reveals multiple proviral copies of HIV. Blue represents DAPI staining of cellular DNA, Green dots represent proviral HIV copies and red dots represent centromeric control probes. B) Frequency distribution of the number of HIV proviral copies per cell in two patients (adapted from Jung et al., 2002). [94]

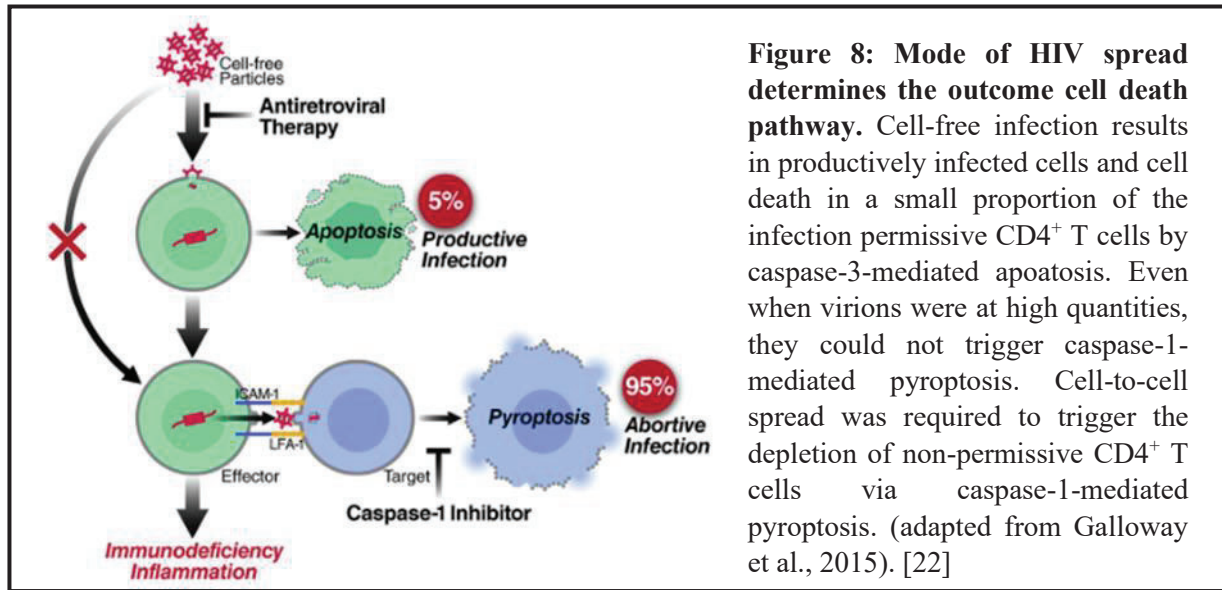
318 However, not all *in vivo* data concur that multiply infected cells make up a significant proportion of the
319 overall infected cell population. Josefsson et al. demonstrated that majority (greater than 90%) of
320 infected CD4⁺ cells from peripheral blood as well as lymph node clinical samples contained only one
321 copy of HIV [106, 107]. One explanation for the discrepancy in the findings of these studies and the
322 before mentioned studies in this section is that the cell types analysed were different. It is possible that
323 certain cell sub-types may be infectable to different degrees and therefore a closer look into specific
324 cell types will clarify to what extent multiple infection occurs and how it contributes to the HIV
325 reservoir and evolution. More recent work supports this explanation, finding that CD3 positive, CD32a
326 high, CD4 T cell subset have a greater than one average of HIV DNA copies per cell in 3 out of 12
327 individuals in the in the face of ART [108].

328 Another explanation for the inconsistency is that multiply infected cell have a higher probability of cell
329 death and are therefore not readily detected [10, 28, 109]. It is also possible that even if the proportion
330 of multiply infected cells generated by cell-to-cell spread is relatively small proportion (less than 10%)
331 they still contribute significantly to genetic diversity. Modelling suggests, that only about 10% of
332 infected cells would need to be multiply infected for the rate at which recombination is observed
333 clinically [110].

334 **1.4 HIV induced cell death**

335 HIV infection results in extensive depletion of CD4⁺ T cells in the lymphatic tissue, where the infection
336 most intense [28-30, 111-114]. Counterintuitively, only approximately 5% of HIV induced cell death
337 occurs in productively infected cells with the remaining majority resulting in bystander cells [30, 114].
338 Cell death in the productively infected CD4⁺ T cell fraction occurs by caspase-3-mediated apoptosis
339 [29]. In contrast, cell death in non-permissive bystander cells is caused by abortive HIV infection.
340 Incomplete reverse transcripts accumulate [30], which are sensed by interferon- γ -inducible protein 16
341 (*IFI16*) [31], triggering caspase-1-dependent pyroptosis [29].

342 Mode of HIV infection has been shown to determine specific cell death pathways [28]. Cell-free
343 infection can elicit the caspase-3-mediated apoptosis in the small percentage of permissive CD4⁺ T cell,
344 whereas infection by cell-to-cell is required to trigger widespread pyroptotic death in non-permissive
345 CD4⁺ T cells of lymphoid tissue [28, 29] (Figure 8). It was also demonstrated that HIV induces cell
346 death by double stranded breaks generated during integration of the reverse transcribed virus in the host
347 DNA [32]. Since, multiple integration attempts are likely during cell-to-cell spread [36, 37], an
348 increased number of double stranded breaks and a higher probability of cell death may be associated
349 with this mode of infection.



350

351 The viral proteins, Tat and Env, may also play a role in inducing cell death of infected cells through
 352 CD95-mediated apoptosis following T cell activation however this mechanism has not yet been
 353 demonstrated as mode of infection specific [33-35].

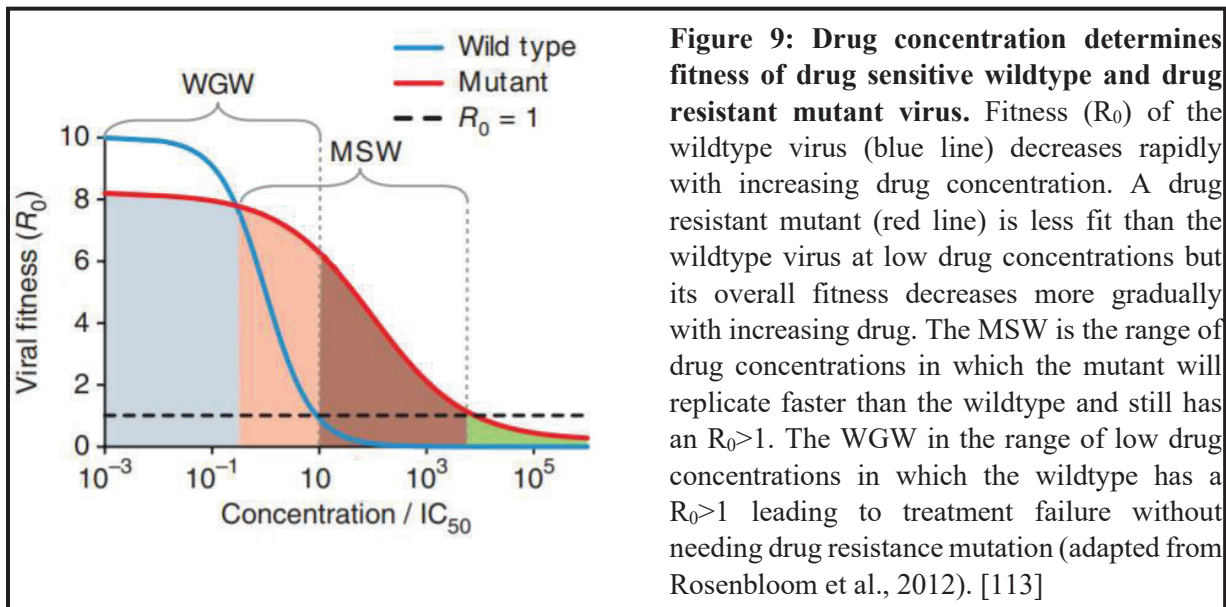
354 1.5 HIV evolution of drug resistance

355 Treatment of HIV with antiretroviral therapy (ART) has been successful in suppressing the virus
 356 replication and reducing patient mortality and morbidities. Although ART prevents HIV disease
 357 progression, HIV evolution of drug resistance remains a considerable concern as it leads to virologic
 358 failure, the replication of HIV in the face of ART due to acquisition of drug resistance mutations.
 359 Prevalence of drug resistance mutations in HIV infected individuals on ART is between 3-12% [115-
 360 117]. For evolution to occur under a selective pressure, like drug, genetic variation is required. HIV is
 361 well suited to this due to its high mutation rate, which generates mutations at $\sim 3 \times 10^{-5}$ per base per
 362 replication cycle [40]. It is therefore predicted that one in every three replication cycles results in a
 363 mutated genome [39].

364 Drug resistance may arise either due to mutations that were present within the viral population before
 365 treatment initiation (standing genetic variation) or due to low levels of ongoing replication during
 366 treatment [118]. Modelling suggests, that in patients initiating ART, 6% will evolve drug resistance in
 367 the first year due to standing genetic variation, which favours the selection of drug resistant mutants
 368 present at the time of ART initiation. In addition, drug resistant mutations which arise during therapy
 369 accounts for a further 3.7% of patients evolving drug resistance for every year on treatment [118].

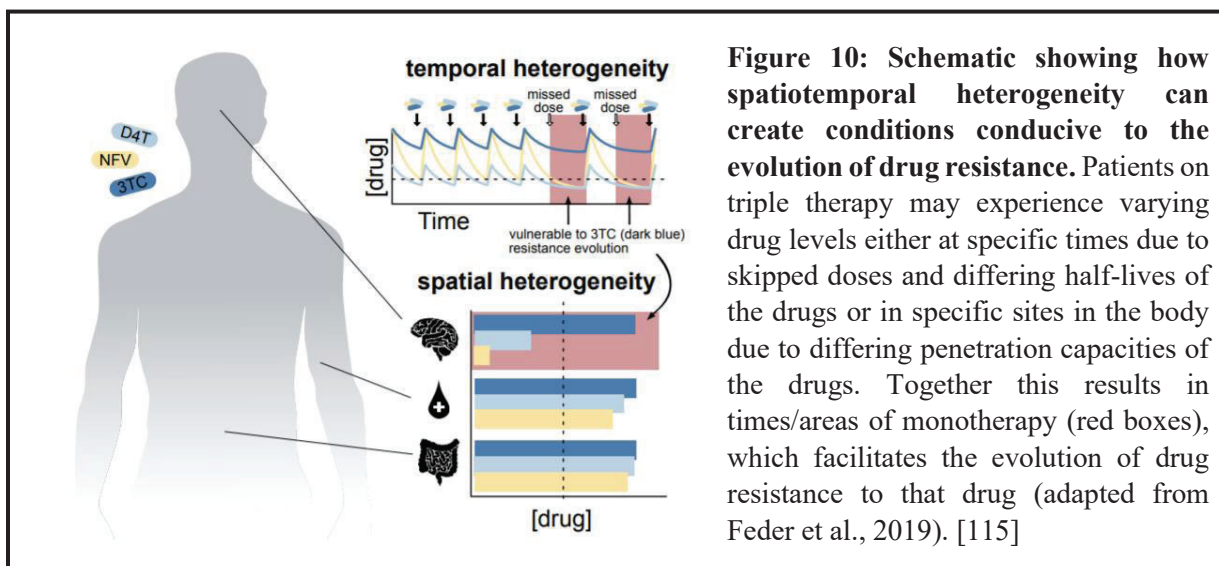
370 Drug resistance mutations are selected for depending on whether they confer a fitness advantage under
 371 the given conditions. In the absence of drug, drug resistant mutants carry a fitness cost and therefore

372 are not selected over the wildtype (drug sensitive) virus [119]. However, when drug concentration is
 373 high both the mutant and the wildtype virus have low fitness (R_0) leading to fully suppressed viral
 374 replication. Thus, there is a specific range of intermediate drug concentrations, termed the mutant
 375 selection window (MSW), in which mutants conferring drug resistance are selected over wildtype virus
 376 [39, 120] (Figure 9).



377
 378

379 Keeping the drug concentration above the MSW is key to preventing mutant selection resulting in drug
 380 resistance although this may not always be achieved. Poor adherence to drug regimens as well as
 381 imperfect drug penetration in anatomical compartments allows continued viral replication in the face of
 382 ART, [50, 51, 121, 122]. Combined, inconsistent adherence and imperfect drug penetration contribute
 383 to spatiotemporal heterogeneity which set up an environment for HIV evolution of drug resistance
 384 [122] (Figure 10).



385

386 Poor ART adherence is associated with drug resistance in HIV patients [42, 47-49]. ART is normally
 387 comprised of at least three drugs from at least two different drug classes. This aims to prevent the
 388 evolution of drug resistance as only a virus carrying drug resistance mutations to all three drugs would
 389 be able to replicate. The probability of multiple drug resistance mutations arising simultaneously is very
 390 low. Yet, the probability of evolution of multidrug resistance over time is dependent on drug half-lives,
 391 where skipped doses may result in a period of monotherapy of the drug with the longest half-life [122].
 392 Non-nucleoside reverse transcriptase inhibitors (NNRTIs), like efavirenz (EFV), have particularly long
 393 half-lives [123, 124]. Treatment interruptions of a few days are long enough for all other drugs in the
 394 formulated regime to leave the body but not long enough for the NNRTI to completely be removed,
 395 leaving what is termed the NNRTI tail [123-126]. Therefore, skipped doses may result in a time period
 396 within the MSW allowing drug resistance evolution.

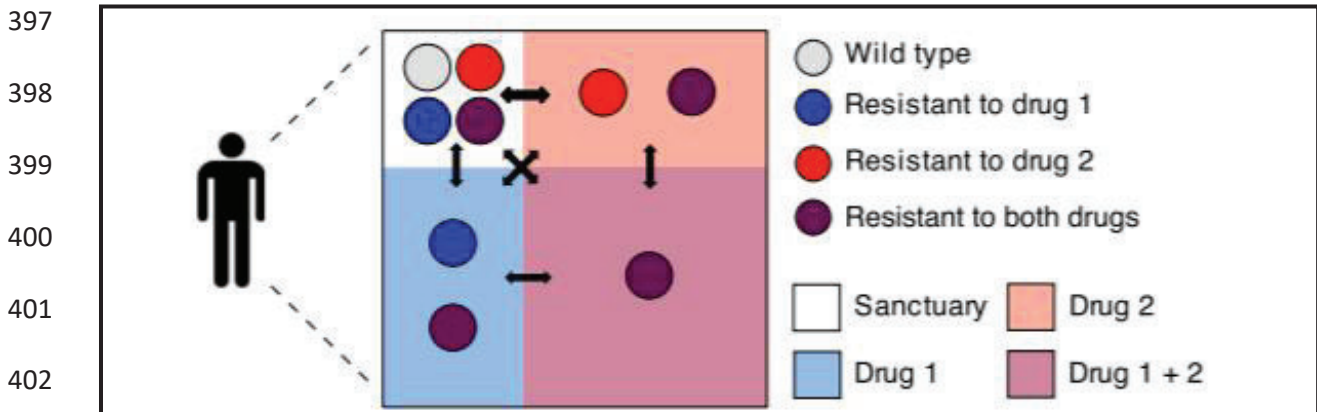


Figure 11: Model of stepwise evolution of multidrug resistance. The box represents a patient's body. A combination therapy of two drugs is represented. Mismatched drug penetration creates areas of monotherapy. White represents a sanctuary where both wildtype and mutant virus can replicate, while blue, orange and red shaded areas represent compartments in the body where only drug 1, drug 2 or both drugs are present respectively. Coloured circles represent viral genotypes: wildtype (light grey), resistant to drug 1 (blue), resistant to drug 2 (red), and resistant to both drugs (purple). In the sanctuary all viruses can replicate as no drugs are present. In the compartments with only a single drug present, only the virus carrying a resistance mutation for that drug can replicate. Finally, in the compartment with both drugs only the virus carrying both resistance mutations will be able to replicate. Arrows indicate connections between compartments allowing migration of virus between them. Drug resistance mutants evolved in the sanctuary site will be able to replicate in the single drug compartment for which the mutation confers resistance to. Following this first step, the virus now replicating in the presence of one drug must only evolve one more drug resistance mutation to allow it to replicate in the presence of both drugs. This spatial drug heterogeneity permits the evolution of multidrug resistance one step at a time (adapted from Moreno-Gamez et al., 2015). [44]

403 It has been shown that drug concentrations in the lymph nodes [38] and the central nervous system
 404 (CNS) [52, 127-129] do not reach the same concentration as those found in the peripheral blood. Indeed,
 405 evolution of HIV sequences occurs in the lymph nodes of patients on ART [13]. Drug resistant
 406 mutations are detected in the cerebral spinal fluid (CSF) of ART treated patient, despite having
 407 undetectable viral load (VL) in the blood [14-16, 130, 131], which may indicate ongoing HIV evolution

408 occurring in the CNS even though HIV is suppressed elsewhere in the body. Furthermore, the lowered
 409 drug levels and potential monotherapy found in tissue compartments could favour the evolution of
 410 multidrug resistance, as it provides the opportunity for HIV to accumulate drug resistance mutations in
 411 a stepwise fashion [50] (Figure 11).

412 **1.6 Gene expression in HIV infection**

413 HIV infection alters the host gene expression, leading to dramatic changes in the functioning of the host
 414 immune system. The interactions between the virus and host, which drive HIV disease progression and
 415 persistence, are complex. In depth study of host gene expression in response to HIV infection is
 416 therefore required to identify targets for new therapies or effective vaccines. Microarrays and the more
 417 recently developed RNA-seq platforms are methods used to identify differentially expressed genes
 418 (DEGs) in HIV infection [58, 132, 133]. General trends in studies of gene expression have found that
 419 genes expressed during HIV infection are dependent on cell/tissue type, stage of the infection, level of
 420 viremia as well as treatment status [58].

421 CD4⁺ T cells are the primary targets of HIV infection and are gradually depleted throughout the course
 422 of infection resulting in AIDS in HIV infected patients. Given their central role, in HIV pathogenesis,
 423 it is of great importance to understand the host transcriptional changes which occur in this specific
 424 group of cells during HIV infection. Common gene pathways differentially expressed in infected CD4⁺
 425 T cells related to cell-cycle modulation, apoptosis, inflammation, metabolism, and type-1 interferon
 426 related genes (Figure 12).

427

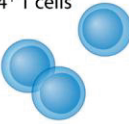
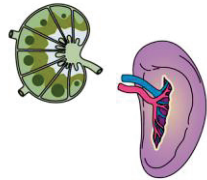
Sample type	Key findings
 CD4 ⁺ T cells	<ul style="list-style-type: none"> • Pre-treatment samples – upregulation of cell cycle, immune response, type-1 interferon related genes, and modulation of apoptosis pathways • Heightened viraemia – greater upregulation of cell cycle and differentiation genes, cellular metabolism, processing and transport • Cell death may be driven by increased cell cycle entry, with G2 or M arrest • Resting CD4⁺ T cells are polarised toward Th1 functions • Resting compartment may secrete HIV virions in the absence of activation stimuli, contributing to chronic viraemia
 Lymphoid tissues	<ul style="list-style-type: none"> • Lymph nodes – striking changes in gene expression during HIV infection. Upregulation of immune defence, apoptosis, metabolism and tissue repair pathways in the acute phase. 46 genes remain differentially expressed throughout infection; possible core host genes responding to virus • Viraemia – inverse correlation with 95% of gene expression in lymph nodes(54)

Figure 12: Summary of key findings per cell population type. (adapted from Judge et al., 2020). [58]

428 Studies of *in vivo* infected CD4⁺ T cells have examined gene expression within total CD4⁺ T cell
 429 population, with infected cells in the minority, but are likely better reflections of the systemic host
 430 response. Gene expression in pre-treatment CD4⁺ T cells from HIV infected individuals demonstrate

431 significant upregulation of genes relating to cell cycle, type 1 interferon response, immune pathways
 432 and modulation of apoptosis [54, 56-58]. These host transcriptional responses may contribute to CD4⁺
 433 T cell depletion during HIV infection, in untreated individuals, by disrupting CD4⁺ T cell
 434 differentiation. It was suggested that, in HIV infected individuals, activated CD4⁺ T cells may enter a
 435 hyperproliferative state modulated by type I interferon, resulting in a greater number of short lived
 436 effector cells and fewer long lived memory cells [54] (Figure 13).

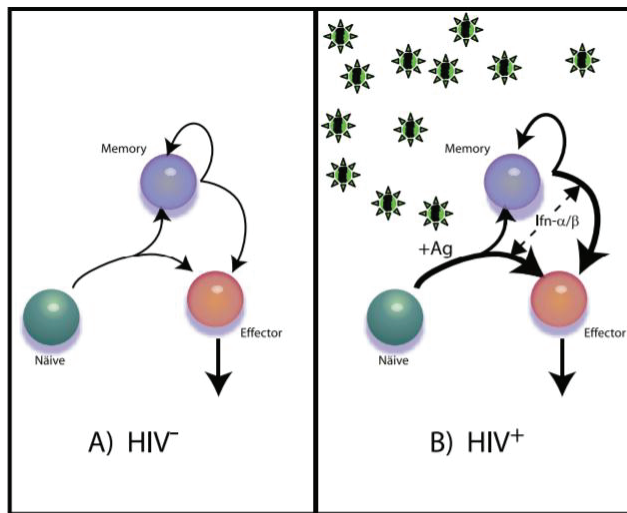


Figure 13: Model of CD4⁺ T cell differentiation. Thickness of the arrows represent the proportion of differentiation in the direction of the arrow. A) Differentiation in a healthy individual B) Differentiation in the presence of HIV antigens, results in an upregulation of interferon type 1 which increases the proportion of cells differentiating towards short-lived effector cells (adapted from Sedaghat et al., 2008). [48]

437

438 Additionally, the observed upregulation of interferon-stimulated genes (ISGs) positively correlates with
 439 high viremia and disease progression [55, 57]. Some of the ISGs associated with high viremia include,
 440 *MX1*, *TAP1*, *IFI35*, *ISG15* and *IFIT3* [57]. Studies demonstrated an increase of expression for ISGs in
 441 CD4⁺ T cells from acute and chronically infected samples from non-controllers but not in samples from
 442 elite controllers [55, 57]. The gene expression of non-controllers on ART, with undetectable viral loads,
 443 was comparable to that of majority of elite controllers [57, 134], further highlighting the positive
 444 correlation between high viremia/disease progression and the upregulation of interferon genes. Central
 445 memory CD4⁺ T cell in HIV infected individuals also showed an increase in expression of interferon
 446 signalling and inflammatory genes [135]. Other genes upregulated in the CD4⁺ T cells in viremic
 447 patients, but not in aviremic patients, involve transcriptional regulation, RNA processing and
 448 modification, protein trafficking/vesicle transport [136].

449 Lymphatic tissue is a site of substantial HIV infection [18, 19]. The large number of infectable cells
 450 [18, 137, 138], close cell-cell contacts [3, 20-24, 139] and decreased penetration of ART [38] in this
 451 tissue makes it an environment well suited to HIV infection and a likely site of the HIV reservoir. It is
 452 therefore an important site to study the changes in gene expression during HIV infection. Common gene
 453 pathways differentially expressed in infected lymph node tissues relate to immune defence, apoptosis,
 454 metabolism, and tissue repair pathways (Figure 12). Li et al. determined that gene expression, of mixed
 455 cell populations, from the lymph nodes of HIV infected untreated individuals depended on the stage of
 456 infection [59]. Lymph nodes from acute HIV infection generated the highest number of differentially

457 expressed genes (DGEs) which related to upregulation of immune activation, immune defences,
458 apoptosis, and tissue repair. The asymptomatic stage which followed saw a return to baseline level
459 expression of majority of the genes in the lymph nodes [59]. Gene expression during the AIDS stage
460 reflected mostly downregulation of genes regulating to immune activation, apoptosis and tissue repair
461 [59]. The authors noted that 47 differentially expressed genes were common to all stages of HIV
462 infection including the upregulation of many genes involved in interferon related antiviral response,
463 activation and cell-cycle regulation [59]. Re-analysis of the same data, found that 95% of the DGEs
464 negatively correlated with viral load; however, similar in the studies of CD4⁺ T cells, ISGs positively
465 correlated with viral replication in the lymph nodes [60].

466

467

468

469

470

471

472

473

474

475

476

477

478

479

480

481

482

483

484

485 **REFERENCES**

486

- 487 1. Sattentau, Q., *Avoiding the void: cell-to-cell spread of human viruses*. Nature Reviews
488 Microbiology, 2008. **6**(11): p. 815-826.
- 489 2. Chen, P., et al., *Predominant mode of human immunodeficiency virus transfer between T*
490 *cells is mediated by sustained Env-dependent neutralization-resistant virological synapses*.
491 Journal of virology, 2007. **81**(22): p. 12582-12595.
- 492 3. Jolly, C., et al., *HIV-1 cell to cell transfer across an Env-induced, actin-dependent synapse*.
493 Journal of Experimental Medicine, 2004. **199**(2): p. 283-293.
- 494 4. Kim, J.T., et al., *Dendritic cells efficiently transmit HIV to T Cells in a tenofovir and raltegravir*
495 *insensitive manner*. PloS one, 2018. **13**(1): p. e0189945.
- 496 5. Geijtenbeek, T.B., et al., *DC-SIGN, a dendritic cell-specific HIV-1-binding protein that*
497 *enhances trans-infection of T cells*. Cell, 2000. **100**(5): p. 587-597.
- 498 6. Sigal, A. and D. Baltimore, *As good as it gets? The problem of HIV persistence despite*
499 *antiretroviral drugs*. Cell host & microbe, 2012. **12**(2): p. 132-138.
- 500 7. Agosto, L.M., et al., *HIV-1-infected CD4+ T cells facilitate latent infection of resting CD4+ T*
501 *cells through cell-cell contact*. Cell reports, 2018. **24**(8): p. 2088-2100.
- 502 8. Sigal, A., et al., *Cell-to-cell spread of HIV permits ongoing replication despite antiretroviral*
503 *therapy*. Nature, 2011. **477**(7362): p. 95-98.
- 504 9. Duncan, C.J., R.A. Russell, and Q.J. Sattentau, *High multiplicity HIV-1 cell-to-cell transmission*
505 *from macrophages to CD4+ T cells limits antiretroviral efficacy*. AIDS (London, England),
506 2013. **27**(14): p. 2201.
- 507 10. Jackson, L., et al., *Incomplete inhibition of HIV infection results in more HIV infected lymph*
508 *node cells by reducing cell death*. Elife, 2018. **7**: p. e30134.
- 509 11. Abela, I.A., et al., *Cell-cell transmission enables HIV-1 to evade inhibition by potent CD4bs*
510 *directed antibodies*. PLoS Pathog, 2012. **8**(4): p. e1002634.
- 511 12. Duncan, C.J., et al., *High-multiplicity HIV-1 infection and neutralizing antibody evasion*
512 *mediated by the macrophage-T cell virological synapse*. Journal of virology, 2014. **88**(4): p.
513 2025-2034.
- 514 13. Lorenzo-Redondo, R., et al., *Persistent HIV-1 replication maintains the tissue reservoir during*
515 *therapy*. Nature, 2016. **530**(7588): p. 51.
- 516 14. Peluso, M.J., et al., *Cerebrospinal fluid HIV escape associated with progressive neurologic*
517 *dysfunction in patients on antiretroviral therapy with well-controlled plasma viral load*. AIDS
518 (London, England), 2012. **26**(14).
- 519 15. Soulie, C., et al., *Antiretroviral-treated HIV-1 patients can harbour resistant viruses in CSF*
520 *despite an undetectable viral load in plasma*. Journal of Antimicrobial Chemotherapy, 2017.
521 **72**(8): p. 2351-2354.
- 522 16. Kugathasan, R., et al., *Diffuse white matter signal abnormalities on magnetic resonance*
523 *imaging are associated with human immunodeficiency virus type 1 viral escape in the central*
524 *nervous system among patients with neurological symptoms*. Clinical Infectious Diseases,
525 2017. **64**(8): p. 1059-1065.
- 526 17. Horiike, M., et al., *Lymph nodes harbor viral reservoirs that cause rebound of plasma viremia*
527 *in SIV-infected macaques upon cessation of combined antiretroviral therapy*. Virology, 2012.
528 **423**(2): p. 107-118.
- 529 18. Embretson, J., et al., *Massive covert infection of helper T lymphocytes and macrophages by*
530 *HIV during the incubation period of AIDS*. Nature, 1993. **362**(6418): p. 359-362.
- 531 19. Pantaleo, G., et al., *HIV infection is active and progressive in lymphoid tissue during the*
532 *clinically latent stage of disease*. Nature, 1993. **362**(6418): p. 355-358.
- 533 20. Groot, F., S. Welsch, and Q.J. Sattentau, *Efficient HIV-1 transmission from macrophages to T*
534 *cells across transient virological synapses*. Blood, The Journal of the American Society of
535 Hematology, 2008. **111**(9): p. 4660-4663.

- 536 21. Hübner, W., et al., *Quantitative 3D video microscopy of HIV transfer across T cell virological*
537 *synapses*. *Science*, 2009. **323**(5922): p. 1743-1747.
- 538 22. Dale, B.M., et al., *Cell-to-cell transfer of HIV-1 via virological synapses leads to endosomal*
539 *virion maturation that activates viral membrane fusion*. *Cell host & microbe*, 2011. **10**(6): p.
540 551-562.
- 541 23. Baxter, A.E., et al., *Macrophage infection via selective capture of HIV-1-infected CD4+ T cells*.
542 *Cell host & microbe*, 2014. **16**(6): p. 711-721.
- 543 24. Sourisseau, M., et al., *Inefficient human immunodeficiency virus replication in mobile*
544 *lymphocytes*. *Journal of virology*, 2007. **81**(2): p. 1000-1012.
- 545 25. Bousso, P. and E.A. Robey, *Dynamic behavior of T cells and thymocytes in lymphoid organs as*
546 *revealed by two-photon microscopy*. *Immunity*, 2004. **21**(3): p. 349-355.
- 547 26. Iwami, S., et al., *Cell-to-cell infection by HIV contributes over half of virus infection*. *Elife*,
548 2015. **4**: p. e08150.
- 549 27. Komarova, N.L., et al., *Relative contribution of free-virus and synaptic transmission to the*
550 *spread of HIV-1 through target cell populations*. *Biology letters*, 2013. **9**(1): p. 20121049.
- 551 28. Galloway, N.L., et al., *Cell-to-cell transmission of HIV-1 is required to trigger pyroptotic death*
552 *of lymphoid-tissue-derived CD4 T cells*. *Cell reports*, 2015. **12**(10): p. 1555-1563.
- 553 29. Doitsh, G., et al., *Cell death by pyroptosis drives CD4 T-cell depletion in HIV-1 infection*.
554 *Nature*, 2014. **505**(7484): p. 509-514.
- 555 30. Doitsh, G., et al., *Abortive HIV infection mediates CD4 T cell depletion and inflammation in*
556 *human lymphoid tissue*. *Cell*, 2010. **143**(5): p. 789-801.
- 557 31. Monroe, K.M., et al., *IFI16 DNA sensor is required for death of lymphoid CD4 T cells*
558 *abortively infected with HIV*. *Science*, 2014. **343**(6169): p. 428-432.
- 559 32. Cooper, A., et al., *HIV-1 causes CD4 cell death through DNA-dependent protein kinase during*
560 *viral integration*. *Nature*, 2013. **498**(7454): p. 376.
- 561 33. Banda, N.K., et al., *Crosslinking CD4 by human immunodeficiency virus gp120 primes T cells*
562 *for activation-induced apoptosis*. *Journal of Experimental Medicine*, 1992. **176**(4): p. 1099-
563 1106.
- 564 34. Westendorp, M., et al., *HIV-1 Tat potentiates TNF-induced NF-kappa B activation and*
565 *cytotoxicity by altering the cellular redox state*. *The EMBO journal*, 1995. **14**(3): p. 546.
- 566 35. Westendorp, M.O., et al., *Sensitization of T cells to CD95-mediated apoptosis by HIV-1 Tat*
567 *and gp120*. *Nature*, 1995. **375**(6531): p. 497-500.
- 568 36. Del Portillo, A., et al., *Multiploid inheritance of HIV-1 during cell-to-cell infection*. *Journal of*
569 *virology*, 2011. **85**(14): p. 7169-7176.
- 570 37. Russell, R.A., et al., *Multiple proviral integration events after virological synapse-mediated*
571 *HIV-1 spread*. *Virology*, 2013. **443**(1): p. 143-149.
- 572 38. Fletcher, C.V., et al., *Persistent HIV-1 replication is associated with lower antiretroviral drug*
573 *concentrations in lymphatic tissues*. *Proceedings of the National Academy of Sciences*, 2014.
574 **111**(6): p. 2307-2312.
- 575 39. Hill, A.L., D.I. Rosenbloom, and M.A. Nowak, *Evolutionary dynamics of HIV at multiple spatial*
576 *and temporal scales*. *Journal of molecular medicine*, 2012. **90**(5): p. 543-561.
- 577 40. Mansky, L.M. and H.M. Temin, *Lower in vivo mutation rate of human immunodeficiency virus*
578 *type 1 than that predicted from the fidelity of purified reverse transcriptase*. *Journal of*
579 *virology*, 1995. **69**(8): p. 5087-5094.
- 580 41. Parienti, J.-J., et al., *Not all missed doses are the same: sustained NNRTI treatment*
581 *interruptions predict HIV rebound at low-to-moderate adherence levels*. *PloS one*, 2008. **3**(7):
582 p. e2783.
- 583 42. Oyugi, J.H., et al., *Treatment interruptions predict resistance in HIV-positive individuals*
584 *purchasing fixed-dose combination antiretroviral therapy in Kampala, Uganda*. *Aids*, 2007.
585 **21**(8): p. 965-971.

- 586 43. Musinguzi, N., et al., *Duration of viral suppression and risk of rebound viremia with first-line*
587 *antiretroviral therapy in rural Uganda*. *AIDS and behavior*, 2017. **21**(6): p. 1735-1740.
- 588 44. Rosenblum, M., et al., *The risk of virologic failure decreases with duration of HIV suppression,*
589 *at greater than 50% adherence to antiretroviral therapy*. *PLoS one*, 2009. **4**(9): p. e7196.
- 590 45. Bangsberg, D.R., A.R. Moss, and S.G. Deeks, *Paradoxes of adherence and drug resistance to*
591 *HIV antiretroviral therapy*. *Journal of Antimicrobial Chemotherapy*, 2004. **53**(5): p. 696-699.
- 592 46. Genberg, B.L., et al., *Patterns of antiretroviral therapy adherence and impact on HIV RNA*
593 *among patients in North America*. *AIDS (London, England)*, 2012. **26**(11): p. 1415.
- 594 47. Sethi, A.K., et al., *Association between adherence to antiretroviral therapy and human*
595 *immunodeficiency virus drug resistance*. *Clinical Infectious Diseases*, 2003. **37**(8): p. 1112-
596 1118.
- 597 48. Lima, V.D., et al., *Risk of viral failure declines with duration of suppression on HAART,*
598 *irrespective of adherence level*. *Journal of acquired immune deficiency syndromes (1999)*,
599 2010. **55**(4): p. 460.
- 600 49. Bangsberg, D.R., et al., *Adherence-resistance relationships for protease and non-nucleoside*
601 *reverse transcriptase inhibitors explained by virological fitness*. *Aids*, 2006. **20**(2): p. 223-231.
- 602 50. Moreno-Gamez, S., et al., *Imperfect drug penetration leads to spatial monotherapy and rapid*
603 *evolution of multidrug resistance*. *Proceedings of the National Academy of Sciences*, 2015.
604 **112**(22): p. E2874-E2883.
- 605 51. Kepler, T.B. and A.S. Perelson, *Drug concentration heterogeneity facilitates the evolution of*
606 *drug resistance*. *Proceedings of the National Academy of Sciences*, 1998. **95**(20): p. 11514-
607 11519.
- 608 52. Best, B.M., et al., *Efavirenz concentrations in CSF exceed IC50 for wild-type HIV*. *Journal of*
609 *Antimicrobial Chemotherapy*, 2011. **66**(2): p. 354-357.
- 610 53. Solas, C., et al., *Discrepancies between protease inhibitor concentrations and viral load in*
611 *reservoirs and sanctuary sites in human immunodeficiency virus-infected patients*.
612 *Antimicrobial agents and chemotherapy*, 2003. **47**(1): p. 238-243.
- 613 54. Sedaghat, A.R., et al., *Chronic CD4+ T-cell activation and depletion in human*
614 *immunodeficiency virus type 1 infection: type I interferon-mediated disruption of T-cell*
615 *dynamics*. *Journal of virology*, 2008. **82**(4): p. 1870-1883.
- 616 55. Hycrca, M.D., et al., *Distinct transcriptional profiles in ex vivo CD4+ and CD8+ T cells are*
617 *established early in human immunodeficiency virus type 1 infection and are characterized by*
618 *a chronic interferon response as well as extensive transcriptional changes in CD8+ T cells*.
619 *Journal of virology*, 2007. **81**(7): p. 3477-3486.
- 620 56. Xu, C., et al., *Comparison of transcriptional profiles between CD4+ and CD8+ T cells in HIV*
621 *type 1-infected patients*. *AIDS research and human retroviruses*, 2014. **30**(2): p. 134-141.
- 622 57. Rotger, M., et al., *Genome-wide mRNA expression correlates of viral control in CD4+ T-cells*
623 *from HIV-1-infected individuals*. *PLoS Pathog*, 2010. **6**(2): p. e1000781.
- 624 58. Judge, M., et al., *Gene Expression: the Key to Understanding HIV-1 Infection?* *Microbiology*
625 *and Molecular Biology Reviews*, 2020. **84**(2).
- 626 59. Li, Q., et al., *Microarray analysis of lymphatic tissue reveals stage-specific, gene expression*
627 *signatures in HIV-1 infection*. *The Journal of Immunology*, 2009. **183**(3): p. 1975-1982.
- 628 60. Smith, A.J., et al., *Host genes associated with HIV-1 replication in lymphatic tissue*. *The*
629 *Journal of Immunology*, 2010. **185**(9): p. 5417-5424.
- 630 61. Barré-Sinoussi, F., et al., *Isolation of a T-lymphotropic retrovirus from a patient at risk for*
631 *acquired immune deficiency syndrome (AIDS)*. *Science*, 1983. **220**(4599): p. 868-871.
- 632 62. Gallo, R.C., et al., *Frequent detection and isolation of cytopathic retroviruses (HTLV-III) from*
633 *patients with AIDS and at risk for AIDS*. *science*, 1984. **224**(4648): p. 500-503.
- 634 63. UNAIDS, *Global AIDS Update*. 2020.
- 635 64. Martinez-Picado, J. and S.G. Deeks, *Persistent HIV-1 replication during antiretroviral therapy*.
636 *Current Opinion in HIV and AIDS*, 2016. **11**(4): p. 417.

- 637 65. Mzingwane, M.L. and C.T. Tiemessen, *Mechanisms of HIV persistence in HIV reservoirs*.
638 *Reviews in medical virology*, 2017. **27**(2): p. e1924.
- 639 66. Levy, J.A., *Pathogenesis of human immunodeficiency virus infection*. *Microbiology and*
640 *Molecular Biology Reviews*, 1993. **57**(1): p. 183-289.
- 641 67. Kuiken, C., et al., *HIV sequence compendium 2001*. Theoretical Biology and Biophysics Group,
642 Los Alamos National Laboratory, Los Alamos, NM, 2001.
- 643 68. Barré-Sinoussi, F., *HIV as the cause of AIDS*. *The Lancet*, 1996. **348**(9019): p. 31-35.
- 644 69. Freed, E.O., *HIV-1 replication*. *Somatic cell and molecular genetics*, 2001. **26**(1-6): p. 13-33.
- 645 70. Arrildt, K.T., S.B. Joseph, and R. Swanstrom, *The HIV-1 env protein: a coat of many colors*.
646 *Current Hiv/aids Reports*, 2012. **9**(1): p. 52-63.
- 647 71. Turner, B.G. and M.F. Summers, *Structural biology of HIV*. *Journal of molecular biology*,
648 1999. **285**(1): p. 1-32.
- 649 72. Ferguson, M.R., et al., *HIV-1 replication cycle*. *Clinics in laboratory medicine*, 2002. **22**(3): p.
650 611-635.
- 651 73. Nie, Z., et al., *The putative alpha helix 2 of human immunodeficiency virus type 1 Vpr*
652 *contains a determinant which is responsible for the nuclear translocation of proviral DNA in*
653 *growth-arrested cells*. *Journal of Virology*, 1998. **72**(5): p. 4104-4115.
- 654 74. Wieggers, K., et al., *Sequential steps in human immunodeficiency virus particle maturation*
655 *revealed by alterations of individual Gag polyprotein cleavage sites*. *Journal of virology*,
656 1998. **72**(4): p. 2846-2854.
- 657 75. Zhong, P., et al., *Cell-to-cell transmission of viruses*. *Current opinion in virology*, 2013. **3**(1): p.
658 44-50.
- 659 76. Bracq, L., et al., *Mechanisms for cell-to-cell transmission of HIV-1*. *Frontiers in immunology*,
660 2018. **9**: p. 260.
- 661 77. Martin, N. and Q. Sattentau, *Cell-to-cell HIV-1 spread and its implications for immune*
662 *evasion*. *Current Opinion in HIV and AIDS*, 2009. **4**(2): p. 143-149.
- 663 78. Piguet, V. and Q. Sattentau, *Dangerous liaisons at the virological synapse*. *The Journal of*
664 *clinical investigation*, 2004. **114**(5): p. 605-610.
- 665 79. Law, K., et al., *Cell-to-cell spread of HIV and viral pathogenesis*, in *Advances in virus research*.
666 2016, Elsevier. p. 43-85.
- 667 80. McDonald, D., et al., *Recruitment of HIV and its receptors to dendritic cell-T cell junctions*.
668 *Science*, 2003. **300**(5623): p. 1295-1297.
- 669 81. Sattentau, Q.J., *Cell-to-cell spread of retroviruses*. *Viruses*, 2010. **2**(6): p. 1306-1321.
- 670 82. McKEATING, J.A., A. McKNIGHT, and J.P. Moore, *Differential loss of envelope glycoprotein*
671 *gp120 from virions of human immunodeficiency virus type 1 isolates: effects on infectivity*
672 *and neutralization*. *Journal of virology*, 1991. **65**(2): p. 852-860.
- 673 83. Agosto, L.M., P.D. Uchil, and W. Mothes, *HIV cell-to-cell transmission: effects on*
674 *pathogenesis and antiretroviral therapy*. *Trends in microbiology*, 2015. **23**(5): p. 289-295.
- 675 84. Zhong, P., et al., *Cell-to-cell transmission can overcome multiple donor and target cell*
676 *barriers imposed on cell-free HIV*. *PloS one*, 2013. **8**(1): p. e53138.
- 677 85. Pedro, K.D., A.J. Henderson, and L.M. Agosto, *Mechanisms of HIV-1 cell-to-cell transmission*
678 *and the establishment of the latent reservoir*. *Virus research*, 2019. **265**: p. 115-121.
- 679 86. Durham, N.D., et al., *Neutralization resistance of virological synapse-mediated HIV-1*
680 *Infection is regulated by the gp41 cytoplasmic tail*. *Journal of virology*, 2012. **86**(14): p. 7484-
681 7495.
- 682 87. Boullé, M., et al., *HIV cell-to-cell spread results in earlier onset of viral gene expression by*
683 *multiple infections per cell*. *PLoS pathogens*, 2016. **12**(11): p. e1005964.
- 684 88. Jolly, C., I. Mitar, and Q.J. Sattentau, *Requirement for an intact T-cell actin and tubulin*
685 *cytoskeleton for efficient assembly and spread of human immunodeficiency virus type 1*.
686 *Journal of virology*, 2007. **81**(11): p. 5547-5560.

- 687 89. Cameron, P.U., et al., *Dendritic cells exposed to human immunodeficiency virus type-1*
688 *transmit a vigorous cytopathic infection to CD4+ T cells*. *Science*, 1992. **257**(5068): p. 383-
689 387.
- 690 90. Piguet, V. and R.M. Steinman, *The interaction of HIV with dendritic cells: outcomes and*
691 *pathways*. *Trends in immunology*, 2007. **28**(11): p. 503-510.
- 692 91. Carr, J., et al., *Rapid and efficient cell-to-cell transmission of human immunodeficiency virus*
693 *infection from monocyte-derived macrophages to peripheral blood lymphocytes*. *Virology*,
694 1999. **265**(2): p. 319-329.
- 695 92. Gousset, K., et al., *Real-time visualization of HIV-1 GAG trafficking in infected macrophages*.
696 *PLoS Pathog*, 2008. **4**(3): p. e1000015.
- 697 93. Dupont, M. and Q.J. Sattentau, *Macrophage cell-cell interactions promoting HIV-1 infection*.
698 *Viruses*, 2020. **12**(5): p. 492.
- 699 94. Lee, B., et al., *Quantification of CD4, CCR5, and CXCR4 levels on lymphocyte subsets, dendritic*
700 *cells, and differentially conditioned monocyte-derived macrophages*. *Proceedings of the*
701 *National Academy of Sciences*, 1999. **96**(9): p. 5215-5220.
- 702 95. Chen, B.K., R.T. Gandhi, and D. Baltimore, *CD4 down-modulation during infection of human T*
703 *cells with human immunodeficiency virus type 1 involves independent activities of vpu, env,*
704 *and nef*. *Journal of virology*, 1996. **70**(9): p. 6044-6053.
- 705 96. Wilke, C.O. and I.S. Novella, *Phenotypic mixing and hiding may contribute to memory in viral*
706 *quasispecies*. *BMC microbiology*, 2003. **3**(1): p. 11.
- 707 97. Jackson, L., et al., *Complementation can maintain a quasispecies of drug sensitive and*
708 *resistant HIV*. *bioRxiv*, 2020.
- 709 98. Chen, J., et al., *Mechanisms of nonrandom human immunodeficiency virus type 1 infection*
710 *and double infection: preference in virus entry is important but is not the sole factor*. *Journal*
711 *of virology*, 2005. **79**(7): p. 4140-4149.
- 712 99. Dang, Q., et al., *Nonrandom HIV-1 infection and double infection via direct and cell-mediated*
713 *pathways*. *Proceedings of the National Academy of Sciences of the United States of America*,
714 2004. **101**(2): p. 632-637.
- 715 100. Law, K.M., et al., *In vivo HIV-1 cell-to-cell transmission promotes multicopy micro-*
716 *compartmentalized infection*. *Cell reports*, 2016. **15**(12): p. 2771-2783.
- 717 101. Jung, A., et al., *Recombination: Multiply infected spleen cells in HIV patients*. *Nature*, 2002.
718 **418**(6894): p. 144-144.
- 719 102. Meyerhans, A., et al., *The non-clonal and transitory nature of HIV in vivo*. *Swiss medical*
720 *weekly*, 2003. **133**(33/34): p. 451-454.
- 721 103. Gratton, S., et al., *Highly restricted spread of HIV-1 and multiply infected cells within splenic*
722 *germinal centers*. *Proceedings of the National Academy of Sciences*, 2000. **97**(26): p. 14566-
723 14571.
- 724 104. Dixit, N.M. and A.S. Perelson, *HIV dynamics with multiple infections of target cells*.
725 *Proceedings of the National Academy of Sciences of the United States of America*, 2005.
726 **102**(23): p. 8198-8203.
- 727 105. Ito, Y., et al., *Number of infection events per cell during HIV-1 cell-free infection*. *Scientific*
728 *reports*, 2017. **7**(1): p. 1-11.
- 729 106. Josefsson, L., et al., *Majority of CD4+ T cells from peripheral blood of HIV-1-infected*
730 *individuals contain only one HIV DNA molecule*. *Proceedings of the National Academy of*
731 *Sciences*, 2011. **108**(27): p. 11199-11204.
- 732 107. Josefsson, L., et al., *Single cell analysis of lymph node tissue from HIV-1 infected patients*
733 *reveals that the majority of CD4+ T-cells contain one HIV-1 DNA molecule*. *PLoS pathogens*,
734 2013. **9**(6): p. e1003432.
- 735 108. Descours, B., et al., *CD32a is a marker of a CD4 T-cell HIV reservoir harbouring replication-*
competent proviruses. *Nature*, 2017. **543**(7646): p. 564-567.

- 737 109. Doitsh, G., et al., *Pyroptosis drives CD4 T-cell depletion in HIV-1 infection*. *Nature*, 2014.
738 **505**(7484): p. 509.
- 739 110. Neher, R.A. and T. Leitner, *Recombination rate and selection strength in HIV intra-patient*
740 *evolution*. *PLoS Comput Biol*, 2010. **6**(1): p. e1000660.
- 741 111. Sanchez, J.L., et al., *Lymphoid fibrosis occurs in long-term nonprogressors and persists with*
742 *antiretroviral therapy but may be reversible with curative interventions*. *The Journal of*
743 *infectious diseases*, 2014. **211**(7): p. 1068-1075.
- 744 112. Brenchley, J.M., et al., *CD4+ T cell depletion during all stages of HIV disease occurs*
745 *predominantly in the gastrointestinal tract*. *Journal of Experimental Medicine*, 2004. **200**(6):
746 p. 749-759.
- 747 113. Mattapallil, J.J., et al., *Massive infection and loss of memory CD4+ T cells in multiple tissues*
748 *during acute SIV infection*. *Nature*, 2005. **434**(7037): p. 1093-1097.
- 749 114. Finkel, T., et al., *Apoptosis occurs predominantly in bystander cells and not in productively*
750 *infected cells of HIV-and SIV-infected lymph nodes*. *Nature medicine*, 1995. **1**(2): p. 129-134.
- 751 115. Rocheleau, G., et al., *Longitudinal trends of HIV drug resistance in a large Canadian cohort,*
752 *1996–2016*. *Clinical Microbiology and Infection*, 2018. **24**(2): p. 185-191.
- 753 116. Gupta, R.K., et al., *Global trends in antiretroviral resistance in treatment-naive individuals*
754 *with HIV after rollout of antiretroviral treatment in resource-limited settings: a global*
755 *collaborative study and meta-regression analysis*. *The Lancet*, 2012. **380**(9849): p. 1250-
756 1258.
- 757 117. WHO, *HIV Drug Resistance Report 2019*. 2019.
- 758 118. Pennings, P.S., *Standing genetic variation and the evolution of drug resistance in HIV*. *PLoS*
759 *Comput Biol*, 2012. **8**(6): p. e1002527.
- 760 119. Sampah, M.E.S., et al., *Dose–response curve slope is a missing dimension in the analysis of*
761 *HIV-1 drug resistance*. *Proceedings of the National Academy of Sciences*, 2011. **108**(18): p.
762 7613-7618.
- 763 120. Rosenbloom, D.I., et al., *Antiretroviral dynamics determines HIV evolution and predicts*
764 *therapy outcome*. *Nature medicine*, 2012. **18**(9): p. 1378-1385.
- 765 121. Pennings, P.S., *HIV drug resistance: problems and perspectives*. *Infectious disease reports*,
766 2013. **5**(Suppl 1).
- 767 122. Feder, A., K. Harper, and P.S. Pennings, *Challenging conventional wisdom on the evolution of*
768 *resistance to multi-drug HIV treatment: Lessons from data and modeling*. *bioRxiv*, 2019: p.
769 807560.
- 770 123. Vrouenraets, S.M., et al., *Efavirenz: a review*. *Expert opinion on pharmacotherapy*, 2007.
771 **8**(6): p. 851-871.
- 772 124. Ribaudou, H.J., et al., *Pharmacogenetics of plasma efavirenz exposure after treatment*
773 *discontinuation: an Adult AIDS Clinical Trials Group Study*. *Clinical infectious diseases*, 2006.
774 **42**(3): p. 401-407.
- 775 125. Taylor, S., et al., *Stopping antiretroviral therapy*. *Aids*, 2007. **21**(13): p. 1673-1682.
- 776 126. Sadiq, S.T., et al., *Efavirenz detectable in plasma 8 weeks after stopping therapy and*
777 *subsequent development of non-nucleoside reverse transcriptase inhibitor-associated*
778 *resistance*. *Aids*, 2005. **19**(15): p. 1716-1717.
- 779 127. Lustig, G., et al., *The CNS in the face of ART contains T cell origin HIV which can lead to drug*
780 *resistance*. *bioRxiv*, 2019: p. 588426.
- 781 128. Best, B., et al. *Efavirenz and emtricitabine concentrations consistently exceed wild-type IC50*
782 *in cerebrospinal fluid: CHARTER findings*. in *16th Conference on Retroviruses and*
783 *Opportunistic Infections*. 2009.
- 784 129. Calcagno, A., et al., *Tenofovir and emtricitabine cerebrospinal fluid-to-plasma ratios correlate*
785 *to the extent of blood-brainbarrier damage*. *Aids*, 2011. **25**(11): p. 1437-1439.

- 786 130. Mukerji, S.S., et al., *Temporal patterns and drug resistance in CSF viral escape among ART-*
787 *experienced HIV-1 infected adults*. Journal of acquired immune deficiency syndromes (1999),
788 2017. **75**(2): p. 246.
- 789 131. Dravid, A.N., et al., *Discordant CSF/plasma HIV-1 RNA in individuals on virologically*
790 *suppressive antiretroviral therapy in Western India*. Medicine, 2018. **97**(8).
- 791 132. Giri, M.S., et al., *Microarray data on gene modulation by HIV-1 in immune cells: 2000–2006*.
792 Journal of leukocyte biology, 2006. **80**(5): p. 1031-1043.
- 793 133. Mehla, R. and V. Ayyavoo, *Gene array studies in HIV-1 infection*. Current HIV/AIDS Reports,
794 2012. **9**(1): p. 34-43.
- 795 134. Vigneault, F., et al., *Transcriptional profiling of CD4 T cells identifies distinct subgroups of*
796 *HIV-1 elite controllers*. Journal of virology, 2011. **85**(6): p. 3015-3019.
- 797 135. Olvera-García, G., et al., *A transcriptome-based model of central memory CD4 T cell death in*
798 *HIV infection*. BMC genomics, 2016. **17**(1): p. 1-14.
- 799 136. Chun, T.-W., et al., *Gene expression and viral production in latently infected, resting CD4+ T*
800 *cells in viremic versus aviremic HIV-infected individuals*. Proceedings of the National
801 Academy of Sciences, 2003. **100**(4): p. 1908-1913.
- 802 137. Tenner-Racz, K., et al., *The unenlarged lymph nodes of HIV-1–infected, asymptomatic*
803 *patients with high CD4 T cell counts are sites for virus replication and CD4 T cell proliferation.*
804 *The impact of highly active antiretroviral therapy*. The Journal of experimental medicine,
805 1998. **187**(6): p. 949-959.
- 806 138. Deleage, C., et al., *Defining HIV and SIV reservoirs in lymphoid tissues*. Pathogens &
807 immunity, 2016. **1**(1): p. 68.
- 808 139. Gropelli, E., S. Starling, and C. Jolly, *Contact-induced mitochondrial*. 2015.

809

810

811

812

813

814

815

816

CHAPTER 2:

Incomplete inhibition of HIV infection results in more HIV infected lymph node cells by reducing cell death

In this chapter I demonstrate, that HIV infection by infection modes cell-free and cell-to-cell spread results in different patterns of survival of infected cells at intermediate drug strengths. The observed patterns correlate with the number of infections per cell, with many HIV copies per cell correlating with fewer live infected cells and fewer HIV copies per cell resulting in a higher number of live infected cells likely due to the reduction of cytotoxicity. My contributions to this work are as follows: the development of an assay for detection of individual infections in single cells, using the developed assay to determine the number of infections per cell in *in vitro* infected lymph node cells, validation of this assay in the ACH-2 cell line, sub-cloning of the ACH-2 cell line, curation of data into figures and writing of manuscript.

Incomplete inhibition of HIV infection results in more HIV infected lymph node cells by reducing cell death

Laurelle Jackson^{1,2†}, Jessica Hunter^{1,2†}, Sandile Cele¹,
Isabella Markham Ferreira^{1,2}, Andrew C Young^{1,3}, Farina Karim¹,
Rajhmun Madansein^{4,5}, Kaylesh J Dullabh⁴, Chih-Yuan Chen⁴, Noel J Buckels⁴,
Yashica Ganga¹, Khadija Khan¹, Mikael Boule¹, Gila Lustig¹, Richard A Neher^{6,7},
Alex Sigal^{1,2,8*}

¹Africa Health Research Institute, Durban, South Africa; ²School of Laboratory Medicine and Medical Sciences, University of KwaZulu-Natal, Durban, South Africa; ³Department of Neurology, Massachusetts General Hospital and Harvard Medical School, Boston, United States; ⁴Department of Cardiothoracic Surgery, University of KwaZulu-Natal, Durban, South Africa; ⁵Centre for the AIDS Programme of Research in South Africa, Durban, South Africa; ⁶Biozentrum, University of Basel, Basel, Switzerland; ⁷SIB Swiss Institute of Bioinformatics, Basel, Switzerland; ⁸Max Planck Institute for Infection Biology, Berlin, Germany

Abstract HIV has been reported to be cytotoxic in vitro and in lymph node infection models. Using a computational approach, we found that partial inhibition of transmissions of multiple virions per cell could lead to increased numbers of live infected cells. If the number of viral DNA copies remains above one after inhibition, then eliminating the surplus viral copies reduces cell death. Using a cell line, we observed increased numbers of live infected cells when infection was partially inhibited with the antiretroviral efavirenz or neutralizing antibody. We then used efavirenz at concentrations reported in lymph nodes to inhibit lymph node infection by partially resistant HIV mutants. We observed more live infected lymph node cells, but with fewer HIV DNA copies per cell, relative to no drug. Hence, counterintuitively, limited attenuation of HIV transmission per cell may increase live infected cell numbers in environments where the force of infection is high.

DOI: <https://doi.org/10.7554/eLife.30134.001>

*For correspondence:

alex.sigal@k-rith.org

†These authors contributed equally to this work

Competing interest: See page 17

Funding: See page 17

Received: 18 July 2017

Accepted: 08 March 2018

Published: 20 March 2018

Reviewing editor: Wenying Shou, Fred Hutchinson Cancer Research Center, United States

© Copyright Jackson et al. This article is distributed under the terms of the [Creative Commons Attribution License](https://creativecommons.org/licenses/by/4.0/), which permits unrestricted use and redistribution provided that the original author and source are credited.

Introduction

HIV infection is known to result in extensive T cell depletion in lymph node environments (Sanchez et al., 2015), where infection is most robust (Brenchley et al., 2004; Doitsh et al., 2010; Doitsh et al., 2014; Finkel et al., 1995; Galloway et al., 2015; Mattapallil et al., 2005). Depletion of HIV infectable target cells, in addition to onset of immune control, is thought to account for the decreased replication ratio of HIV from an initial peak in early infection (Bonhoeffer et al., 1997; Nowak and May, 2000; Perelson, 2002; Phillips, 1996; Quiñones-Mateu and Arts, 2006; Ribeiro et al., 2010; Wodarz and Levy, 2007). This is consistent with observations that individuals are most infectious in the initial, acute stage of infection, where the target cell population is relatively intact and produces high viral loads (Hollingsworth et al., 2008; Wawer et al., 2005).

T-cell death occurs by several mechanisms, which are either directly or indirectly mediated by HIV infection. Accumulation of incompletely reverse transcribed HIV transcripts is sensed by interferon- γ -inducible protein 16 (Monroe et al., 2014) and leads to pyroptotic death of incompletely infected

eLife digest The HIV virus infects cells of the immune system. Once inside, it hijacks the cellular molecular machineries to make more copies of itself, which are then transmitted to new host cells. HIV eventually kills most cells it infects, either in the steps leading to the infection of the cell, or after the cell is already producing virus. HIV can spread between cells in two ways, known as cell-free or cell-to-cell. In the first, individual viruses are released from infected cells and move randomly through the body in the hope of finding new cells to infect. In the second, infected cells interact directly with uninfected cells. The second method is often much more successful at infecting new cells since they are exposed to multiple virus particles.

HIV infections can be controlled by using combinations of antiretroviral drugs, such as efavirenz, to prevent the virus from making more of itself. With a high enough dose, the drugs can in theory completely stop HIV infections, unless the virus becomes resistant to treatment. However, some patients continue to use these drugs even after the virus they are infected with develops resistance. It is not clear what effect taking ineffective, or partially effective, drugs has on how HIV progresses.

Using efavirenz, Jackson, Hunter et al. partially limited the spread of HIV between human cells grown in the laboratory. The experiments mirrored the situation where a partially resistant HIV strain spreads through the body. The results show that the success of cell-free infection is reduced as drug dose increases. Yet paradoxically, in cell-to-cell infection, the presence of drug caused more cells to become infected. This can be explained by the fact that, in cell-to-cell spread, each cell is exposed to multiple copies of the virus. The drug dose reduced the number of viral copies per cell without stopping the virus from infecting completely. The reduced number of viral copies per cell made it more likely that infected cells would survive the infection long enough to produce virus particles themselves.

Viruses that can kill cells, such as HIV, must balance the need to make more of themselves against the speed that they kill their host cell to maximize the number of infected cells. If transmission between cells is too effective and too many virus particles are delivered to the new cell, the virus may not manage to infect new hosts before killing the old ones. These findings highlight this delicate balance. They also indicate a potential issue in using drugs to treat partially resistant virus strains. Without care, these treatments could increase the number of infected cells in the body, potentially worsening the effects of living with HIV.

DOI: <https://doi.org/10.7554/eLife.30134.002>

cells by initiating a cellular defence program involving the activation of caspase 1 (Doitsh et al., 2010; Doitsh et al., 2014; Galloway et al., 2015). HIV proteins Tat and Env have also been shown to lead to cell death of infected cells through CD95-mediated apoptosis following T-cell activation (Banda et al., 1992; Westendorp et al., 1995a; Westendorp et al., 1995b, 1995). Using SIV infection, it has been shown that damage to lymph nodes due to chronic immune activation leads to an environment less conducive to T-cell survival (Zeng et al., 2012). Finally, double strand breaks in the host DNA caused by integration of the reverse transcribed virus results in cell death by the DNA-PK-mediated activation of the p53 response (Cooper et al., 2013).

The lymph node environment is conducive to HIV infection due to: (1) presence of infectable cells (Deleage et al., 2016; Embretson et al., 1993; Tenner-Racz et al., 1998); (2) proximity of cells to each other and lack of flow which should enable cell-to-cell HIV spread (Baxter et al., 2014; Dale et al., 2011; Groot et al., 2008; Gropelli et al., 2015; Gummuluru et al., 2002; Hübner et al., 2009; Jolly et al., 2004; Jolly et al., 2011; Münch et al., 2007; Sherer et al., 2007; Sourisseau et al., 2007; Sowinski et al., 2008); (3) decreased penetration of antiretroviral therapy (ART) (Fletcher et al., 2014a). Multiple infections per cell have been reported in cell-to-cell spread of HIV (Baxter et al., 2014; Boullé et al., 2016; Dang et al., 2004; Del Portillo et al., 2011; Dixit and Perelson, 2004; Duncan et al., 2013; Law et al., 2016; Reh et al., 2015; Russell et al., 2013; Sigal et al., 2011; Zhong et al., 2013). In this mode of HIV transmission, an interaction between the infected donor cell and the uninfected target results in directed transmission of large numbers of virions (Baxter et al., 2014; Gropelli et al., 2015; Hübner et al., 2009; Sowinski et al., 2008). This is in contrast to cell-free infection, where free-floating virus finds target

cells through diffusion. Both modes occur simultaneously when infected donor cells are cocultured with targets. However, the cell-to-cell route is thought to be the main cause of multiple infections per cell (Hübner et al., 2009). In the lymph nodes, several studies showed multiple infections (Gratton et al., 2000; Jung et al., 2002; Law et al., 2016) while another study did not (Josefsson et al., 2013). One explanation for the divergent results is that different cell subsets are infected to different degrees. For example, T cells were shown not to be multiply infected in the peripheral blood compartment (Josefsson et al., 2011). However, more recent work investigating markers associated with HIV latency in the face of ART found that the average number of HIV DNA copies per cell is greater than one in 3 out of 12 individuals. This occurred in the face of ART in the CD3-positive, CD32a high CD4 T-cell subset (Descours et al., 2017). In the absence of suppressive ART, it would be expected that the number of HIV DNA copies per cell would be higher.

Multiple viral integration attempts per cell may increase the probability of death. One consequence of HIV-mediated death may be that attenuation of infection may increase viral replication by increasing the number of live targets. Indeed, it has been suggested that more attenuated HIV strains result in more successful infections in terms of the ability of the virus to replicate in the infected individual (Ariën et al., 2005; Nowak and May, 2000; Payne et al., 2014; Quiñones-Mateu and Arts, 2006; Wodarz and Levy, 2007).

Here, we experimentally examined the effect of attenuating cell-to-cell spread by using HIV inhibitors. We observed that partially inhibiting infection with drug or antibody resulted in an increase in the number of live infected cells in both a cell line and in lymph node cells. This is, to our knowledge, the first experimental demonstration at the cellular level that attenuation of HIV infection can result in an increase in live infected cells under specific infection conditions.

Results

We introduce a model of infection where each donor to target transmission leads to an infection probability r and death probability q per infection attempt. In our experimental system, one infection attempt is measured as one HIV DNA copy, whether integrated or unintegrated. The probability of successful infection of a target cell given n infection attempts is $1-(1-r)^n$ (Sigal et al., 2011). We define L_n as the probability of a cell to survive infection in the face of n infection attempts. Assuming infection attempts act independently, $L_n=(1-q)^n$. The probability of a cell to be infected and not die after it has been exposed to n infection attempts is therefore:

$$P_n = (1 - (1 - r)^n)(1 - q)^n \quad (1)$$

This model makes several simplifying assumptions: (1) all infection attempts have equal probabilities to infect targets. (2) The probability for a cell to die from each transmission is equal between transmissions. (3) Infection attempts act independently, and productive infection and death are independent events. In this model, r and q capture the probabilities for a cell to be infected or die post-reverse transcription. For example, mutations which reduce viral fitness by decreasing the probability of HIV to integrate would reduce r , while mutations which reduce the probability of successful reverse transcription would reduce q .

If the number of infection attempts n is Poisson distributed with mean λ , the probability for a cell to be infected is $1-e^{-\lambda r}$ and the probability of a cell to live is $L_n = e^{-q\lambda}$ (see **Supplementary file 1** for parameters and definitions). As derived in Appendix 1, the probability that a cell is productively infected will be:

$$P_\lambda = e^{-\lambda q} \left(1 - e^{-\lambda r(1-q)} \right) \quad (2)$$

Since antiretroviral drugs lead to a reduction in the number of infection attempts by, for example, decreasing the probability of reverse transcription in the case of reverse transcriptase inhibitors, we introduced a drug strength value d , where $d = 1$ in the absence of drug and $d > 1$ in the presence of drug. In the presence of drug, λ is decreased to λ/d . The drug therefore tunes λ , and if the antiretroviral regimen is fully suppressive, λ/d is expected to be below what is required for ongoing replication. The probability of a cell to be infected and live given drug strength d is therefore:

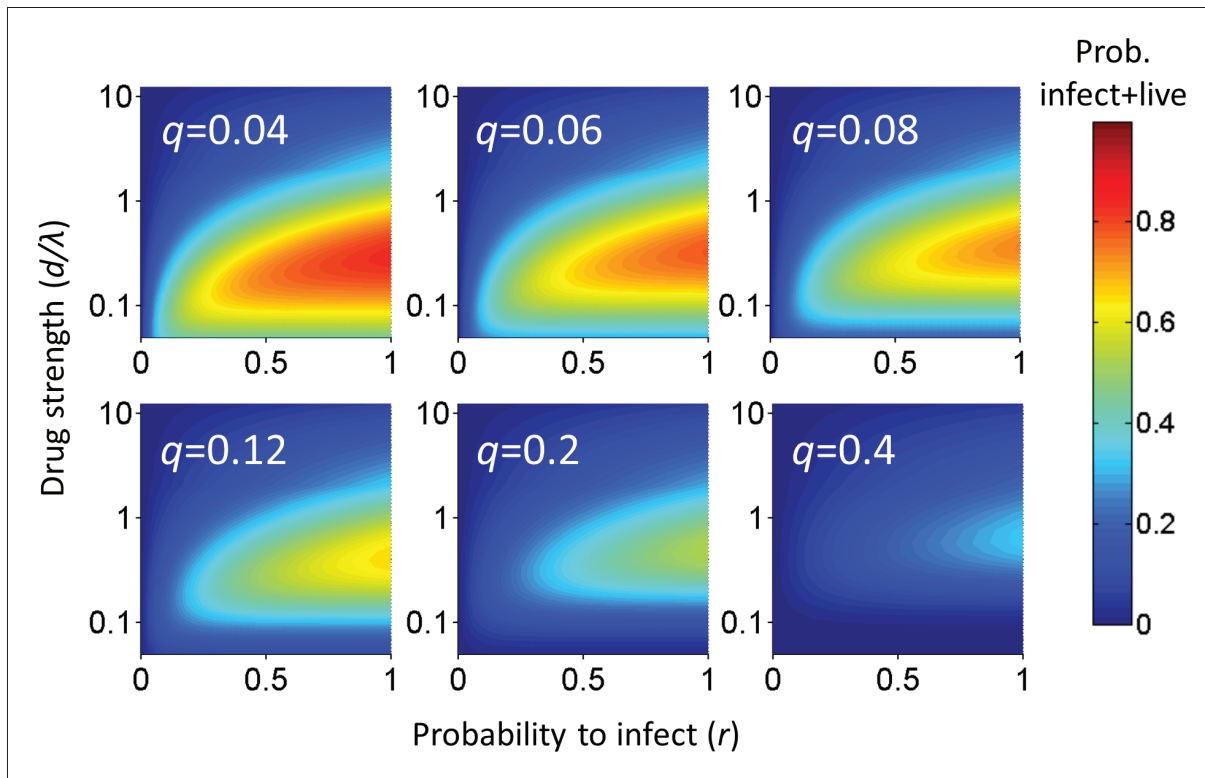


Figure 1. Probability for a cell to be infected and live as a function of inhibitor. Probability for a cell to be infected and live was calculated for 20 infection attempts (λ) and represented as a heat map. Drug strength (d/λ) is on the y-axis, and the probability per infection attempt to infect (r) is on the x-axis. Each plot is the calculation for one value of the probability per infection attempt to die (q) denoted in white in the top left corner. DOI: <https://doi.org/10.7554/eLife.30134.003>

$$P_{\lambda/d} = e^{-\lambda q/d} \left(1 - e^{-\lambda r(1-q)/d} \right) \quad (3)$$

Analysis of the probability of a cell to survive and be infected as a function of r and q shows that at each drug strength d/λ , P_{λ} increases as the probability of infection r increases (Figure 1). Hence, the value of r strongly influences the amplitude of P_{λ} . How P_{λ} behaves when drug strength d/λ increases depends on the parameter values of r and q . A subset of parameter values results in a peak in the number of infected cells at intermediate d/λ , decreasing as drug strength increases further (Figure 1). We refer to such a peak in infected numbers as an infection optimum. As q increases, the cost of multiple infections per cell increases, and the infection optimum shifts to higher d/λ values. A fall from the infection optimum at decreasing d/λ is driven by increasing cell death as a result of increasing infection attempts per cell. This slope is therefore shallower, and peaks broader, at low q values (Figure 1).

Our model assumes that cellular infection and death due to an HIV infection attempt are independent processes. This is based on observations that support a role for cell death as a cellular defence mechanism which may occur before productive infection, such as programmed cell death triggered by HIV integration induced DNA damage (Cooper et al., 2013). An alternative model is that HIV-mediated cell death depends on productive infection. This would be consistent with cell death due to, for example, expression of viral proteins (Westendorp et al., 1995b, 1995). Since the concentration of viral proteins may also scale with the number of infections per cell, we derived the mathematical model for such a process in the supplementary mathematical analysis. The models are equivalent, showing that independence of cell death and infection is not a necessary condition for an infection optimum to occur in the presence of inhibitor.

Given that an infection optimum is dependent on parameter values, we next examined whether these parameter values occur experimentally in HIV infection. We therefore first tested for an infection optimum in the RevCEM cell line engineered to express GFP upon HIV Rev protein expression (Wu *et al.*, 2007). We subcloned the cell line to maximize the frequency of GFP-positive cells upon infection (Boullé *et al.*, 2016). We needed to detect the number of infection attempts per cell λ . To estimate this, we used PCR to detect the number of reverse transcribed copies of viral DNA in the cell by splitting each individual infected cell over multiple wells. We then detected the number of wells with HIV DNA by PCR amplification of the reverse transcriptase gene. Hence, the number of positive wells indicated the minimum number of viral DNA copies per cell, since more than one copy can be contained within the same well (Josefsson *et al.*, 2011; Josefsson *et al.*, 2013). We first measured the number of viral DNA copies in ACH-2 cells, reported to contain a single inactive HIV integration per genome (Chun *et al.*, 1997; O'Doherty *et al.*, 2002). We sorted a total of 166 ACH-2 cells at one cell per well into lysis buffer and subdivided single-cell lysates into four wells (Figure 2—figure supplement 1A). About one quarter of cells showed a PCR product of the expected size. Cells with more than one HIV copy per cell were very rare and may reflect either errors in cell sorting or dividing cells (Figure 2—figure supplement 1B). Similar frequencies were obtained when the ACH-2 cell line was subcloned or split over 10 wells (Figure 2—figure supplement 1C). Given that each ACH-2 cell contains one HIV DNA copy, the frequency of detection indicated our detection efficiency per HIV DNA copy.

To investigate the effect of multiple infection attempts per cell, we used coculture infection, where infected (donor) cells are co-incubated with uninfected (target) cells and lead to cell-to-cell spread. We used approximately 2% infected donor cells as our input, and detected the number of HIV DNA copies per cell by flow cytometric sorting of individual GFP-positive cells followed by splitting each cell lysate over 10 wells. Wells were then amplified by PCR and visualized on an agarose gel (Figure 2A). We assayed 60 cells and obtained a wide distribution of viral DNA copies per cell, which ranged from 0 to 9 copies (Figure 2B). The range of HIV DNA copies per cell fit a Poisson distribution with two means better than either a single mean Gaussian or Poisson distribution. However, the fit of the two mean Poisson distribution did not show two obvious peaks, and instead seemed to fit the data better due to the addition of fit parameters (Figure 2—figure supplement 2). Hence we cannot conclude that the distribution is bimodal. We also detected the HIV copy number in 30 GFP-positive cells infected by cell-free HIV. HIV in cell-free form was obtained by filtering supernatant from HIV producing cells to exclude cells or cell fragments, then infecting target cells with the filtered virus. Infection with this virus is defined here as cell-free infection. In this case, we detected either zero or one HIV copy per cell (Figure 2B inset). The frequency of single HIV DNA copies was 0.23, identical to the measured result in the ACH-2 cell line. We computationally corrected the detected number of DNA copies in coculture infection for the sensitivity of our PCR reaction as determined by the ACH-2 results (Materials and methods). On average we obtained 15 ± 3 copies per cell after correction.

To tune λ , we added the HIV reverse transcriptase inhibitor efavirenz (EFV) to infections. To calculate d , we used cell-free infection (Figure 2C, see Figure 2—figure supplement 3 for logarithmic y-axis plot), which as verified above, results in single HIV copies per cell. For cell-free infection, we approximate $d = 1/Tx$, where Tx is defined as the number of infected cells with drug divided by the number of infected cells without drug with single infection attempts (see Materials and methods and (Sigal *et al.*, 2011)). This is equivalent to $1-\varepsilon$ in a commonly used model describing the effect of inhibitors on infection. In this model, ε is drug effectiveness, with the 50% inhibitory drug concentration (IC_{50}) and the Hill coefficient for drug action as parameter values (Canini and Perelson, 2014; Shen *et al.*, 2008). We fit the observed response of infection to EFV using this approach to estimate d across a range of EFV concentrations. Fit of the model to the cell-free data using wild type, EFV-sensitive HIV showed a monotonic decrease with $IC_{50} = 2.9$ nM and Hill coefficient of 2.1 (Figure 2C, black line).

We next dialed in EFV to tune λ/d in coculture infection. To obtain the number of infected target cells, and specifically exclude donor cells or donor-target cell fusions, target cells were marked by the expression of mCherry. Donor cells were stained with the vital stain Cell Trace Far Red (CTFR). The concentration of live infected cells was determined after 2 days in coculture with infected donors. Live infected cells were identified based on the absence of cell death indicator dye DAPI fluorescence, and presence of GFP. The input of infected donor cells was excluded from the count

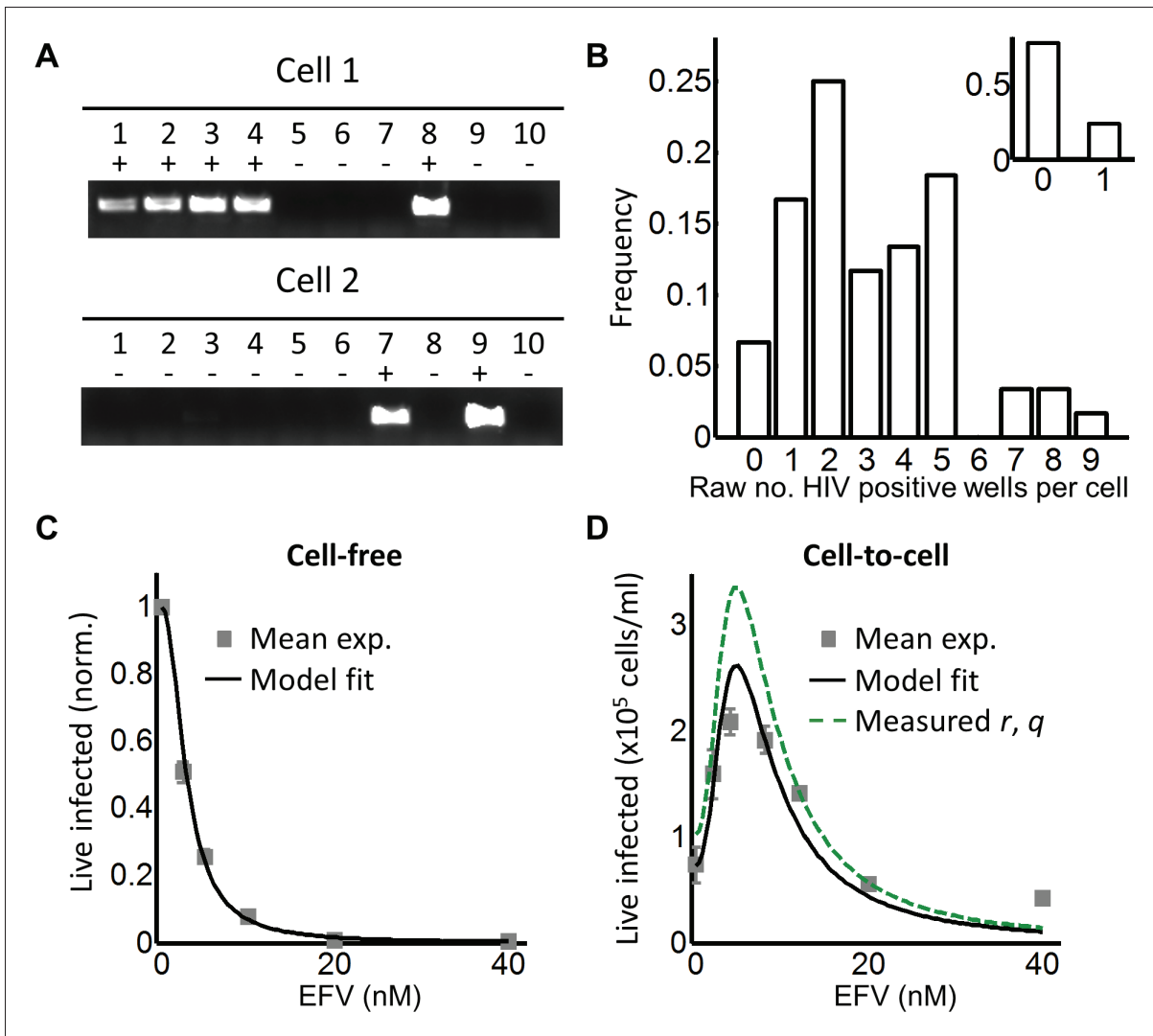


Figure 2. Partial inhibition increases the number of live infected cells. (A) To quantify HIV DNA copy number per cell, GFP-positive cells were sorted into individual wells and lysed. Each lysate was subdivided into 10 wells and PCR performed to detect HIV DNA, with the sum of positive wells being the raw HIV copy number for that cell. (B) Histogram of raw HIV DNA copies per cell in coculture infection ($n = 60$ cells, four independent experiments). Inset shows raw HIV DNA copies per cell in cell-free infection ($n = 30$, two independent experiments) (C) Number of live infected cells normalized by maximum number of live infected cells in cell-free infection with EFV. Black line is best-fit for EFV suppression of cell-free infection ($IC_{50} = 2.9$ nM, $h = 2.1$). Means and standard errors for three independent experiments. (D) Number of live infected cells/ml 2 days post-infection resulting from coculture infection of 10^6 cells/ml in the presence of EFV. Means and standard errors for three independent experiments. Black line is best-fit of **Equation (3)** with $r = 0.22$ and $q = 0.17$. Dashed green line is the result of **Equation (3)** with experimentally measured $r = 0.28$, $q = 0.15$.

DOI: <https://doi.org/10.7554/eLife.30134.004>

The following figure supplements are available for figure 2:

Figure supplement 1. Detected integrations in ACH-2 cells.

DOI: <https://doi.org/10.7554/eLife.30134.005>

Figure supplement 2. Fitting of different distributions to the frequency of HIV DNA copies per cell.

DOI: <https://doi.org/10.7554/eLife.30134.006>

Figure supplement 3. The number of live infected cells in cell-free infection with wild-type HIV.

DOI: <https://doi.org/10.7554/eLife.30134.007>

Figure supplement 4. Gating strategy for coculture infection with wild type HIV.

DOI: <https://doi.org/10.7554/eLife.30134.008>

Figure supplement 5. Experimental measurement of r and q .

DOI: <https://doi.org/10.7554/eLife.30134.009>

Figure 2 continued on next page

Figure 2 continued

Figure supplement 6. Time-lapse microscopy of HIV infection in the absence and presence of EFV.

DOI: <https://doi.org/10.7554/eLife.30134.010>

of infected cells based on the absence of mCherry fluorescence. Donor-target cell fusions were excluded by excluding CTFR-positive cells (see **Figure 2—figure supplement 4** for gating strategy).

While the percent of infected cells was reduced with drug, the concentration of live infected cells increased (**Figure 2—figure supplement 4**). We observed a peak in the number of live infected target cells at 4 nM EFV (**Figure 2D**). We then fit the number of live infected cells using **Equation (3)**, where P_λ was multiplied by the input number of target cells per ml (10^6 cells/ml) to obtain the predicted number of live infected cells per ml of culture. This was done to constrain r in the model, which strongly determines the amplitude of $P_{\lambda/d}$ as described above. **Equation (3)** best fit the behaviour of infection when $r = 0.22$ and $q = 0.17$, resulting in a peak at 4.8 nM EFV (**Figure 2D**, black line). Hence an infection optimum is present in the cell line infection system.

In order to determine whether the fitted r and q values were within a reasonable range, we measured these values experimentally. To measure r , we infected with cell-free HIV to avoid the broad distribution of HIV copy numbers observed in cell-to-cell spread, and determined the fraction of live infected cells P_λ (**Figure 2—figure supplement 5A**). We then determined the mean number of HIV copies per cell λ for the same set of experiments corrected by the efficiency of detection (**Figure 2—figure supplement 5B**). The parameter r was calculated as $-\ln(1-P_\lambda)/\lambda$ (**Supplementary file 2**). To measure q , we blocked cell division using serum starvation to measure differences in cell concentration due to cell death only, and not due to proliferation of uninfected cells (**Figure 2—figure supplement 5C**). We then infected with cell-free HIV and measured L_λ , defined as the fraction of live cells remaining upon infection with λ HIV DNA copies relative to infection blocked with EFV (see below). To specifically detect the decrease in live cells as a result of events downstream of reverse transcription, we compared infected cells to cells exposed to the same virus concentration but treated with 40 nM EFV, a drug concentration where infection by cell-free virus is negligible (**Figure 2—figure supplement 3**). q was then calculated as $-\ln(L_\lambda)/\lambda$, where L_λ was the probability of a cell to live given transmission with λ copies (**Supplementary file 2**). Measured r and q values were 0.28 ± 0.08 and 0.15 ± 0.07 (mean \pm standard deviation), respectively. The solution to **Equation (3)** using these values showed similar behavior to the solution with the fitted values for wild-type HIV infection, indicating that the fitted values gave a reasonable approximation of the behavior of the system (**Figure 2D**, dashed green line).

In order to investigate the dynamics of cell depletion due to cell-to-cell HIV spread and its modulation by the addition of an inhibitor, we performed time-lapse microscopy over a two day infection window. While infection parameters were different due to the constraints of visualizing cells (Materials and methods), the general trend from the data was deterioration in the number of live cells in the time-lapse culture starting at 1 day post-infection when no drug was added. The deterioration in live cell numbers was averted by the addition of EFV (**Figure 2—figure supplement 6**).

We next investigated whether an infection optimum occurs with EFV-resistant HIV. To derive the resistant mutant, we cultured wild-type HIV in our reporter cell line in the presence of EFV. We obtained the L100I partially resistant mutant. We then replaced the reverse transcriptase of the wild-type molecular clone with the mutant reverse transcriptase gene (Materials and methods). We derived d_{mut} for the L100I mutant using cell-free mutant infection (**Figure 3A**, see **Figure 3—figure supplement 1** for logarithmic y-axis plot). The L100I mutant was found to have an $IC_{50} = 29$ nM EFV and a Hill coefficient of 2.0 (**Figure 3A**, black line).

We next performed coculture infection (see **Figure 3—figure supplement 2** for gating strategy). Similarly to wild-type HIV coculture infection, there was a peak in the number of live infected target cells for the L100I mutant infection. However, the peak in live infected cells was shifted to 40 nM EFV (**Figure 3B**). Fits were obtained to **Equation (3)** using d_{mut} values and λ measured for wild-type infection. The fits recapitulated the experimental results when $r = 0.29$ and $q = 0.13$, with a fitted peak at 45 nM EFV (**Figure 3B**, black line). The solution to **Equation (3)** using the measured values for r and q showed a similar pattern to that obtained with the fitted values (**Figure 3B**, dashed green line). We note that both wild type and mutant coculture infection has data points above the fit line at the highest drug concentrations. This may be a limitation of our model at drug values much higher

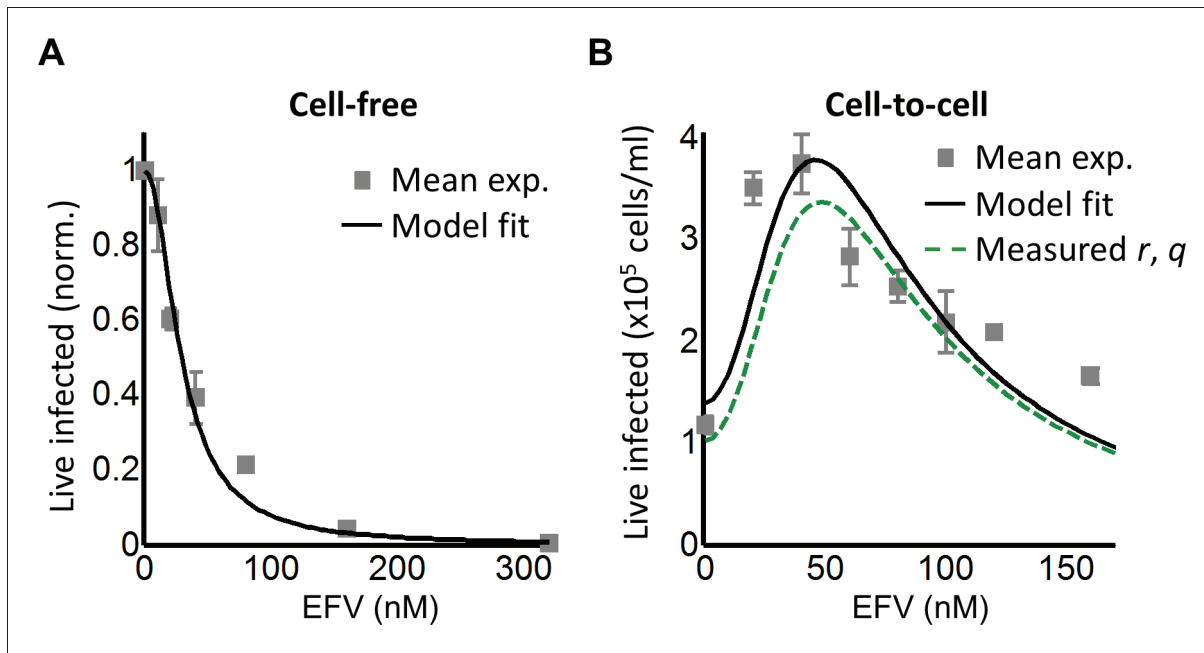


Figure 3. Partial inhibition of the EFV-resistant L100I mutant shifts the peak of live infected cells to higher EFV concentrations. (A) The number of live infected cells normalized by the maximum number of live infected cells in cell-free infection as a function of EFV for the L100I mutant. Black line is best-fit for EFV suppression of cell-free infection ($IC_{50} = 29$ nM, $h = 2.0$). Shown are means and standard errors for three independent experiments. (B) Number of live infected cells/ml 2 days post-infection resulting from coculture infection of 10^6 cells/ml in the presence of EFV. Means and standard errors for three independent experiments. Black line is best-fit of **Equation (3)** with $r = 0.29$ and $q = 0.13$. Dashed green line is the result of **Equation (3)** with the experimentally measured $r = 0.28$ and $q = 0.15$ for wild-type HIV infection.

DOI: <https://doi.org/10.7554/eLife.30134.011>

The following figure supplements are available for figure 3:

Figure supplement 1. The number of live infected cells in cell-free infection with the L100I mutant.

DOI: <https://doi.org/10.7554/eLife.30134.012>

Figure supplement 2. Gating strategy for coculture infection with mutant HIV.

DOI: <https://doi.org/10.7554/eLife.30134.013>

than observed at the infection optimum. In this range of drug values, our model predicts a more pronounced decline in the number of infected cells than is observed experimentally.

In order to examine whether a peak in live infected targets can be obtained with an unrelated inhibitor, we used the HIV neutralizing antibody b12. This antibody is effective against cell-to-cell spread of HIV (Baxter et al., 2014; Reh et al., 2015). We obtained a peak in live infected cells at 5 μ g/ml b12 (Figure 4). The b12 concentration that resulted in a peak number of live infected cells was the same for wild-type virus and the L100I mutant, showing that L100I mutant fitness gain was EFV specific. In contrast, cell-free infection in the face of b12 showed a sharp and monotonic drop in live infected cells for both wild type and mutant virus (Figure 4—figure supplement 1).

While the RevCEM cell line is a useful tool to illustrate the principles governing the formation of an infection optimum, the sensitivity of such an optimum to parameter values would make its presence in primary HIV target cells speculative. We therefore investigated whether a fitness optimum occurs in primary human lymph node cells, the anatomical site which would be most likely to have a high force of infection. We derived human lymph nodes from HIV-negative individuals from indicated lung resections (Supplementary file 3), cellularized the lymph node tissue using mechanical separation, and infected the resulting lymph node cells with HIV. A fraction of the cells was infected by cell-free virus and used as infected donor cells. We added these to uninfected target cells from the same lymph node to test coculture infection, and detected the number of live infected cells 4 days post-infection with the L100I EFV-resistant mutant in the face of EFV. We detected the number of

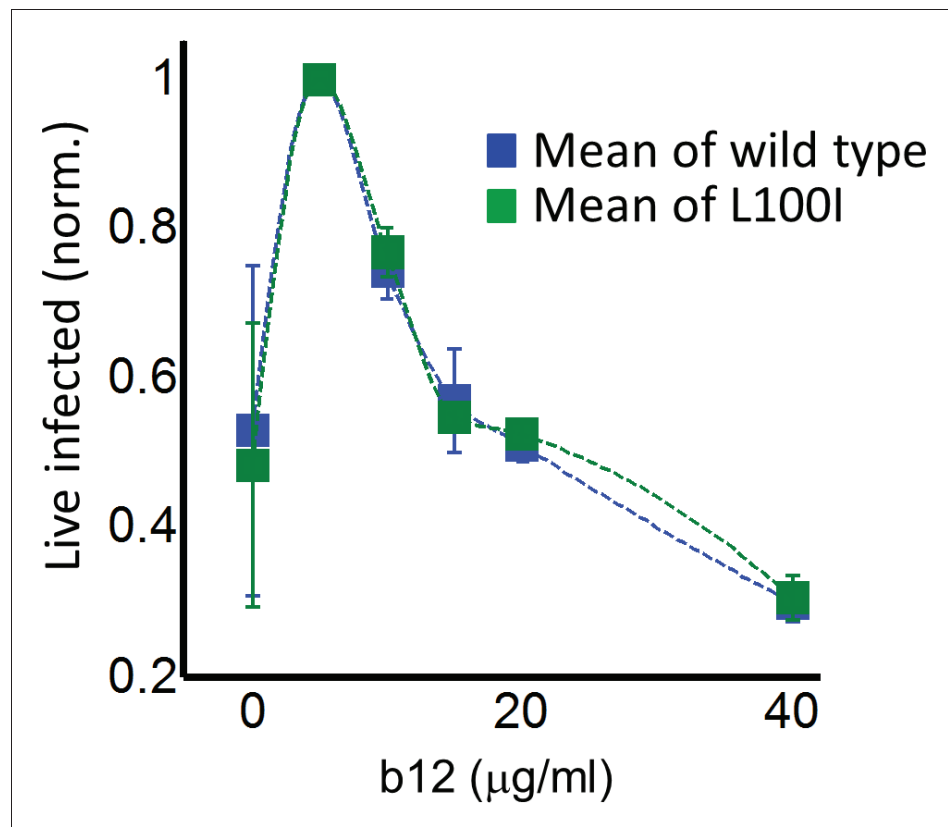


Figure 4. Partial inhibition of coculture infection with neutralizing antibody results in higher numbers of live infected cells. Shown are the numbers of live infected cells normalized by the maximum number of live infected cells in coculture infection as a function of b12 antibody concentration. Infection was by either EFV-sensitive HIV (blue) or the L100I EFV-resistant mutant (green). Dashed lines are a guide to the eye. Shown are means and standard errors for three independent experiments.

DOI: <https://doi.org/10.7554/eLife.30134.014>

The following figure supplement is available for figure 4:

Figure supplement 1. The number of live infected cells with cell-free infection in the face of neutralizing antibody b12.

DOI: <https://doi.org/10.7554/eLife.30134.015>

live infected cells by the exclusion of dead cells with the fixable death detection dye eFluor660 followed by single cell staining for HIV Gag using anti-p24 antibody (**Figure 5A**).

In each of the lymph nodes tested, we observed a peak in live infected cells at intermediate EFV concentrations. Lymph node cells from participant 205 showed a peak of live infected cells at 100 nM EFV (**Figure 5A**, first row). The infection optimum in the lymph node cells of study participant 257 was visible as a plateau between 50 and 200 nM EFV. In the presence of EFV, there was a decrease in the fraction of dead cells that was offset by a similar increase in the fraction of live infected cells for lymph nodes from all participants. There were more overall detectable cells with EFV, resulting in differences in the absolute concentrations of live infected cells being larger than the differences in the fractions of live infected cells between EFV and non-drug-treated cells (right two columns in **Figure 5A**, with absolute number of live infected cells shown in parentheses in the flow cytometry plots). This is most likely due to cells which died early becoming fragments and so being excluded from the total population in the absence of EFV. Peaks in the number of live infected cells in the face of drug may be specific to lymph node derived cells. Cell-to-cell infection of peripheral blood mononuclear cells (PBMC) with wild-type HIV showed a slight peak at a very low EFV concentration in cells from one blood donor, which was not repeated in cells from two other donors (**Figure 5—figure supplement 1**).

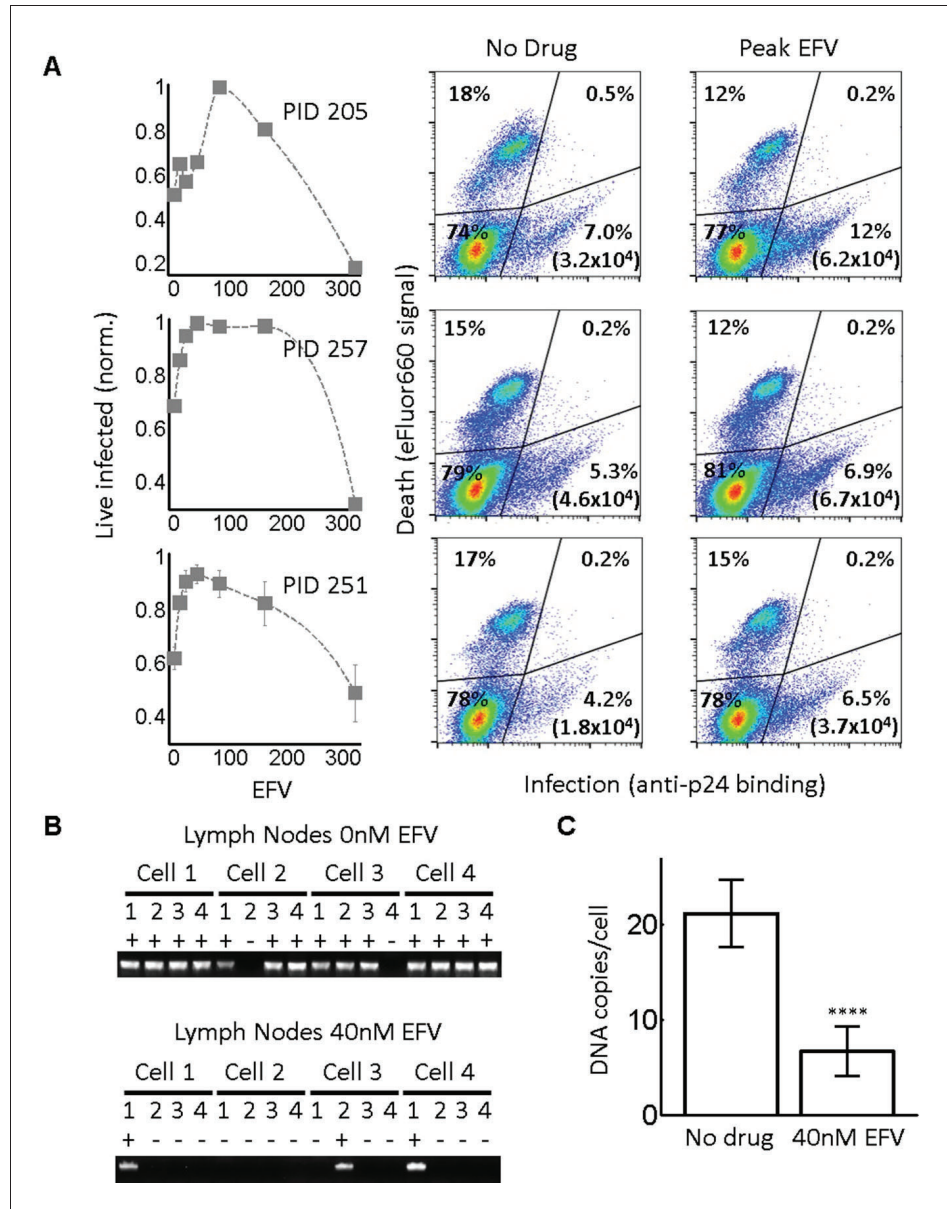


Figure 5. Infection optimum with EFV in lymph node cells. (A) Number of live infected cells as a function of EFV. Each row shows in vitro infected lymph node cells from one participant. Left column is the number of live infected cells normalized by maximum number of live infected cells in coculture infection. Middle and right columns are flow cytometry dot plots of infection without drug and at the infection optimum, with HIV p24 on x-axis and death detection by eFluor660 on y-axis. Infected live cells are bottom right. Number in brackets represents live infected cell density per ml. PID, participant identification number. For PID205 and 257, cells were sufficient for one experiment. For PID251, means and standard errors for three independent experiments are shown. Dashed lines are a guide to the eye. (B) HIV DNA copy number per cell was quantified by sorting fixed p24-positive cells from PID251 into individual wells. Cells were lysed and de-crosslinking performed. Each lysate was divided into four wells and PCR performed to detect HIV DNA. First row is representative of cells with no drug, second row is representative of 40 nM EFV. (C) Mean and standard error of the number of HIV DNA copies without drug and with 40 nM EFV after assay sensitivity correction. N = 56 cells from three independent experiments for each condition. ****p=4x10⁻⁹, two tailed t-test.

DOI: <https://doi.org/10.7554/eLife.30134.016>

The following figure supplements are available for figure 5:

Figure 5 continued on next page

Figure 5 continued

Figure supplement 1. Cell-to-cell infection of peripheral blood mononuclear cells in the presence of EFV does not lead to a discernable peak in live infected cells.

DOI: <https://doi.org/10.7554/eLife.30134.017>

Figure supplement 2. Raw HIV DNA copy numbers per lymph node cell.

DOI: <https://doi.org/10.7554/eLife.30134.018>

We used a lymph node from study participant 251, where we obtained more cells, to examine the number of HIV DNA copies per cell. Cells from this lymph node showed an infection optimum at 50 nM EFV (**Figure 5A**, third row). To detect the effect of EFV on integrations per cell, we sorted single cells based on p24-positive signal, de-crosslinked to remove the fixative (Materials and methods), then divided each cell lysate into four wells. Using fewer wells saved reagents without changing sensitivity, as demonstrated in the ACH-2 cell line (**Figure 2—figure supplement 1C**). We detected HIV DNA copies by PCR 2 days post-infection. We observed multiple DNA copies in EFV-untreated lymph node cells. The number of copies decreased with EFV (**Figure 5B**). We corrected for sensitivity of detection as quantified in ACH-2 cells (Materials and methods). The corrected numbers were 21 HIV DNA copies with no drug, and five copies in the presence of EFV at the infection optimum (**Figure 5C**, see **Figure 5—figure supplement 2** for histograms of raw HIV DNA copy numbers per cell). Hence, the decrease in the number of copies still results in sufficient copies to infect the cell.

Since L100I does not often occur in the absence of other drug resistance mutations according to the Stanford HIV Drug Resistance Database (*Rhee et al., 2003*), we repeated the experiment with the K103N mutant, a frequently observed mutation in virologic failure with a higher level of resistance to EFV relative to the L100I mutant. We used cell-free infection to obtain drug inhibition per virion at each level of EFV, which we denote d_{103} (**Figure 6A**, see **Figure 6—figure supplement 1** for logarithmic y-axis plot). The fits showed a monotonic decrease with $IC_{50} = 26.0$ nM and Hill coefficient of 1.5 (**Figure 6A**, black line). We then proceeded to use the K103N mutant in coculture infection, using cells from two different lymph nodes in different experiments (see **Figure 6—figure supplement 2** for results of individual experiments). We observed an infection optimum with EFV in lymph node cells. The peak in the number of live infected cells in the presence of drug was between 80 and 160 nM EFV (**Figure 6B**). We fit the experimental data with **Equation (3)** using d_{103} values and the number of DNA copies in the absence of drug measured for L100I infection. We did not calculate the predicted number of infected cells for $P_{\lambda/d}$ values since the lymph node is a complex environment containing different cell subsets (*Sallusto et al., 1999*) and the number of infectable target cells at the start of infection is difficult to determine. Hence, we normalized both the experimental number of live infected cells and the $P_{\lambda/d}$ values from **Equation (3)** to the maximum value in each case. The fits recapitulated the experimental results when $r = 0.91$ and $q = 0.15$, with a fitted peak at 90 nM EFV (**Figure 6B**, black line). The q value matched the measured result in the cell line, while the r value was much higher. However, the fitted r value in this case is not expected to be accurate since we were unable to constrain it with the number of infected cells relative to the starting number of target cells.

To examine if the observed peak in live cells may be due to EFV alone, we measured cell viability in lymph node cells from one of the study participants used in the above experiment as a function of EFV without infection. No clear dependence on EFV in the absence of infection was detected (**Figure 6—figure supplement 3**).

Discussion

The optimal virulence concept in ecology proposes that virulence needs to be balanced against host survival for optimal pathogen spread (*Bonhoeffer et al., 1996; Bonhoeffer and Nowak, 1994; Gandon et al., 2001; Jensen et al., 2006*). At the cellular level, this implies that the number of successfully infected cells may increase when infection virulence is reduced. The current study is, to our knowledge, the first to address this question experimentally at the level of individual cells infected with HIV.

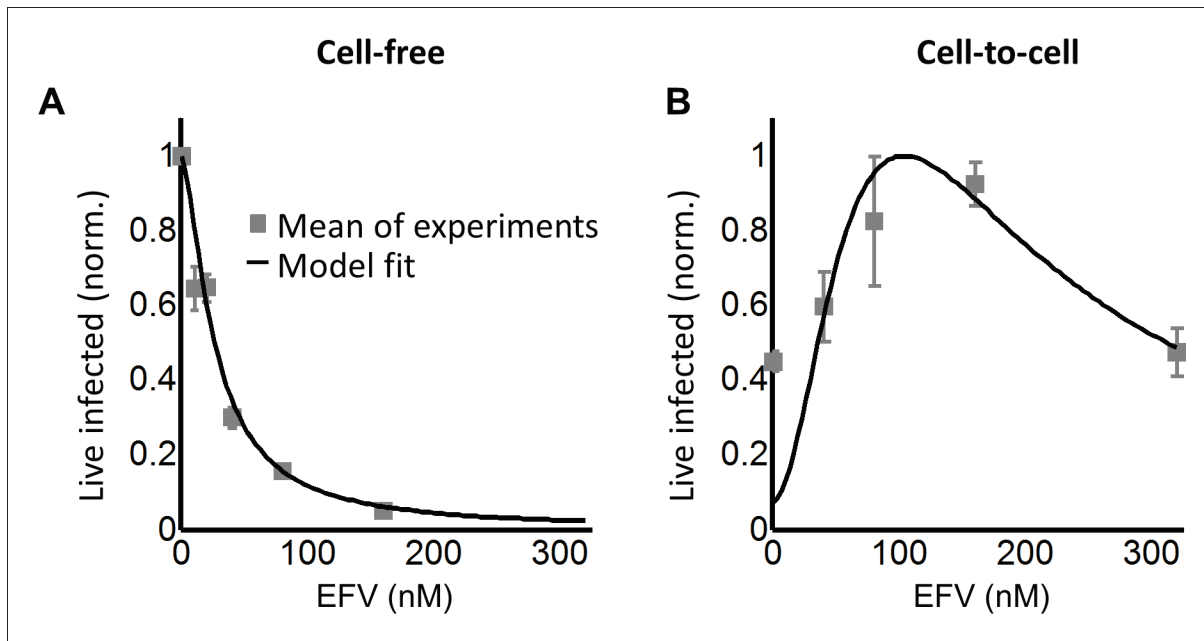


Figure 6. Infection with the K103N mutant shows an infection optimum at clinically observed lymph node EFV concentrations. (A) The number of live infected cells normalized by the maximum number of live infected cells in cell-free infection as a function of EFV for the K103N mutant. Black line is best-fit for EFV suppression of cell-free infection ($IC_{50} = 26$ nM, $h = 1.5$). Shown are means and standard errors for two independent experiments using cells from PID251. (B) The number of live infected cells normalized by the maximum number of live infected cells in coculture infection as a function of EFV for the K103N mutant. Black line represents best-fit model for the effect of EFV on coculture infection according to **Equation (3)**, with d values calculated based on the cell-free infection data for the K103N mutant, and the mean number of HIV DNA copies in the absence of drug determined for L1001. The fits recapitulated the experimental results when $r = 0.91$ and $q = 0.15$. Shown are means and standard errors for three independent experiments. There were sufficient lymph node cells from PID251 for two of the three experiments, and the third experiment was performed with lymph node cells from PID274.

DOI: <https://doi.org/10.7554/eLife.30134.019>

The following figure supplements are available for figure 6:

Figure supplement 1. The number of live infected cells in cell-free infection with the K103N mutant.

DOI: <https://doi.org/10.7554/eLife.30134.020>

Figure supplement 2. Response of K103N coculture infection to EFV in individual experiments.

DOI: <https://doi.org/10.7554/eLife.30134.021>

Figure supplement 3. Effect of EFV on viability of uninfected lymph node cells from PID274.

DOI: <https://doi.org/10.7554/eLife.30134.022>

Using a model where cells are infected and die in a probabilistic way, we found that there were two possible outcomes of partially inhibiting infection. In the case where cells were infected by single infection attempts, inhibition always led to a decline in the number of live infected cells, since inhibition reduced the number of infections per cell from one to zero. In contrast, in the case of multiple infection attempts per cell, the possibility existed that inhibition reduced the number of integrating HIV DNA copies, without extinguishing infection of the cell completely. If each HIV DNA copy increases the probability of cell death, reducing the number of HIV DNA copies without eliminating infection should lead to an increased probability of infected cell survival. This would consequently lead to an increase in the number of live infected cells.

We investigated the outcome of partial inhibition of infection in both a cell line and primary lymph node cells. In both systems, we observed that there was a peak in live infected cell number at intermediate inhibitor concentrations. This correlated to a decreased number of viral DNA copies per cell. Further increasing inhibitor concentration led to a decline in live infected cell numbers, and infecting with EFV resistant mutants shifted the peak in live infected number to higher EFV concentrations. Our model as described by **Equation (3)** reproduced the essential behaviour of the experimental results. Construction of the model assumed independence of productive infection and cell

death. However, as shown in the Appendix 1, an equivalent model can be constructed assuming a dependence of cell death on infection. Neither model accurately captures infection dynamics at high-drug concentrations, away from the infection optimum. In this range, where the number of infection attempts per cell is much lower than 1, infection declined more slowly with drug than predicted. The model can be further refined using a distribution for the number of DNA copies per cell. Moreover, the probability of death per HIV DNA copy we denote q may be dependent on how many infection attempts preceded the current infection attempt, and the model can be improved by measuring this dependence.

Physiologically, an infection optimum in the face of an antiretroviral drug may be important in HIV infection of lymph node cells and may be less pronounced in cells from peripheral blood. We used EFV in our study since it is a common component of first line antiretroviral therapy, with frequent drug resistance mutations. However, the infection optimum we describe should occur with other classes of antiretroviral drugs, since all drugs should decrease the multiplicity of infection between cells. In terms of modeling, a future therapy component such as the integrase inhibitor dolutegravir would exert its effect on r and not λ in our model. However, the effect is symmetrical since $e^{-(\lambda/d)} r = e^{-\lambda(r/d)}$. The more complex outcome of partial inhibition of infection should also be considered in other infections where multiple pathogens infect one cell and host cell death is a possible outcome (Mahamed *et al.*, 2017).

These observations reinforce previous results showing that successful completion of reverse transcription leads to cellular cytotoxicity. In addition to HIV cytotoxicity caused by viral integrations through the mechanism of double strand breaks (Cooper *et al.*, 2013), other mechanisms of HIV-induced death are also present, including IFI16-dependent innate immune system sensing of abortive reverse transcripts following non-productive infection of resting T cells (Doitsh *et al.*, 2014; Monroe *et al.*, 2014). The experiments presented here reflect the effect of partial inhibition on productive infection of HIV target cells, which mostly consist of activated T-cell subsets, not resting T cells. More complex models would be needed to decipher the effect of partial inhibition of HIV infection on resting T-cell numbers and the outcome of this in terms of available T-cell targets in future infection cycles.

This study may have implications for the establishment of viral reservoirs in the context of poorly controlled infections, infections with some degree of drug resistance, or infections where some replication may take place in the face of ART, since infected cell survival is a pre-requisite for long-term persistence. The clinical implications of an infection optimum in the presence of EFV with EFV-sensitive HIV strains are likely to be negligible, since the drug concentrations at which the infection optimum occurs are extremely low. However, for EFV-resistant HIV, the infection optimum shifts to the range of EFV concentrations observed in lymph nodes (~100 nM) (Fletcher *et al.*, 2014b), and can be expected to shift to even higher EFV concentrations with more resistant mutants. As EFV has a longer half-life than the other antiretroviral drugs co-formulated with it, it may be the only agent present in partially adherent individuals for substantial periods of time (Taylor *et al.*, 2007). Therefore, partial inhibition of HIV infection with EFV may provide a surprising advantage to EFV resistant mutants, and may allow individuals failing therapy to better transmit drug resistant strains.

Materials and methods

Ethical statement

Lymph nodes were obtained from the field of surgery of participants undergoing surgery for diagnostic purposes and/or complications of inflammatory lung disease. Informed consent was obtained from each participant, and the study protocol approved by the University of KwaZulu-Natal Institutional Review Board (approval BE024/09). Blood for PBMC was obtained from healthy blood donors under the same study protocol.

Inhibitors, viruses and cell lines

The following reagents were obtained through the AIDS Research and Reference Reagent Program, National Institute of Allergy and Infectious Diseases, National Institutes of Health: the antiretroviral EFV; RevCEM cells from Y. Wu and J. Marsh; HIV molecular clone pNL4-3 from M. Martin; ACH-2 cells from T. Folks. Cell-free viruses were produced by transfection of HEK293 cells with pNL4-3

using TransIT-LT1 (Mirus, Madison, WI) or Fugene HD (Roche, [Risch-Rotkreuz, Switzerland](#)) transfection reagents. Virus containing supernatant was harvested after 2 days of incubation and filtered through a 0.45 μm filter (Corning, New York, NY). b12 antibody was produced from transfecting HEK293 cells with a b12 expression plasmid (expressed under a CMV promoter on a pHAGE6 lentiviral plasmid backbone, gift from A. Balazs), followed by harvesting of cell supernatant and purification at the California Institute of Technology protein expression core. The number of virus genomes in viral stocks was determined using the RealTime HIV-1 viral load test (Abbott Diagnostics, Santa Clara, CA). For r and q measurement, 0.45 μm filtered cell-free supernatants from infected RevCEM cells were used, to include any secreted factors which may modulate cell-death. The L100I and K103N mutants were evolved by serial passages of wild-type NL4-3 in RevCEM cells in the presence of 20 nM EFV. After 16 days of selection, the reverse transcriptase gene was cloned from the proviral DNA and the mutant reverse transcriptase gene was inserted into the NL4-3 molecular clone. RevCEM clones E7 and G2 used in this study were generated as previously described ([Boullé et al., 2016](#)). Briefly, the E7 clone was generated by subcloning RevCEM cells at single-cell density. Surviving clones were subdivided into replicate plates. One of the plates was screened for the fraction of GFP expressing cells upon HIV infection using microscopy, and the clone with the highest fraction of GFP-positive cells was selected. To generate the G2 clone, E7 cells were stably infected with the mCherry gene under the EF-1 α promoter on a pHAGE2-based lentiviral vector (gift from A. Balazs), subcloned, and screened for >99% mCherry-positive cells. All cell lines not authenticated, and mycoplasma negative. Cell culture and experiments were performed in complete RPMI 1640 medium supplemented with L-Glutamine, sodium pyruvate, HEPES, non-essential amino acids (Lonza, [Basel, Switzerland](#)), and 10% heat-inactivated FBS (GE Healthcare Bio-Sciences, Pittsburgh, PA).

Primary cells

Lymph node cells were obtained by mechanical separation of lymph nodes and frozen at 5×10^6 cells/ml in a solution of 90% FBS and 10% DMSO with 2.5 $\mu\text{g/ml}$ Amphotericin B (Lonza). Cells were stored in liquid nitrogen until use, then thawed and resuspended at 10^6 cells/ml in complete RPMI 1640 medium supplemented with L-Glutamine, sodium pyruvate, HEPES, non-essential amino acids (Lonza), 10% heat-inactivated FBS (Hyclone), and IL-2 at 5 ng/ml (PeproTech). Phytohemagglutinin at 10 $\mu\text{g/ml}$ (Sigma-Aldrich, St Louis, MO) was added to activate cells. PBMCs were isolated by density gradient centrifugation using Histopaque 1077 (Sigma-Aldrich) and cultured at 10^6 cells/ml in complete RPMI 1640 medium supplemented with L-Glutamine, sodium pyruvate, HEPES, non-essential amino acids (Lonza), 10% heat-inactivated FBS (GE Healthcare Bio-Sciences, Pittsburgh, PA), and IL-2 at 5 ng/ml (PeproTech, Rocky Hill, NJ). Phytohemagglutinin at 10 $\mu\text{g/ml}$ (Sigma-Aldrich) was added to activate cells. For both primary cell types, donor cells for coculture infection were cultured for one day then infected by cell-free virus, while target cells were cultured for three days and infected with either cell-free HIV or infected donor cells.

Subcloning of ACH-2 cells

Cells from the parental ACH-2 cell line were diluted to 10 cells/ml in conditioned medium, with conditioned medium generated by culturing ACH-2 cells to 10^6 cells/ml, then filtering through a 0.22 μm filter (Corning). 25 μl of the diluted cell suspension was then distributed to each well of a Greiner μClear 384-well plate (mean of 0.5 cells per well). Clones were cultured for 3 weeks, where each week an additional 25 μl of conditioned medium was added to each well. Clones were detected in 5% of wells and two clones, designated D6 and C3, were randomly chosen and further expanded.

Infection

For a cell-free infection of RevCEM clones, PBMC and lymph node cells, 10^6 cells/ml were infected with 2×10^8 NL4-3 viral copies/ml ($\sim 20\text{ng}$ p24 equivalent) for 2 days. For coculture infection, infected cells from the cell-free infection were used as the donors and cocultured with 10^6 cells/ml target cells. For RevCEM clones, 2% infected donor cells were added to uninfected targets and cocultured for 2 days in tissue culture experiments, and 20% infected donor cells were added to uninfected targets and cocultured for 2 days for time-lapse experiments. For lymph node cells and

PBMCs, a ratio of 1:4 donor to target cells was used. Infection was over 2 days in PBMC infection and for 4 days for infection of lymph node cells.

Staining and flow cytometry

To determine the number of live infected cells in reporter cell line experiments, E7 RevCEM reporter cells were infected as above used as donor cells. Prior to co-incubation with target cells, donor cells were stained with CellTrace Far Red (CTFR, Thermo Fisher Scientific, Waltham, MA) at 1 μ M and washed according to manufacturer's instructions. The G2 mCherry-positive reporter cells were used as infection targets, and cocultured with 2% infected donor cells for 2 days. The coculture infection was pulsed with 100 ng/ml DAPI (Sigma-Aldrich) immediately before flow cytometry and the number of live infected target cells was determined by the number of DAPI negative, CTFR negative and mCherry and GFP double positive cells on a FACSAria Fusion machine (BD Biosciences, Sparks, MD) using the 355, 488 and 633 nm laser lines. For cell-free infections where fewer fluorescence channels were used, a pulse of 300 nM of the far-red live cell impermeable dye DRAQ7 (Biolegend, San Diego, CA) immediately before flow cytometry was substituted for DAPI, and live infected cells detected as the number of DRAQ7-negative, GFP-positive cells on a FACSCaliber machine using 488 and 633 nm laser lines. Lymph node cells were resuspended in 1 ml of phosphate buffered saline (PBS) and stained at a 1:1000 dilution of the eFluor660 dye (Thermo Fisher Scientific) according to the manufacturer's instructions. Cells were then fixed and permeabilized using the BD Cytofix/Cytoperm Fixation/Permeabilization kit (BD Biosciences) according to the manufacturer's instructions. Cells were then stained with anti-p24 FITC conjugated antibody (KC57, Beckman Coulter, Brea, CA). Live infected lymph node cells were detected as the number of eFluor660-negative, p24-positive cells. Cells were acquired with a FACSAriaIII or FACSCaliber machine (BD Biosciences) using 488 and 633 nm laser lines. Results were analysed with FlowJo 10.0.8 software. For single-cell sorting to detect the number of HIV DNA copies per cell, cells were single-cell sorted using 85 micron nozzle in a FACSAriaIII machine. GFP-positive, DRAQ7-negative RevCEM clones were sorted 1 day post-infection into 96 well plates (Biorad, Hercules, CA) containing 30 μ l lysis buffer (2.5 μ l 0.1M Dithiothreitol, 5 μ l 5% NP40 and 22.5 μ l molecular biology grade water [Kurimoto *et al.*, 2007]). For experiments to determine the number of HIV DNA copies to measure r and q , the DRAQ7-negative subset was sorted. Fixed, p24-positive, eFluor660-negative lymph node cells were single-cell sorted two days post-infection into 96-well plates containing 5 μ l of PKD buffer (Qiagen, Hilden, Germany) with 1:16 proteinase K solution (Qiagen) (Thomsen *et al.*, 2016). Sorted plates were snap frozen and kept at -80°C until ready for PCR. For analysis by flow cytometry, a minimum of 50,000 cells were collected per data point.

Time-lapse microscopy and image analysis

For imaging infection by time-lapse microscopy, cell density was reduced to 5×10^4 cells/ml and cells were attached to ploy-l-lysine (Sigma-Aldrich) coated optical six-well plates (MatTek, Ashland, MA). Infections with and without EFV were imaged in tandem using a Metamorph-controlled Nikon TiE motorized microscope with a Yokogawa spinning disk with a 20x, 0.75 NA phase objective in a biosafety level three facility. Excitation sources were 488 (GFP) and 561 (mCherry) laser lines and emission was detected through a Semrock Brightline quad band 440–40/521–21/607–34/700–45 nm filter. Images were captured using an 888 EMCCD camera (Andor, Belfast, UK). Temperature (37°C), humidity and CO_2 (5%) were controlled using an environmental chamber (OKO Labs, Naples, Italy). Fields of view were captured every 20 min. To facilitate automated image analysis of time-lapse experiment data, mCherry expressing G2 clone cells were used as targets and E7 clone cells used as infected donors. The number of live cells was measured as the number of cells expressing mCherry since intracellular mCherry protein is soluble and hence lost upon cell death when cellular membrane integrity is compromised. The number of live infected cells was measured as the number of cells expressing both mCherry and GFP. Three independent experiments were performed. Movies were analyzed using custom code developed with the Matlab R2014a Image Analysis Toolbox. Images in the mCherry channel were thresholded and the `imfindcircle` function used to detect round objects within the cell radius range. Cell centers were found. GFP signal underwent the same binary thresholding. The number of mCherry-positive 16 pixel² squares around the cell centers was used as the

the number of total target cells at each time-point, and the number of squares double positive for fluorescence in the GFP channel was used as the number of infected target cells.

Determination of HIV DNA copy number in individual cells

96-well plates of cells previously sorted at 1 cell per well were thawed at room temperature and spun down. Fixed cells were de-crosslinked by incubating in a thermocycler at 56°C for 1 hr. The lysate from each well was split equally over 10 wells (2.5 µl each well after correction for evaporation) for E7 RevCEM or four wells (6.8 µl each well after correction for evaporation) for lymph nodes, containing 50 µl of Phusion hot start II DNA polymerase (New England Biolabs, Ipswich, MA) PCR reaction mix (10 µl 5X Phusion HF buffer, 1 µl dNTPs, 2.5 µl of the forward primer, 2.5 µl of the reverse primer, 0.5 µl Phusion hot start II DNA polymerase, 2.5 µl of DMSO and molecular biology grade water to 50 µl reaction volume). Two rounds of PCR were performed. The first round reaction amplified a 700 bp region of the reverse transcriptase gene using the forward primer 5' CCTACACCTG TCAACATAATTGGAAG 3' and reverse primer 5' GAATGGAGTTCTTTCTGATG 3'. Cycling program was 98°C for 30 s, then 34 cycles of 98°C for 10 s, 63°C for 30 s and 72°C for 15 s with a final extension of 72°C for 5 min. 1 µl of the first round product was then transferred into a PCR mix as above, with nested second round primers (forward 5' TAAAAGCATTAGTAGAAATTTGTACAGA 3', reverse 5' GGTAATCCCCACCTCAACAGATG 3'). The second round PCR amplified a 550 bp product which was then visualized on a 1% agarose gel. PCR reactions were found to work best if sorted plates were thawed no more than once, and plates which underwent repeated freeze-thaw cycles showed poor amplification.

Correction of raw number of detected DNA copies for detection sensitivity

A stochastic simulation in Matlab was used to generate a distribution for the number of positive wells per cell for each mean number of DNA copies per cell λ . The probability for a DNA copy to be present within a given well and be detected was set as σ/w , where σ was the detection sensitivity calculated as the number of ACH-2 with detectable integrations divided by the total number of ACH-2 cells assayed (38/166, $\sigma = 0.23$), and w was the number of wells. A random number m representing DNA copies per cell from a Poisson distribution with a mean λ was drawn, and a vector R of m random numbers from a uniform distribution was generated. If there existed an element R_i of the vector with a value between 0 and σ/w , the first well was occupied. If an element existed with a value between $\sigma/w + \gamma$ and $2(\sigma/w)$, where $\gamma \ll 1$, the second well was occupied, and if between $(\sigma/w + \gamma)(n-1)$ and $n(\sigma/w)$, the n th well was occupied. The sum of wells occupied at least once was determined, and the process repeated j times for each λ , where j was the number of cells in the experimental data. A least squares fit was performed to select λ which best fit the experimental results across well frequencies, and mean and standard deviation for λ was derived by repeating the simulation 10 times.

Fit of the EFV response for single infections using IC₅₀ and Hill coefficient

To obtain d , we normalized Equation (2) by the fraction of infected cells in the absence of drug (Sigal et al., 2011) to obtain $T_x = (\text{infected targets with EFV}) / (\text{infected targets no EFV}) = ((1 - (1 - r)^{\lambda/d}) (1 - q)^{\lambda/d}) / ((1 - (1 - r)^{\lambda}) (1 - q)^{\lambda})$. We approximate the result at small r, q to $T_x = (1 - e^{-r\lambda/d}) e^{-q\lambda/d} / (1 - e^{-r\lambda}) e^{-q\lambda} = e^{q\lambda(1-1/d)} ((1 - e^{-r\lambda/d}) / (1 - e^{-r\lambda}))$. Expanding the exponentials we obtain $T_x = (1 + q\lambda(1-1/d)) ((-r\lambda/d) / -r\lambda) = (1 + q\lambda(1-1/d))(1/d)$. We note that at $\lambda < 1$, $q\lambda(1-1/d) \ll 1$, and hence $T_x \cong 1/d$. T_x was measured from the experiments to obtain d values at the EFV concentrations used for cell-free infection, where $\lambda < 1$. To obtain a fit of d as a function of the concentration of drug that gives half-maximal inhibition (IC₅₀) and Hill coefficient (h) for EFV, we used the relation for the fraction cells remaining infected in the face of drug (Canini and Perelson, 2014), whose definition is equivalent to T_x at $\lambda < 1$:

$$\frac{1}{d} = 1 - \frac{[EFV]^h}{[EFV]^h + IC_{50}^h}. \quad (4)$$

Measurement of r

Cell-free supernatant used in infection was derived as follows: 10^6 cells/ml were infected with 2×10^8 NL4-3 viral copies/ml (~ 20 ng p24 equivalent) for 2 days. Thereafter 0.2% of the infected cells from the cell-free infection were added to 10^6 cells/ml target cells. The infected supernatant from the coculture 2 days post-infection was filtered using a $0.45 \mu\text{m}$ filter (Corning) and added to cells at a 1:8 dilution, where the dilution was calibrated to result in non-saturating infection in terms of GFP expression. A fraction of the cells were sorted into lysis buffer at one cell per well 1 day post infection, split over four wells, and PCR performed as described above to determine HIV copy number per cell. The remaining cells from the same infection were used to determine frequency of DRAQ-7-negative, GFP-positive cells 2 days post-infection using flow cytometry.

Measurement of q

Cell-free supernatant used in infection was derived as for r , except that 1 day before harvesting of the viral supernatant from infected cells, infected cells were washed twice with PBS and serum-free growth medium added. At the same time, the target cells for the infection were washed twice with PBS and serum-free growth medium added. Cells were split into two wells, and EFV to a final concentration of 40 nM was added to one of the wells. Supernatant was harvested and filtered as described for r , and added to cells at a 1:2 dilution. A fraction of the cells were sorted into lysis buffer at one cell per well 1 day post-infection, split over four wells, and PCR performed as described above to determine HIV copy number per cell. The remaining cells from the same infection were used to determine the frequency of live and dead cells two days post-infection. The concentration of live cells was measured using the TC20TM automated cell counter (Bio-Rad) with trypan blue staining (Lonza).

Acknowledgements

This work was supported by National Institutes of Health Grant R21MH104220. AS was supported by a Human Frontiers Science Program Career Development Award CDA 00050/2013. RAN is supported by the European Research Council through grant Stg. 260686. LJ and JH are supported by a fellowship from the South African National Research Foundation. IMF is supported through a Sub-Saharan African Network for TB/HIV Research Excellence (SANTHE, a DELTAS Africa Initiative (grant #DEL-15-006)) fellowship, and a Poliomyelitis Research Foundation fellowship 17/59. Open access publication of this article has been made possible through support from the Victor Daitz Information Gateway, an initiative of the Victor Daitz Foundation and the University of KwaZulu-Natal.

Additional information

Competing interests

Richard A Neher: Reviewing editor, *eLife*. The other authors declare that no competing interests exist.

Funding

Funder	Grant reference number	Author
Human Frontier Science Program	CDA 00050/2013	Alex Sigal
European Research Council	Stg. 260686	Richard A Neher
DELTAS Africa Initiative	Graduate Fellowship (DEL-15-006)	Isabella Markham Ferreira
National Research Foundation	Graduate Fellowship	Laurelle Jackson Jessica Hunter
National Institutes of Health	R21MH104220	Alex Sigal
Poliomyelitis Research Foundation	Graduate Fellowship	Isabella Markham Ferreira

The funders had no role in study design, data collection and interpretation, or the decision to submit the work for publication.

Author contributions

Laurelle Jackson, Conceptualization, Data curation, Validation, Investigation, Visualization, Methodology, Writing—original draft, Project administration, Writing—review and editing; Jessica Hunter, Data curation, Validation, Investigation, Visualization, Methodology, Writing—original draft; Sandile Cele, Isabella Markham Ferreira, Andrew C Young, Yashica Ganga, Mikael Boulle, Investigation, Methodology; Farina Karim, Rajhmun Madansein, Resources, Project administration; Kaylesh J Dullabh, Resources, Data curation, Validation, Investigation; Chih-Yuan Chen, Resources, Investigation; Noel J Buckels, Khadija Khan, Resources; Gila Lustig, Resources, Investigation, Methodology, Project administration; Richard A Neher, Conceptualization, Methodology; Alex Sigal, Conceptualization, Resources, Data curation, Software, Formal analysis, Supervision, Funding acquisition, Validation, Investigation, Visualization, Writing—original draft, Project administration, Writing—review and editing

Author ORCIDs

Andrew C Young  <http://orcid.org/0000-0003-3616-7956>

Richard A Neher  <http://orcid.org/0000-0003-2525-1407>

Alex Sigal  <http://orcid.org/0000-0001-8571-2004>

Ethics

Human subjects: Lymph nodes were obtained from the field of surgery of participants undergoing surgery for diagnostic purposes and/or complications of inflammatory lung disease. Informed consent was obtained from each participant, and the study protocol approved by the University of Kwa-Zulu-Natal Institutional Review Board (approval BE024/09).

Decision letter and Author response

Decision letter <https://doi.org/10.7554/eLife.30134.039>

Author response <https://doi.org/10.7554/eLife.30134.040>

Additional files

Supplementary files

- Supplementary file 1. S Table 1: Parameters and definitions.

DOI: <https://doi.org/10.7554/eLife.30134.023>

- Supplementary file 2. S Table 2: Measurement of r and q

DOI: <https://doi.org/10.7554/eLife.30134.024>

- Supplementary file 3. S Table 3: Participant information.

DOI: <https://doi.org/10.7554/eLife.30134.025>

- Source code 1. script1r2.m: Matlab source code for **Figure 1**.

DOI: <https://doi.org/10.7554/eLife.30134.026>

- Source code 2. script2r2: Matlab source code for copy number correction for RevCEM clones based on HIV copy detection efficiency in ACH-2 cells.

DOI: <https://doi.org/10.7554/eLife.30134.027>

- Source code 3. script3r2.m: Matlab source code for cell-free and coculture infection model fits for RevCEM cells infected with wild-type HIV in **Figure 2**.

DOI: <https://doi.org/10.7554/eLife.30134.028>

- Source code 4. Script4.m: Matlab source code for histograms of raw HIV copy numbers for cell-free and coculture infection and fits of different distributions to coculture copy number frequencies.

DOI: <https://doi.org/10.7554/eLife.30134.029>

- Source code 5. Script5.m: Matlab source code for image analysis of time-lapse data for **Figure 2—figure supplement 5**.

DOI: <https://doi.org/10.7554/eLife.30134.030>

• Source code 6. script6r2.m: Matlab source code for cell-free and coculture infection model fits for RevCEM cells infected with L100I mutant HIV in **Figure 3**.

DOI: <https://doi.org/10.7554/eLife.30134.031>

• Source code 7. Script7.m: Matlab source code for copy number correction for lymph node cells based on HIV copy detection efficiency is ACH-2 cells.

DOI: <https://doi.org/10.7554/eLife.30134.032>

• Source code 8. script8r2.m: Matlab source code for cell-free and coculture infection model fits for lymph node cells infected with K103N mutant HIV in **Figure 6**.

DOI: <https://doi.org/10.7554/eLife.30134.033>

• Transparent reporting form

DOI: <https://doi.org/10.7554/eLife.30134.034>

References

- Ariën KK, Troyer RM, Gali Y, Colebunders RL, Arts EJ, Vanham G. 2005. Replicative fitness of historical and recent HIV-1 isolates suggests HIV-1 attenuation over time. *AIDS* **19**:1555–1564. DOI: <https://doi.org/10.1097/01.aids.0000185989.16477.91>, PMID: 16184024
- Banda NK, Bernier J, Kurahara DK, Kurrle R, Haigwood N, Sekaly RP, Finkel TH. 1992. Crosslinking CD4 by human immunodeficiency virus gp120 primes T cells for activation-induced apoptosis. *Journal of Experimental Medicine* **176**:1099–1106. DOI: <https://doi.org/10.1084/jem.176.4.1099>, PMID: 1402655
- Baxter AE, Russell RA, Duncan CJ, Moore MD, Willberg CB, Pablos JL, Finzi A, Kaufmann DE, Ochsenbauer C, Kappes JC, Groot F, Sattentau QJ. 2014. Macrophage infection via selective capture of HIV-1-infected CD4+ T cells. *Cell Host & Microbe* **16**:711–721. DOI: <https://doi.org/10.1016/j.chom.2014.10.010>, PMID: 25467409
- Bonhoeffer S, Lenski RE, Ebert D. 1996. The curse of the pharaoh: the evolution of virulence in pathogens with long living propagules. *Proceedings of the Royal Society B: Biological Sciences* **263**:715–721. DOI: <https://doi.org/10.1098/rspb.1996.0107>, PMID: 8763793
- Bonhoeffer S, May RM, Shaw GM, Nowak MA. 1997. Virus dynamics and drug therapy. *PNAS* **94**:6971–6976. DOI: <https://doi.org/10.1073/pnas.94.13.6971>, PMID: 9192676
- Bonhoeffer S, Nowak MA. 1994. Mutation and the evolution of virulence. *Proceedings of the Royal Society B: Biological Sciences* **258**:133–140. DOI: <https://doi.org/10.1098/rspb.1994.0153>
- Boullé M, Müller TG, Dähling S, Ganga Y, Jackson L, Mahamed D, Oom L, Lustig G, Neher RA, Sigal A. 2016. HIV Cell-to-Cell Spread Results in Earlier Onset of Viral Gene Expression by Multiple Infections per Cell. *PLoS Pathogens* **12**:e1005964. DOI: <https://doi.org/10.1371/journal.ppat.1005964>, PMID: 27812216
- Brenchley JM, Schacker TW, Ruff LE, Price DA, Taylor JH, Beilman GJ, Nguyen PL, Khoruts A, Larson M, Haase AT, Douek DC. 2004. CD4+ T cell depletion during all stages of HIV disease occurs predominantly in the gastrointestinal tract. *The Journal of Experimental Medicine* **200**:749–759. DOI: <https://doi.org/10.1084/jem.20040874>, PMID: 15365096
- Canini L, Perelson AS. 2014. Viral kinetic modeling: state of the art. *Journal of Pharmacokinetics and Pharmacodynamics* **41**:431–443. DOI: <https://doi.org/10.1007/s10928-014-9363-3>, PMID: 24961742
- Chun TW, Carruth L, Finzi D, Shen X, DiGiuseppe JA, Taylor H, Hermankova M, Chadwick K, Margolick J, Quinn TC, Kuo YH, Brookmeyer R, Zeiger MA, Barditch-Crovo P, Siliciano RF. 1997. Quantification of latent tissue reservoirs and total body viral load in HIV-1 infection. *Nature* **387**:183–188. DOI: <https://doi.org/10.1038/387183a0>, PMID: 9144289
- Cooper A, García M, Petrovas C, Yamamoto T, Koup RA, Nabel GJ. 2013. HIV-1 causes CD4 cell death through DNA-dependent protein kinase during viral integration. *Nature* **498**:376–379. DOI: <https://doi.org/10.1038/nature12274>, PMID: 23739328
- Dale BM, McNerney GP, Thompson DL, Hubner W, de Los Reyes K, Chuang FY, Huser T, Chen BK. 2011. Cell-to-cell transfer of HIV-1 via virological synapses leads to endosomal virion maturation that activates viral membrane fusion. *Cell Host & Microbe* **10**:551–562. DOI: <https://doi.org/10.1016/j.chom.2011.10.015>, PMID: 22177560
- Dang Q, Chen J, Unutmaz D, Coffin JM, Pathak VK, Powell D, KewalRamani VN, Maldarelli F, Hu WS, Ws H. 2004. Nonrandom HIV-1 infection and double infection via direct and cell-mediated pathways. *PNAS* **101**:632–637. DOI: <https://doi.org/10.1073/pnas.0307636100>, PMID: 14707263
- Del Portillo A, Tripodi J, Najfeld V, Wodarz D, Levy DN, Chen BK. 2011. Multiploid inheritance of HIV-1 during cell-to-cell infection. *Journal of Virology* **85**:7169–7176. DOI: <https://doi.org/10.1128/JVI.00231-11>, PMID: 21543479
- Deleage C, Wietgreffe SW, Del Prete G, Morcock DR, Hao XP, Piatak M, Bess J, Anderson JL, Perkey KE, Reilly C, McCune JM, Haase AT, Lifson JD, Schacker TW, Estes JD. 2016. Defining HIV and SIV reservoirs in lymphoid tissues. *Pathogens and Immunity* **1**:68. DOI: <https://doi.org/10.20411/pai.v1i1.100>, PMID: 27430032
- Descours B, Petitjean G, López-Zaragoza JL, Bruel T, Raffel R, Psomas C, Reynes J, Lacabaratz C, Levy Y, Schwartz O, Lelievre JD, Benkirane M. 2017. CD32a is a marker of a CD4 T-cell HIV reservoir harbouring

- replication-competent proviruses. *Nature* **543**:564–567. DOI: <https://doi.org/10.1038/nature21710>, PMID: 28297712
- Dixit NM, Perelson AS. 2004. Multiplicity of human immunodeficiency virus infections in lymphoid tissue. *Journal of Virology* **78**:8942–8945. DOI: <https://doi.org/10.1128/JVI.78.16.8942-8945.2004>, PMID: 15280505
- Doitsh G, Cavrois M, Lassen KG, Zepeda O, Yang Z, Santiago ML, Hebbeler AM, Greene WC. 2010. Abortive HIV infection mediates CD4 T cell depletion and inflammation in human lymphoid tissue. *Cell* **143**:789–801. DOI: <https://doi.org/10.1016/j.cell.2010.11.001>, PMID: 21111238
- Doitsh G, Galloway NL, Geng X, Yang Z, Monroe KM, Zepeda O, Hunt PW, Hatano H, Sowinski S, Muñoz-Arias I, Greene WC. 2014. Cell death by pyroptosis drives CD4 T-cell depletion in HIV-1 infection. *Nature* **505**:509–514. DOI: <https://doi.org/10.1038/nature12940>, PMID: 24356306
- Duncan CJ, Russell RA, Sattentau QJ. 2013. High multiplicity HIV-1 cell-to-cell transmission from macrophages to CD4+ T cells limits antiretroviral efficacy. *AIDS* **27**:2201–2206. DOI: <https://doi.org/10.1097/QAD.0b013e3283632ec4>, PMID: 24005480
- Embretson J, Zupancic M, Ribas JL, Burke A, Racz P, Tenner-Racz K, Haase AT. 1993. Massive covert infection of helper T lymphocytes and macrophages by HIV during the incubation period of AIDS. *Nature* **362**:359–362. DOI: <https://doi.org/10.1038/362359a0>, PMID: 8096068
- Finkel TH, Tudor-Williams G, Banda NK, Cotton MF, Curiel T, Monks C, Baba TW, Ruprecht RM, Kupfer A. 1995. Apoptosis occurs predominantly in bystander cells and not in productively infected cells of HIV- and SIV-infected lymph nodes. *Nature Medicine* **1**:129–134. DOI: <https://doi.org/10.1038/nm0295-129>, PMID: 7585008
- Fletcher CV, Staskus K, Wietgreffe SW, Rothenberger M, Reilly C, Chipman JG, Beilman GJ, Khoruts A, Thorkelson A, Schmidt TE, Anderson J, Perkey K, Stevenson M, Perelson AS, Douek DC, Haase AT, Schacker TW. 2014a. Persistent HIV-1 replication is associated with lower antiretroviral drug concentrations in lymphatic tissues. *PNAS* **111**:2307–2312. DOI: <https://doi.org/10.1073/pnas.1318249111>
- Fletcher CV, Staskus K, Wietgreffe SW, Rothenberger M, Reilly C, Chipman JG, Beilman GJ, Khoruts A, Thorkelson A, Schmidt TE, Anderson J, Perkey K, Stevenson M, Perelson AS, Douek DC, Haase AT, Schacker TW. 2014b. Persistent HIV-1 replication is associated with lower antiretroviral drug concentrations in lymphatic tissues. *PNAS* **111**:2307–2312. DOI: <https://doi.org/10.1073/pnas.1318249111>, PMID: 24469825
- Galloway NL, Doitsh G, Monroe KM, Yang Z, Muñoz-Arias I, Levy DN, Greene WC. 2015. Cell-to-cell transmission of hiv-1 is required to trigger pyroptotic death of lymphoid-tissue-derived CD4 T Cells. *Cell Reports* **12**:1555–1563. DOI: <https://doi.org/10.1016/j.celrep.2015.08.011>, PMID: 26321639
- Gandon S, Mackinnon MJ, Nee S, Read AF. 2001. Imperfect vaccines and the evolution of pathogen virulence. *Nature* **414**:751–756. DOI: <https://doi.org/10.1038/414751a>, PMID: 11742400
- Gratton S, Cheynier R, Dumaurier MJ, Oksenhendler E, Wain-Hobson S. 2000. Highly restricted spread of HIV-1 and multiply infected cells within splenic germinal centers. *PNAS* **97**:14566–14571. DOI: <https://doi.org/10.1073/pnas.97.26.14566>, PMID: 11121058
- Groot F, Welsch S, Sattentau QJ. 2008. Efficient HIV-1 transmission from macrophages to T cells across transient virological synapses. *Blood* **111**:4660–4663. DOI: <https://doi.org/10.1182/blood-2007-12-130070>, PMID: 18296630
- Groppelli E, Starling S, Jolly C. 2015. Contact-induced mitochondrial polarization supports HIV-1 virological synapse formation. *Journal of Virology* **89**:14–24. DOI: <https://doi.org/10.1128/JVI.02425-14>, PMID: 25320323
- Gummuru S, KewalRamani VN, Emerman M. 2002. Dendritic cell-mediated viral transfer to T cells is required for human immunodeficiency virus type 1 persistence in the face of rapid cell turnover. *Journal of Virology* **76**:10692–10701. DOI: <https://doi.org/10.1128/JVI.76.21.10692-10701.2002>, PMID: 12368311
- Hollingsworth TD, Anderson RM, Fraser C. 2008. HIV-1 transmission, by stage of infection. *The Journal of Infectious Diseases* **198**:687–693. DOI: <https://doi.org/10.1086/590501>, PMID: 18662132
- Hübner W, Mc Nerney GP, Chen P, Dale BM, Gordon RE, Chuang FY, Li XD, Asmuth DM, Huser T, Chen BK. 2009. Quantitative 3D video microscopy of HIV transfer across T cell virological synapses. *Science* **323**:1743–1747. DOI: <https://doi.org/10.1126/science.1167525>, PMID: 19325119
- Jensen KH, Little TJ, Little T, Skorpung A, Ebert D. 2006. Empirical support for optimal virulence in a castrating parasite. *PLoS Biology* **4**:e197. DOI: <https://doi.org/10.1371/journal.pbio.0040197>, PMID: 16719563
- Jolly C, Kashafi K, Hollinshead M, Sattentau QJ. 2004. HIV-1 cell to cell transfer across an Env-induced, actin-dependent synapse. *The Journal of Experimental Medicine* **199**:283–293. DOI: <https://doi.org/10.1084/jem.20030648>, PMID: 14734528
- Jolly C, Welsch S, Michor S, Sattentau QJ. 2011. The regulated secretory pathway in CD4(+) T cells contributes to human immunodeficiency virus type-1 cell-to-cell spread at the virological synapse. *PLoS Pathogens* **7**:e1002226. DOI: <https://doi.org/10.1371/journal.ppat.1002226>, PMID: 21909273
- Josefsson L, King MS, Makitalo B, Brännström J, Shao W, Maldarelli F, Kearney MF, Hu WS, Chen J, Gaines H, Mellors JW, Albert J, Coffin JM, Palmer SE. 2011. Majority of CD4+ T cells from peripheral blood of HIV-1-infected individuals contain only one HIV DNA molecule. *PNAS* **108**:11199–11204. DOI: <https://doi.org/10.1073/pnas.1107729108>, PMID: 21690402
- Josefsson L, Palmer S, Faria NR, Lemey P, Casazza J, Ambrozak D, Kearney M, Shao W, Kottlil S, Sneller M, Mellors J, Coffin JM, Maldarelli F. 2013. Single cell analysis of lymph node tissue from HIV-1 infected patients reveals that the majority of CD4+ T-cells contain one HIV-1 DNA molecule. *PLoS Pathogens* **9**:e1003432. DOI: <https://doi.org/10.1371/journal.ppat.1003432>, PMID: 23818847
- Jung A, Maier R, Vartanian JP, Bocharov G, Jung V, Fischer U, Meese E, Wain-Hobson S, Meyerhans A. 2002. Recombination: Multiply infected spleen cells in HIV patients. *Nature* **418**:144. DOI: <https://doi.org/10.1038/418144a>, PMID: 12110879

- Kurimoto K**, Yabuta Y, Ohinata Y, Saitou M. 2007. Global single-cell cDNA amplification to provide a template for representative high-density oligonucleotide microarray analysis. *Nature Protocols* **2**:739–752. DOI: <https://doi.org/10.1038/nprot.2007.79>, PMID: 17406636
- Law KM**, Komarova NL, Yewdall AW, Lee RK, Herrera OL, Wodarz D, Chen BK. 2016. In Vivo HIV-1 Cell-to-Cell transmission promotes multicopy micro-compartmentalized infection. *Cell Reports* **15**:2771–2783. DOI: <https://doi.org/10.1016/j.celrep.2016.05.059>, PMID: 27292632
- Mahamed D**, Bouille M, Ganga Y, Mc Arthur C, Skroch S, Oom L, Catinas O, Pillay K, Naicker M, Rampersad S, Mathonsi C, Hunter J, Wong EB, Suleman M, Sreejit G, Pym AS, Lustig G, Sigal A. 2017. Intracellular growth of *Mycobacterium tuberculosis* after macrophage cell death leads to serial killing of host cells. *eLife* **6**:e22028. DOI: <https://doi.org/10.7554/eLife.22028>, PMID: 28130921
- Mattapallil JJ**, Douek DC, Hill B, Nishimura Y, Martin M, Roederer M. 2005. Massive infection and loss of memory CD4+ T cells in multiple tissues during acute SIV infection. *Nature* **434**:1093–1097. DOI: <https://doi.org/10.1038/nature03501>, PMID: 15793563
- Monroe KM**, Yang Z, Johnson JR, Geng X, Doitsh G, Krogan NJ, Greene WC. 2014. IFI16 DNA sensor is required for death of lymphoid CD4 T cells abortively infected with HIV. *Science* **343**:428–432. DOI: <https://doi.org/10.1126/science.1243640>, PMID: 24356113
- Münch J**, Rücker E, Ständker L, Adermann K, Goffinet C, Schindler M, Wildum S, Chinnadurai R, Rajan D, Specht A, Giménez-Gallego G, Sánchez PC, Fowler DM, Koulov A, Kelly JW, Mothes W, Grivel JC, Margolis L, Keppler OT, Forssmann WG, et al. 2007. Semen-derived amyloid fibrils drastically enhance HIV infection. *Cell* **131**:1059–1071. DOI: <https://doi.org/10.1016/j.cell.2007.10.014>, PMID: 18083097
- Nowak M**, May RM. 2000. *Virus dynamics: mathematical principles of immunology and virology: mathematical principles of immunology and virology*. UK: Oxford University Press.
- O’Doherty U**, Swiggard WJ, Jeyakumar D, McGain D, Malim MH. 2002. A sensitive, quantitative assay for human immunodeficiency virus type 1 integration. *Journal of Virology* **76**:10942–10950. DOI: <https://doi.org/10.1128/JVI.76.21.10942-10950.2002>, PMID: 12368337
- Payne R**, Muenchhoff M, Mann J, Roberts HE, Matthews P, Adland E, Hempenstall A, Huang KH, Brockman M, Brumme Z, Sinclair M, Miura T, Frater J, Essex M, Shapiro R, Walker BD, Ndung’u T, McLean AR, Carlson JM, Goulder PJ. 2014. Impact of HLA-driven HIV adaptation on virulence in populations of high HIV seroprevalence. *PNAS* **111**:E5393–E5400. DOI: <https://doi.org/10.1073/pnas.1413339111>, PMID: 25453107
- Perelson AS**. 2002. Modelling viral and immune system dynamics. *Nature Reviews Immunology* **2**:28–36. DOI: <https://doi.org/10.1038/nri700>, PMID: 11905835
- Phillips AN**. 1996. Reduction of HIV concentration during acute infection: independence from a specific immune response. *Science* **271**:497–499. DOI: <https://doi.org/10.1126/science.271.5248.497>, PMID: 8560262
- Quiñones-Mateu ME**, Arts EJ. 2006. Virus fitness: concept, quantification, and application to HIV population dynamics. *Current Topics in Microbiology and Immunology* **299**:83–140. PMID: 16568897
- Reh L**, Magnus C, Schanz M, Weber J, Uhr T, Rusert P, Trkola A. 2015. Capacity of Broadly Neutralizing Antibodies to Inhibit HIV-1 Cell-Cell Transmission Is Strain- and Epitope-Dependent. *PLoS Pathogens* **11**:e1004966. DOI: <https://doi.org/10.1371/journal.ppat.1004966>, PMID: 26158270
- Rhee SY**, Gonzales MJ, Kantor R, Betts BJ, Ravela J, Shafer RW. 2003. Human immunodeficiency virus reverse transcriptase and protease sequence database. *Nucleic Acids Research* **31**:298–303. DOI: <https://doi.org/10.1093/nar/gkg100>, PMID: 12520007
- Ribeiro RM**, Qin L, Chavez LL, Li D, Self SG, Perelson AS. 2010. Estimation of the initial viral growth rate and basic reproductive number during acute HIV-1 infection. *Journal of Virology* **84**:6096–6102. DOI: <https://doi.org/10.1128/JVI.00127-10>, PMID: 20357090
- Russell RA**, Martin N, Mitar I, Jones E, Sattentau QJ. 2013. Multiple proviral integration events after virological synapse-mediated HIV-1 spread. *Virology* **443**:143–149. DOI: <https://doi.org/10.1016/j.virol.2013.05.005>, PMID: 23722103
- Sallusto F**, Lenig D, Förster R, Lipp M, Lanzavecchia A. 1999. Two subsets of memory T lymphocytes with distinct homing potentials and effector functions. *Nature* **401**:708–712. DOI: <https://doi.org/10.1038/44385>, PMID: 10537110
- Sanchez JL**, Hunt PW, Reilly CS, Hatano H, Beilman GJ, Khoruts A, Jasurda JS, Somsouk M, Thorkelson A, Russ S, Anderson J, Deeks SG, Schacker TW. 2015. Lymphoid fibrosis occurs in long-term nonprogressors and persists with antiretroviral therapy but may be reversible with curative interventions. *Journal of Infectious Diseases* **211**:1068–1075. DOI: <https://doi.org/10.1093/infdis/jiu586>, PMID: 25344521
- Shen L**, Peterson S, Sedaghat AR, McMahon MA, Callender M, Zhang H, Zhou Y, Pitt E, Anderson KS, Acosta EP, Siliciano RF. 2008. Dose-response curve slope sets class-specific limits on inhibitory potential of anti-HIV drugs. *Nature Medicine* **14**:762–766. DOI: <https://doi.org/10.1038/nm1777>, PMID: 18552857
- Sherer NM**, Lehmann MJ, Jimenez-Soto LF, Horensavitz C, Pypaert M, Mothes W. 2007. Retroviruses can establish filopodial bridges for efficient cell-to-cell transmission. *Nature Cell Biology* **9**:310–315. DOI: <https://doi.org/10.1038/ncb1544>, PMID: 17293854
- Sigal A**, Kim JT, Balazs AB, Dekel E, Mayo A, Milo R, Baltimore D. 2011. Cell-to-cell spread of HIV permits ongoing replication despite antiretroviral therapy. *Nature* **477**:95–98. DOI: <https://doi.org/10.1038/nature10347>, PMID: 21849975
- Sourisseau M**, Sol-Foulon N, Porrot F, Blanchet F, Schwartz O. 2007. Inefficient human immunodeficiency virus replication in mobile lymphocytes. *Journal of Virology* **81**:1000–1012. DOI: <https://doi.org/10.1128/JVI.01629-06>, PMID: 17079292

- Sowinski S**, Jolly C, Berninghausen O, Purbhoo MA, Chauveau A, Köhler K, Oddos S, Eissmann P, Brodsky FM, Hopkins C, Onfelt B, Sattentau Q, Davis DM. 2008. Membrane nanotubes physically connect T cells over long distances presenting a novel route for HIV-1 transmission. *Nature Cell Biology* **10**:211–219. DOI: <https://doi.org/10.1038/ncb1682>, PMID: 18193035
- Taylor S**, Boffito M, Khoo S, Smit E, Back D. 2007. Stopping antiretroviral therapy. *AIDS* **21**:1673–1682. DOI: <https://doi.org/10.1097/QAD.0b013e3281c61394>, PMID: 17690564
- Tenner-Racz K**, Stellbrink HJ, van Lunzen J, Schneider C, Jacobs JP, Raschdorff B, Grosschupff G, Steinman RM, Racz P. 1998. The unenlarged lymph nodes of HIV-1-infected, asymptomatic patients with high CD4 T cell counts are sites for virus replication and CD4 T cell proliferation. The impact of highly active antiretroviral therapy. *The Journal of Experimental Medicine* **187**:949–959. DOI: <https://doi.org/10.1084/jem.187.6.949>, PMID: 9500797
- Thomsen ER**, Mich JK, Yao Z, Hodge RD, Doyle AM, Jang S, Shehata SI, Nelson AM, Shapovalova NV, Levi BP, Ramanathan S. 2016. Fixed single-cell transcriptomic characterization of human radial glial diversity. *Nature Methods* **13**:87–93. DOI: <https://doi.org/10.1038/nmeth.3629>, PMID: 26524239
- Wawer MJ**, Gray RH, Sewankambo NK, Serwadda D, Li X, Laeyendecker O, Kiwanuka N, Kigozi G, Kiddugavu M, Lutalo T, Nalugoda F, Wabwire-Mangen F, Meehan MP, Quinn TC. 2005. Rates of HIV-1 transmission per coital act, by stage of HIV-1 infection, in Rakai, Uganda. *The Journal of Infectious Diseases* **191**:1403–1409. DOI: <https://doi.org/10.1086/429411>, PMID: 15809897
- Westendorp MO**, Frank R, Ochsenbauer C, Stricker K, Dhein J, Walczak H, Debatin KM, Krammer PH. 1995a. Sensitization of T cells to CD95-mediated apoptosis by HIV-1 Tat and gp120. *Nature* **375**:497–500. DOI: <https://doi.org/10.1038/375497a0>, PMID: 7539892
- Westendorp MO**, Shatrov VA, Schulze-Osthoff K, Frank R, Kraft M, Los M, Krammer PH, Dröge W, Lehmann V. 1995. HIV-1 Tat potentiates TNF-induced NF-kappa B activation and cytotoxicity by altering the cellular redox state. *The EMBO Journal* **14**:546–554. PMID: 7859743
- Wodarz D**, Levy DN. 2007. Human immunodeficiency virus evolution towards reduced replicative fitness in vivo and the development of AIDS. *Proceedings of the Royal Society B: Biological Sciences* **274**:2481–2491. DOI: <https://doi.org/10.1098/rspb.2007.0413>, PMID: 17666377
- Wu Y**, Beddall MH, Marsh JW. 2007. Rev-dependent indicator T cell line. *Current HIV Research* **5**:394–402. DOI: <https://doi.org/10.2174/157016207781024018>, PMID: 17627502
- Zeng M**, Haase AT, Schacker TW. 2012. Lymphoid tissue structure and HIV-1 infection: life or death for T cells. *Trends in Immunology* **33**:306–314. DOI: <https://doi.org/10.1016/j.it.2012.04.002>, PMID: 22613276
- Zhong P**, Agosto LM, Ilinskaya A, Dorjbal B, Truong R, Derse D, Uchil PD, Heidecker G, Mothes W. 2013. Cell-to-cell transmission can overcome multiple donor and target cell barriers imposed on cell-free HIV. *PLoS One* **8**: e53138. DOI: <https://doi.org/10.1371/journal.pone.0053138>, PMID: 23308151

Appendix 1

DOI: <https://doi.org/10.7554/eLife.30134.035>

Supplementary Mathematical Analysis for Jackson *et al.*

I Derivation of infection model assuming independence of infection and cell death

We consider a model of infection where r is the probability of one HIV DNA copy to successfully infect the cell and q is the probability of the cell to die as a result of the infection attempt. The probability of being infected when virions enter the cell is:

$$P_n = (1 - (1 - r)^n)(1 - q)^n. \tag{AE1}$$

If the number of infection attempts, n , is Poisson distributed with mean λ , the fraction of cells that are productively infected is:

$$\begin{aligned} P_\lambda &= e^{-\lambda} \sum_n \frac{\lambda^n}{n!} P_n = e^{-\lambda} \sum_n \frac{\lambda^n}{n!} (1 - (1 - r)^n)(1 - q)^n \\ &= e^{-\lambda} \sum_n \frac{(\lambda(1-q))^n}{n!} - \frac{(\lambda(1-r)(1-q))^n}{n!} \\ &= e^{-\lambda q} (1 - e^{-\lambda r(1-q)}). \end{aligned} \tag{AE2}$$

We introduce a drug strength value d , where $d = 1$ in the absence of drug and $d > 1$ in the presence of drug. In the presence of drug, λ is decreased to λ/d . The drug therefore tunes λ . The probability of a cell to be infected and live given drug strength d is therefore:

$$P_{\lambda/d} = e^{-\lambda q/d} (1 - e^{-\lambda r(1-q)/d}). \tag{AE3}$$

Experimentally, we measure P_λ , the number of infected cells, and L_λ , the number of live cells remaining two days post-infection for the cell line.

Assuming a Poisson distribution of the number of infection attempts, the probability of being productively infected is

$$P_\lambda = 1 - e^{-\lambda r} \Rightarrow r = -\frac{\log(1 - P_\lambda)}{\lambda}. \tag{AE4}$$

Similarly, the probability of a cell to live is

$$L_\lambda = e^{-\lambda q} \Rightarrow q = -\frac{\log(L_\lambda)}{\lambda}. \tag{AE5}$$

II Derivation of infection model assuming dependence of infection and cell death

Cellular infection and death may be the result of independent processes. For example, cell death may be a programmed response to DNA damage induced by the infection attempt and therefore may occur regardless of whether or not the cell is successfully infected. Infection and death may also be dependent. One example of dependence is the cytotoxicity mediated by expressed viral proteins after integration into the host genome.

In this case, the probability of productive infection and survival of the cell given n attempts is

$$P_n = \sum_{m=1}^n \binom{n}{m} (r'(1-q'))^m (1-r')^{n-m} \tag{AE6}$$

Here, r' and q' are the probabilities for infection and death respectively. Their relationship to the experimentally measured r and q are discussed in the next section. $[r'(1-q')]^m$ is the probability that m infection attempts are successful and none of the attempts triggers cell

death, while $(1 - r')^{n-m}$ accounts for $n - m$ unsuccessful infections. To obtain the total probability of productive infection without cell death given n attempts, we sum over all cases with $m' \geq 1$ successful infections.

Realizing that:

$$\sum_{m=1}^n \binom{n}{m} (r'(1-q'))^m (1-r')^{n-m} = \sum_{m=0}^n \binom{n}{m} (r(1-q))^m (1-r')^{n-m} - (1-r')^n = (r'(1-q') + (1-r'))^n - (1-r')^n, \quad (\text{AE7})$$

we can simplify the above to:

$$P_n = (r'(1-q') + (1-r'))^n - (1-r')^n = (1-r'q')^n - (1-r')^n. \quad (\text{AE8})$$

Averaging this over a Poisson distribution with mean λ , we find:

$$e^{-\lambda} \sum_n \frac{\lambda^n}{n!} P_n = e^{-\lambda} \sum_n \frac{\lambda^n}{n!} ((1-r'q')^n - (1-r')^n) = e^{-\lambda r'q'} - e^{-\lambda r'}. \quad (\text{AE9})$$

III Equivalence of the two models

The two models predict same dependence on λ (the difference of two exponentials) but the parameters r, q and r', q' play slightly different roles. The models are the same if:

$$r'q' = q \quad \text{and} \quad r' = r(1-q) + q. \quad (\text{AE10})$$

Hence the two models are a re-parametrization of the same process. The experimental measurement of r and q , as described in the main manuscript, consists of estimating r as the fraction of infected cells when the fraction of dead cells is low due to a low number of measured DNA copies per cell. The death rate q is derived by measuring the number of live cells remaining when the number of HIV DNA copies per cell is known. If the probability of death is dependent on infection, then death is only of infected cells and is a product of the probability to be infected and die ($r'q'$). Likewise, the underlying probability of infection r' will account for the fraction dead cells (q) and any cells which are infected but not dead ($r(1-q)$).

CHAPTER 3:

HIV cell-to-cell spread slows evolution of drug resistance

In chapter 2, I demonstrated that HIV infection modes resulted in differences in the survival of infected cells at intermediate drug concentrations. Next, I went on to investigate whether modes of HIV infection impact the rate of evolution of drug resistance. The results of this investigation are detailed in this chapter. My contributions to this work are as follows: conceptualization of the project, experimental design of evolution experiments, experimentally measuring the replication ratios of the mutant and wildtype viruses in cell-free infection and cell-to-cell spread, carrying out of evolution experiments in which a second ARV was added to the culture conditions after an initial period of monotherapy, preparation of DNA amplicons for sequencing, DNA library preparation for sequencing of two of the evolution experiments sequenced on the Ion Torrent platform, analyses of sequencing results, curation of data into figures and writing of the manuscript.

HIV cell-to-cell spread slows evolution of drug resistance

1 Jessica Hunter^{1,2}, Sandile Cele^{1,2}, Laurelle Jackson¹, Jennifer Giandhari³, Tulio de Oliveira³, Gila Lustig⁴, Alex Sigal^{1,2,5*},

2 **1** Africa Health Research Institute, Durban 4001, South Africa.

3 **2** School of Laboratory Medicine and Medical Sciences, University of KwaZulu-Natal, Durban, South Africa.

4 **3** KwaZulu-Natal Research Innovation and Sequencing Platform, Durban 4001, South Africa.

5 **4** Centre for the AIDS Programme of Research in South Africa, Durban 4001, South Africa.

6 **5** Max Planck Institute for Infection Biology, Berlin 10117, Germany.

7 * alex.sigal@ahri.org

8 Abstract

9 Many enveloped viruses such as HIV have transmit by two infection modes: cell-free infection and cell-to-cell spread. Cell-to-cell
10 spread is highly efficient as it involves directed viral transmission from the infected to the uninfected cell. In contrast, cell-free
11 infection relies on chance encounters between the virion and cell. Despite the higher efficiency of cell-to-cell spread, there
12 is substantial transmission by cell-free infection in conjunction with cell-to-cell spread. A possible reason is that cell-free
13 infection offers a selective advantage by increasing sensitivity to factors interfering with infection, hence accelerating selection
14 of resistance to these inhibitors relative to cell-to-cell spread alone. Here we investigated whether a combination of cell-free
15 infection and cell-to-cell spread confers a selective advantage in experimental evolution to an antiretroviral drug. We maintained
16 HIV infection using coculture of infected with uninfected cells in the face of moderate inhibition by the reverse transcriptase
17 inhibitor efavirenz. We tested the effect on the rate of drug resistance evolution of replacing one coculture infection cycle with
18 an infection cycle involving cell-free infection only, and observed earlier selection of drug resistance mutations to efavirenz.
19 When we increased selective pressure by adding a second reverse transcriptase inhibitor, emtricitabine, infection with the
20 cell-free step consistently resulted in the selection of multidrug resistance to both drugs and was able to replicate. In contrast,
21 infection without a cell-free step mostly failed to select multidrug resistance. Therefore, HIV cell-to-cell spread decreases the
22 ability of HIV to rapidly select for resistance to inhibitors, which is conferred by cell-free infection.

23 Author summary

24 Cell-to-cell spread of HIV differs from cell-free, diffusion-based HIV infection in that viral transmission is directed from the
25 infected to the uninfected cell through cellular interactions. Cell-to-cell spread has been recognized as a highly efficient infection
26 mode that is able to surmount inhibition by antibodies and antiretroviral drugs. However, the effect of HIV cell-to-cell spread
27 on the rate of selection of viral resistance to infection inhibitors has not been studied. Here we used experimental evolution to
28 investigate the effect of cell-to-cell spread versus cell-free infection on the emergence of drug resistance mutations to one or
29 a combination of antiretroviral drugs. We found that replacing one infection cycle in experimental evolution with cell-free
30 infection, where the filtered supernatant from infected cells, but not the cellular fraction, is used as the viral source, results
31 in more rapid evolution of resistance. The consequences are that multidrug resistance consistently evolves with a cell-free
32 viral cycle, but not when infection is solely by coculture of infected and uninfected cells. A possible consequence is that in
33 environments where HIV cell-to-cell spread may predominate and some residual viral replication occurs in the face of ART, the
34 emergence of drug resistance mutations would be delayed.

35 Introduction

36 Despite the overall success of antiretroviral therapy (ART) at suppressing HIV replication, evolution of drug resistance remains
37 a considerable concern as it leads to the replication of HIV in the face of ART due to acquisition of drug resistance mutations.
38 Incomplete viral suppression of HIV because of treatment interruptions (1–7), and lowered drug levels in some anatomical
39 compartments (8–12) contribute to the selection of drug resistance mutations (13, 14). Drug resistance mutations enable
40 HIV to replicate in the face of what should be suppressive ART concentrations if sufficient mutations are accumulated and
41 result in multidrug resistance (10, 15). The prevalence of drug resistance mutations in HIV infected individuals on ART is
42 about 10% (16, 17), (see also the WHO HIV Drug Resistance Report 2019 at <https://www.who.int/hiv/pub/drugresistance/hivdr-report-2019/en/>).

44 A mechanism for drug insensitivity distinct from acquisition of drug resistance mutations is HIV cell-to-cell spread (18–22).
45 Cell-to-cell spread involves the directed transmission of virions from one cell to another at close range, generally through a
46 virological synapse or other structure which minimizes the distance HIV has to diffuse to reach the uninfected cell (23–30) but
47 does not involve fusion (31). It has been shown to be an efficient mode of infection which decreases sensitivity to antiretroviral
48 drugs (18, 19, 32, 33) and neutralizing antibodies (34–37). It also allows infection under unfavourable conditions (36). This
49 includes infection of cells such as resting T cells and macrophages which have low numbers of CD4 entry receptors (38, 39). In
50 addition to increased efficiency, HIV cell-to-cell spread makes infection more rapid (22) and can more easily cross mucosal
51 barriers (40).

52 Despite the advantages to the virus of infecting by cell-to-cell spread, a considerable amount of virus is not localized to
53 cell-to-cell contacts (25) and transmits by cell-free infection (41–43). More generally, many enveloped viruses are able to infect
54 by both cell-to-cell and cell-free modes (44). This may occur because cell-to-cell spread can be cytotoxic (33, 45) or cell-free
55 virus is needed for transmission between individuals. Here we investigated the possibility that cell-free HIV infection, due to
56 its increased sensitivity to inhibitors, could confer a selective advantage by reducing the time to evolution of drug resistance
57 (8, 46, 47).

58 We performed *in vitro* evolution in the face of the antiretroviral drug efavirenz (EFV) using coculture of infected with
59 uninfected cells. We used a concentration of EFV similar to that predicted upon treatment interruption of several days, due
60 to the increased half-life of EFV relative to the other drug components of the ART regimen (7, 48–53). We introduced a
61 cell-free infection cycle, where we harvested the cell-free virus by filtering out the infected cells and used it as the sole infection
62 source for one infection cycle. The other infection cycles occurring by coculture of infected and uninfected cells which allows
63 cell-to-cell spread (18). We observed a faster fixation of an EFV drug resistance mutant with the cell-free infection cycle
64 relative to coculture alone. Upon transfer of infection with the cell-free step to a culture containing a two drug combination of
65 EFV and the reverse transcriptase inhibitor emtricitabine (FTC), infection containing a cell-free infection cycle was able to

66 evolve drug resistance to both drugs, while infection without the cell-free step failed to evolve multidrug resistance. Therefore,
67 cell-free infection confers the ability to rapidly evolve to selective pressure.

68 Results

69 **Faster evolution of drug resistance to EFV with cell-free infection.** We reasoned that in cell-to-cell spread, which occurs when
70 infected (donor) cells and uninfected (target) cells are cocultured, the frequency of a drug resistant mutant would rise gradually
71 in the face of moderate drug pressure. This would be because the mutant needs to supplant the still replicating drug sensitive
72 (wild-type) HIV genotype. In contrast, cell-free infection is more sensitive to inhibitors, and so wild-type virus would be
73 effectively cleared even at moderate levels of drug. This would rapidly increase the frequency of the drug resistant mutant
74 (Figure 1A).

75 To experimentally measure the effect of drug on wild-type and mutant virus in cell-free infection and cell-to-cell spread, we
76 determined the replication ratio for both infection modes in the face of 20nM of EFV. The replication ratio with cell-to-cell
77 spread (R_{cc}) was derived by measuring the number of infected cells (N_{out}) 2 days (approximately 1 viral cycle) post-infection
78 divided by the number of input infected cells (N_{in}). The cell-free replication ratio (R_{cf}) was derived as for cell-to-cell spread,
79 except that only the supernatant from N_{in} was used (Figure 1B). To determine R_{cf} , input was supernatant from 2×10^5
80 cells/mL infected with wild-type or the L100I EFV resistance mutant, where the L100I confers about 10-fold resistance to
81 EFV (<https://hivdb.stanford.edu/cgi-bin/PositionPhenoSummary.cgi>). We obtained a mean N_{out} of $1.8 \times 10^4 \pm 7.9 \times 10^3$
82 infected cells for the cell-free infection with wild-type virus. When L100I mutant virus was used, the mean N_{out} increased
83 to $8.3 \times 10^5 \pm 1.8 \times 10^4$. To measure R_{cc} , we used a lower input of 1×10^4 /mL of cells infected with wild-type or the L100I
84 EFV resistance mutant to prevent saturation of infection. We obtained a mean N_{out} of $5.5 \times 10^4 \pm 1.7 \times 10^4$ for infection
85 with wild-type and $2.8 \times 10^5 \pm 5.4 \times 10^4$ for infection with the L100I mutant virus respectively. The mean R_{cf} was therefore
86 0.039 ± 0.032 for wild-type virus and 2.0 ± 0.16 for the L100I mutant (Figure 1C). The mean R_{cc} was 5.5 ± 1.7 for wild-type
87 virus and 28 ± 5.4 for the L100I mutant. Therefore, the effect of 20nM of EFV on coculture infection was moderate: wild-type
88 infection could still replicate and expand, as $R > 1$. In contrast, the effect of EFV on cell-free infection of wild-type was much
89 stronger. R_{cc} of the L100I mutant was approximately 5-fold higher compared to wild-type. In contrast, the L100I mutant
90 increased R_{cf} approximately 50-fold. To determine the expected effect of this difference, we calculated the expected frequency
91 of the drug resistant mutant in the total viral pool over time (Figure 1D, Materials and Methods) starting from the measured
92 frequency of the L100I mutant (SFig. 1). We either included or excluded one cell-free infection step at the first infection cycle.
93 The calculation showed that with an initial cell-free infection cycle, the frequency of the L100I EFV resistant mutant was
94 substantially higher at the initial timepoints relative to cell-to-cell spread alone. At later timepoints post-infection, the L100I
95 mutant supplanted the wild-type whether or not a cell-free step was included.

96 To examine whether a cell-free infection step could accelerate evolution of drug resistance, we performed *in vitro* evolution
97 experiments in the face of 20nM EFV by the coculture of infected with uninfected cells. Two cycles of infection were first
98 performed in the absence of drug to obtain a quasispecies (Materials and Methods), allowing selection from a pre-existing
99 pool of single drug resistant mutations which were present at a low but detectable frequency (SFig. 1). Ongoing infection was
100 maintained in the presence of drug by the addition of new uninfected cells every 2 days (Figure 2A). We included a cell-free
101 infection cycle by pelleting the infected cells and filtering the supernatant to obtain cell-free virus and infected cells from
102 the same infected cell population. We then infected new cells by using either the entire cellular fraction or the entire filtered
103 supernatant from the cellular fraction during the first infection cycle in the presence of EFV (Figure 2A). In the latter case,
104 infection would be exclusively by the cell-free mode. 20nM EFV monotherapy, the drug concentration used, may occur in
105 individuals on EFV based ART regimen after several days of treatment interruption due to the longer half-life of EFV relative
106 to other common ART components (7, 48–53).

107 Upon passaging of infection with 20nM EFV, we obtained evolution of the L100I drug resistance mutation (Figure 2B),
108 and with a delay the K103N drug resistance mutation in two out of three experiments (Figure 2C). The K103N is the more
109 commonly detected EFV resistance mutation in the clinical setting and confers approximately 20-fold resistance to EFV
110 (<https://hivdb.stanford.edu/cgi-bin/PositionPhenoSummary.cgi>).

111 In all experiments, a cell-free infection cycle led to a more rapid increase in and higher final frequencies of the L100I
112 mutation. By day 12 post-infection, mean mutant frequency was 0.58 ± 0.040 for evolution with a cell-free infection cycle, and
113 0.11 ± 0.076 without the cell-free infection cycle.

114 The increase in frequency of the K103N mutation was also accelerated for infection with a cell-free infection cycle in
115 experiments where the K103N evolved to substantial levels. Mean K103N mutant frequency at day 12 post-infection was
116 0.21 ± 0.15 in the infection with a cell-free step, and 0.035 ± 0.027 when infection was in the absence of the cell-free step.
117 Therefore, adding a cell-free infection cycle increased the frequencies of both drug resistance mutations in the experiments
118 where they evolved.

119 **Cell-free infection but not cell-to-cell spread leads to the evolution of multidrug resistance.** To determine whether infection
120 with a cell-free step under EFV alone conferred a selective advantage to HIV with a combination of drugs, we added a second
121 drug (FTC) after a period of monotherapy with EFV. As before, the supernatant containing cell-free virus was separated and
122 used to establish an infection with a cell-free step in the face of EFV. The cellular fraction was used for infection without
123 a cell-free infection cycle in the face of EFV. Evolution was carried out at 20nM EFV for the first 3 viral cycles (6 days).
124 Thereafter, a drug combination of 20nM EFV and 770nM FTC was used, where the FTC concentration used similar to that

found in study participants on ART (48, 54, 55). Infected cells were transferred from the one drug to the two drug regimen so that in the two drug regimen infection was initiated with 1% infected cells.

We performed three evolution experiments where we tracked the frequency of drug resistance mutations through time (Figure 3). We observed an increase in the frequency of multidrug resistance (mutations to both EFV and FTC) in the presence of the cell-free step: The EFV resistance mutations L100I or K103N were linked to FTC mutations M184V or M184I. Both M184V and M184I confer high level resistance to FTC (<https://hivdb.stanford.edu/cgi-bin/PositionPhenoSummary.cgi>).

In the first experiment, the infection with a cell-free step evolved the L100I single mutant by day 6 under EFV monotherapy (SFig. 2A). This mutation was supplanted by the K103N single mutant and the L100I/M184I, K103N/M184I, and K103N/M184V multidrug resistant mutants during evolution in the face of EFV and FTC. The K103N and the L100I M184I variants were in turn out-competed, with the K103N/M184I and K103N/M184V multidrug resistant mutants dominating by day 16 (Figure 3, blue squares and diamonds, respectively). In the second experiment, the infection with a cell-free step showed detectable L100I at day 6 (SFig. 2A). The L100I/M184I arose to detectable levels by day 14 and dominated infection by day 18 of the experiment (Figure 3, blue circles). In the third experiment, by day 6 the infection with a cell-free step evolved the L100I mutation to a frequency of 0.4 (SFig. 2A). This mutant was supplanted by the L100I/M184I and L100I/M184V multidrug resistance mutants in the presence of the combined regimen of EFV and FTC (Figure 3, blue circles and triangles, respectively).

Infection without a cell-free step failed to evolve multidrug resistance (Figure 3). The only possible exception was the L100I M184I resistance mutant, which started to be detectable on day 22 of experiment 2 (Figure 3, red circles).

Increased drug pressure leads to more rapid evolution of drug resistance in the absence of cell-free infection. The slower evolution of drug resistant mutations without a cell-free step is consistent with the drug exerting weaker selective pressure in cell-to-cell spread compared with cell-free infection (18, 33). To test the result of increasing selective pressure, we performed the evolution experiments using a higher EFV concentration of 40nM. As previously, the cell-free and cellular fractions were separated from the same infected cell population. The infected cells were used to establish an infection without a cell-free step. After passaging the infection at 40nM EFV, there was an increase in both the rate of evolution as well as the maximal frequency of the L100I mutation (Figure 4A) and the K103N mutation (Figure 4B) when compared to 20nM EFV. Mean mutant frequency for the L100I mutant at day 8 was 0.43 ± 0.15 for infection in the face of 40nM EFV, close to its maximum value in these experiments. In contrast, the L100I frequency was 0.11 ± 0.036 at 20nM EFV. Similarly, the K103N mutant reached its maximum frequency by day 8 at 40nM. The mean K103N frequency at day 8 at 20nM was 0.094 ± 0.070 . In contrast, the frequency was 0.018 ± 0.0035 at 20nM EFV. Therefore, addition of selective pressure by increasing drug concentration results in more rapid evolution by cell-to-cell spread.

Increased drug pressure leads to a minor increase in drug resistance frequency with cell-free infection. We asked whether the evolution of drug resistant mutations with a cell-free step would be further accelerated if drug pressure was increased. We therefore performed the experiments using 40nM EFV, as above, except that the cell-free fraction was used to establish the infection in the face of drug. Interestingly, when we compared the result to the same experiment carried out at 20nM EFV, there was a minor difference in the time to maximal frequency of the L100I mutation (Figure 5A). The L100I mutation frequency reached the near maximal mutation frequency on day 6 for 40nM EFV and day 8 for 20nM EFV. The maximal difference in frequency occurred on day 6, with mean frequency being 0.62 ± 0.080 at 40nM EFV and 0.35 ± 0.28 at 20nM EFV. The rate and the maximal frequency of the K103N mutation for the infection with a cell-free step was moderately increased at 40nM EFV compared to 20nM EFV. (Figure 5B). At the last timepoint tested (day 12), mean frequency for K103N was 0.41 ± 0.20 at 40nM EFV, compared to 0.22 ± 0.16 at 20nM EFV. Therefore, while higher EFV led to an increase in the rate of selection of K103N, 20nM EFV was close to the maximal selective pressure required for rapid evolution of L100I.

Discussion

Materials and Methods

Inhibitors, viruses and cell lines. The antiretrovirals EFV and FTC were obtained through the AIDS Research and Reference Reagent Program, National Institute of Allergy and Infectious Diseases, National Institutes of Health. HIV molecular clone pNL4-3 was obtained from M. Martin. Viral stocks of NL43 were produced by transfection of HEK293 cells with the molecular clone plasmid using TransIT-LT1 (Mirus) transfection reagent. Supernatant containing released virus was harvested two days post-transfection and filtered through a 0.45 micron filter (GVS). The supernatant containing virus was stored in 0.5ml aliquots at -80°C . The L100I pNL4-3 molecular clone was generated as previously described (33). RevCEM cells were obtained from Y. Wu and J. Marsh. RevCEM-E7 cells were generated as described in (22). Briefly, the E7 clone was generated by subcloning RevCEM cells at single cell density. Surviving clones were subdivided into replicate plates. One of the plates was screened for the fraction of GFP expressing cells upon HIV infection using microscopy, and the clone with the highest fraction of GFP positive cells was selected. Cells were cultured in complete RPMI 1640 supplemented with L-Glutamine, sodium pyruvate, HEPES, non-essential amino acids (Lonza), and 10% heat-inactivated FBS (Hyclone).

Measurement of replication ratios for cell-to-cell spread and cell-free infection. To calculate the replication ratio for cell-free infection (R_{cf}), the supernatant of 2×10^5 infected RevCEM-E7 cells were used as the input to 10^6 cells/ml uninfected target RevCEM-E7 cells. For the calculation of the cell-to-cell replication ratio (R_{cc}), 1×10^4 infected donor RevCEM-E7 cells were

181 added as the input to 10^6 cells/ml uninfected target cells. After 48 hours of incubation at $37^\circ C$, the number of output infected
 182 cells determined by flow cytometry as the number of GFP expressing cells.

183 **Calculation of mutant frequency with and without a cell-free infection step.** The calculation was performed using a Matlab
 184 2019a script where mutant frequency was calculated as:

$$F_i^{mt} = N_i^{mt} / (N_i^{mt} + N_i^{wt}).$$

185 Here N_i^{mt} and N_i^{wt} are the number of mutant and wild-type infected cells at infection cycle i , where each infection cycle is
 186 approximately 2 days.

187 N_i^{mt} and N_i^{wt} are determined as:

$$N_i = RN_{i-1}.$$

188 Here R is the replication ratio of the infection for wild-type or mutant virus using the cell-free infection (R_{cf}) or cell-to-cell
 189 spread (R_{cc}), and N_{i-1} is the number of wild-type or mutant infected cells in the previous infection cycle.

190 If a cell-free step was included, the first infection cycle uses R_{cf}^{mt} and R_{cf}^{wt} and the number of infected cells for mutant
 191 infection is calculated as:

$$N_i^{mt} = R_{cf}^{mt} F_0^{mt} N_0.$$

192 Similarly for wild-type virus,

$$N_i^{wt} = R_{cf}^{wt} F_0^{wt} N_0.$$

193 Here F_0^{mt} is the measured initial mutant frequency, where the frequency for the L100I mutant was used ($\mu = 5 \times 10^{-3}$, $\sigma =$
 194 5×10^{-3}) and $F_0^{wt} = 1 - F_0^{mt}$. N_0 is the initial number of infected cells and can be arbitrary.

195 If a cell-free step was excluded, and for all viral cycles after $i = 1$, the calculation uses R_{cc}^{mt} and R_{cc}^{wt} , and the number of
 196 infected cells for mutant infection is calculated as:

$$N_i^{mt} = R_{cc}^{mt} N_{i-1}^{mt}.$$

197 Similarly for wild-type virus,

$$N_i^{wt} = R_{cc}^{wt} N_{i-1}^{wt}.$$

198 **Evolution Experiments.** Two rounds of infection were performed in the absence of drug to establish a quasispecies, followed
 199 by multiple rounds of infection in the presence of EFV or EFV and FTC. The first round of infection in the absence of drug
 200 was initiated by cell-free infection of 2.5×10^6 RevCEM-E7 cells with 5×10^8 viral copies of HIV NL4-3 and incubated for 48
 201 hours. In the second round of infection, cells infected in the first round were added to 3×10^6 uninfected RevCEM-E7 cells to
 202 a final concentration of 0.5% infected cells and incubated for 48 hours. The infection was then separated into infected cells
 203 and cell-free virus by centrifugation at 300 g for 5 minutes followed by filtration of the supernatant through a 0.45 micron
 204 filter (GVS). 1.2×10^6 infected cells or supernatant from 1.2×10^6 infected cells were added to new uninfected target cells
 205 such that the final number of cells in the culture was 6×10^6 at a concentration of 1×10^6 cells/ml. EFV at a concentration of
 206 20nM or 40nM was then added to the cultures. Thereafter, cultures were maintained every 48 hours by the addition of
 207 new uninfected target cells at a 1 : 3 ratio of infected to fresh cells. In the experiments where FTC was added, FTC at the
 208 concentration of 770nM in addition to the the EFV was added 4 days after addition of 20nM EFV alone. Thereafter, cultures
 209 were maintained at a maximum of 1% infected cells by adding fresh cells every 48 hours.

210 **Sequencing for detection of drug resistant mutants.** Genomic DNA from approximately $10^5 - 10^6$ cells was extracted from
 211 the cultures of the evolution experiments every 48 hours using *Quick-DNA* miniprep kits (Zymo Research). The HIV
 212 RT gene amplified by PCR from the proviral RNA using Phusion hot start II DNA polymerase (New England Bio-
 213 labs) PCR reaction mix. The amplicons were sequenced either by Illumina Miseq or Ion Torrent PGM. Illumina for-
 214 ward primer was 5'-tcgtcggcagcgtcagatgtgtataagagacag TTAATAAGAGAACTCAAGATTTTC-3' and the reverse primer
 215 5'-gtctcgtgggctcggagatgtgtataagagacag CAGCACTATAGGCTGTACTGTC-3', where lower case sequences are adaptors for
 216 Illumina sequencing. Ion Torrent forward primer was 5'-TTAATAAGAGAACTCAAGATTTTC-3' and reverse primer was
 217 5'-CATCTGTTGAGGTTGGGATTTACC-3'. The PCR amplicons were visualized on a 1% agarose gel and bands of the
 218 correct size were excised an X-tracta Gel Extraction Tool (Sigma) and product extracted using the QIAquick gel extraction kit
 219 (Qiagen). Input DNA for sequencing was quantified using the Qubit dsDNA HS Assay system. For Illumina sequencing, input
 220 DNA was diluted in molecular-grade water to reach the starting concentration of $0.2\text{ng}/\mu\text{l}$. Barcodes were added to each sample
 221 using the Nextera XT Index kit (Illumina, Whitehead Scientific, SA). Barcoded amplicons were purified using Ampure XP
 222 beads (Beckman Coulter, Atlanta, Georgia) and fragment analysis was performed using the LabChip GX Touch (Perkin Elmer,
 223 Waltham, US). The library was pooled at a final concentration of 4nM and further diluted to 3pM. The library was spiked with
 224 20% PhiX plasmid due to the low diversity of the amplicon library. The spiked library was run on a Miseq v2 with a Nano
 225 Reagent kit (Illumina). For Ion Torrent sequencing, input DNA was purified using AMPure XP beads (Beckman Coulter,

Atlanta, Georgia). Barcoded adapters were added using Ion Plus Fragment Library Kit (Thermo Fisher Scientific) according to manufacturers instructions. Barcoded amplicons were quantified by qPCR using Ion library Quantitation Kit (Thermo Fisher Scientific) and diluted to a concentration of 100pM. Libraries were then pooled and loaded onto chips and sequenced on Ion Torrent PGM using Ion PGM Hi-Q Sequencing Kit (Thermo Fisher Scientific). Fast-q or BAM files from sequencing runs were analysed in Geneious. Drug resistant mutations were found based on a minimum variant frequency of 10^{-3} .

Acknowledgments

This work was supported by National Institute of Allergy and Infectious Diseases, National Institutes of Health Grant 1R01AI138546. JH is supported by a fellowship from the South African National Research Foundation.

References

1. Michael Rosenblum, Steven G Deeks, Mark van der Laan, and David R Bangsberg. The risk of virologic failure decreases with duration of HIV suppression, at greater than 50% adherence to antiretroviral therapy. *PLoS one*, 4(9):e7196, 2009.
2. David R Bangsberg, Andrew R Moss, and Steven G Deeks. Paradoxes of adherence and drug resistance to HIV antiretroviral therapy. *Journal of Antimicrobial Chemotherapy*, 53(5):696–699, 2004.
3. Jessica H Oyugi, Jayne Byakika-Tusiime, Kathleen Ragland, Oliver Laeyendecker, Roy Mugerwa, Cissy Kityo, Peter Mugenyi, Thomas C Quinn, and David R Bangsberg. Treatment interruptions predict resistance in HIV-positive individuals purchasing fixed-dose combination antiretroviral therapy in kampala, uganda. *AIDS*, 21(8):965–971, 2007.
4. Jean-Jacques Parienti, Moupali Das-Douglas, Veronique Massari, David Guzman, Steven G Deeks, Renaud Verdon, and David R Bangsberg. Not all missed doses are the same: sustained nrti treatment interruptions predict HIV rebound at low-to-moderate adherence levels. *PLoS one*, 3(7):e2783, 2008.
5. Jean-Jacques Parienti, Veronique Massari, Diane Descamps, Astrid Vabret, Elisabeth Bouvet, Bernard Larouzé, and Renaud Verdon. Predictors of virologic failure and resistance in HIV-infected patients treated with nevirapine-or efavirenz-based antiretroviral therapy. *Clinical Infectious Diseases*, 38(9):1311–1316, 2004.
6. Nicholas Musinguzi, Rain A Mocello, Yap Boum, Peter W Hunt, Jeffrey N Martin, Jessica E Haberer, David R Bangsberg, and Mark J Siedner. Duration of viral suppression and risk of rebound viremia with first-line antiretroviral therapy in rural uganda. *AIDS and behavior*, 21(6):1735–1740, 2017.
7. B. L. Genberg, I. B. Wilson, D. R. Bangsberg, J. Arnsten, K. Goggin, R. H. Remien, J. Simoni, R. Gross, N. Reynolds, M. Rosen, and H. Liu. Patterns of antiretroviral therapy adherence and impact on HIV RNA among patients in North America. *AIDS*, 26(11):1415–1423, Jul 2012.
8. Daniel IS Rosenbloom, Alison L Hill, S Alireza Rabi, Robert F Siliciano, and Martin A Nowak. Antiretroviral dynamics determines HIV evolution and predicts therapy outcome. *Nature medicine*, 18(9):1378, 2012.
9. Thomas B Kepler and Alan S Perelson. Drug concentration heterogeneity facilitates the evolution of drug resistance. *Proceedings of the National Academy of Sciences*, 95(20):11514–11519, 1998.
10. Stefany Moreno-Gamez, Alison L Hill, Daniel IS Rosenbloom, Dmitri A Petrov, Martin A Nowak, and Pleuni S Pennings. Imperfect drug penetration leads to spatial monotherapy and rapid evolution of multidrug resistance. *Proceedings of the National Academy of Sciences*, 112(22):E2874–E2883, 2015.
11. Philip Greulich, Bartłomiej Waclaw, and Rosalind J Allen. Mutational pathway determines whether drug gradients accelerate evolution of drug-resistant cells. *Physical review letters*, 109(8):088101, 2012.
12. C. V. Fletcher, K. Staskus, S. W. Wietgreffe, M. Rothenberger, C. Reilly, J. G. Chipman, G. J. Beilman, A. Khoruts, A. Thorkelson, T. E. Schmidt, J. Anderson, K. Perkey, M. Stevenson, A. S. Perelson, D. C. Douek, A. T. Haase, and T. W. Schacker. Persistent HIV-1 replication is associated with lower antiretroviral drug concentrations in lymphatic tissues. *Proc Natl Acad Sci U S A*, 111(6):2307–12, 2014. ISSN 1091-6490 (Electronic) 0027-8424 (Linking). URL <https://www.ncbi.nlm.nih.gov/pubmed/24469825>.
13. Soo-Yon Rhee, Matthew J Gonzales, Rami Kantor, Bradley J Betts, Jaideep Ravela, and Robert W Shafer. Human immunodeficiency virus reverse transcriptase and protease sequence database. *Nucleic acids research*, 31(1):298–303, 2003.
14. Annemarie M Wensing, Vincent Calvez, Francesca Ceccherini-Silberstein, Charlotte Charpentier, Huldrych F Günthard, Roger Paredes, Robert W Shafer, and Douglas D Richman. 2019 update of the drug resistance mutations in hiv-1. *Topics in antiviral medicine*, 27(3):111, 2019.
15. Alison Feder, Kristin Harper, and Pleuni S Pennings. Challenging conventional wisdom on the evolution of resistance to multi-drug hiv treatment: Lessons from data and modeling. *bioRxiv*, page 807560, 2019.
16. Ravindra K Gupta, Michael R Jordan, Binta J Sultan, Andrew Hill, Daniel HJ Davis, John Gregson, Anthony W Sawyer, Raph L Hamers, Nicaise Ndembu, Deenan Pillay, et al. Global trends in antiretroviral resistance in treatment-naive individuals with hiv after rollout of antiretroviral treatment in resource-limited settings: a global collaborative study and meta-regression analysis. *The Lancet*, 380(9849):1250–1258, 2012.
17. G Rocheleau, CJ Brumme, J Shoveller, VD Lima, and PR Harrigan. Longitudinal trends of hiv drug resistance in a large canadian cohort, 1996–2016. *Clinical Microbiology and Infection*, 24(2):185–191, 2018.
18. Alex Sigal, Jocelyn T Kim, Alejandro B Balazs, Erez Dekel, Avi Mayo, Ron Milo, and David Baltimore. Cell-to-cell spread of HIV permits ongoing replication despite antiretroviral therapy. *Nature*, 477(7362):95, 2011.
19. Christopher JA Duncan, Rebecca A Russell, and Quentin J Sattentau. High multiplicity HIV-1 cell-to-cell transmission from macrophages to cd4+ t cells limits antiretroviral efficacy. *AIDS (London, England)*, 27(14):2201, 2013.
20. Laurelle Jackson, Sandile Cele, Gila Lustig, Jennifer Giandhari, Tulio de Oliveira, Richard Neher, and Alex Sigal. Complementation can maintain a quasispecies of drug sensitive and resistant HIV. *bioRxiv*, 2020.
21. Ana Moyano, Gila Lustig, Hylton E Rodell, Tibor Antal, and Alex Sigal. Interference with hiv infection of the first cell is essential for viral clearance at sub-optimal levels of drug inhibition. *PLOS Computational Biology*, 16(2):e1007482, 2020.
22. Mikaël Boullé, Thorsten G Müller, Sabrina Dähling, Yashica Ganga, Laurelle Jackson, Deeqa Mahamed, Lance Oom, Gila Lustig, Richard A Neher, and Alex Sigal. HIV cell-to-cell spread results in earlier onset of viral gene expression by multiple infections per cell. *PLoS pathogens*, 12(11):e1005964, 2016.
23. Clare Jolly, Kirk Kashafi, Michael Hollinshead, and Quentin J Sattentau. HIV-1 cell to cell transfer across an env-induced, actin-dependent synapse. *Journal of Experimental Medicine*, 199(2):283–293, 2004.
24. S. Sowinski, C. Jolly, O. Berninghausen, M. A. Purbhoo, A. Chauveau, K. K?hler, S. Oddos, P. Eissmann, F. M. Brodsky, C. Hopkins, B. Onfelt, Q. Sattentau, and D. M. Davis. Membrane nanotubes physically connect T cells over long distances presenting a novel route for HIV-1 transmission. *Nat. Cell Biol.*, 10(2):211–219, Feb 2008.
25. Wolfgang Hübner, Gregory P Mc Nerney, Ping Chen, Benjamin M Dale, Ronald E Gordon, Frank YS Chuang, Xiao-Dong Li, David M Asmuth, Thomas Huser, and Benjamin K Chen. Quantitative 3d video microscopy of HIV transfer across t cell virological synapses. *Science*, 323(5922):1743–1747, 2009.
26. L. Wang, S. Izadmehr, E. Kamau, X. P. Kong, and B. K. Chen. Sequential trafficking of Env and Gag to HIV-1 T cell virological synapses revealed by live imaging. *Retrovirology*, 16(1):2, 01 2019.
27. Dominika Rudnicka, Jérôme Feldmann, Françoise Porrot, Steve Wietgreffe, Stéphanie Guadagnini, Marie-Christine Prévost, Jérôme Estaquier, Ashley T Haase, Nathalie Sol-Foulon, and Olivier Schwartz. Simultaneous cell-to-cell transmission of human immunodeficiency virus to multiple targets through polysynapses. *Journal of virology*, 83(12):6234–6246, 2009.
28. Nathan M Sherer, Maik J Lehmann, Luisa F Jimenez-Soto, Christina Horensavitz, Marc Pypaert, and Walther Mothes. Retroviruses can establish filopodial bridges for efficient cell-to-cell transmission. *Nature cell biology*, 9(3):310, 2007.
29. Benjamin M Dale, Raymond A Alvarez, and Benjamin K Chen. Mechanisms of enhanced hiv spread through t-cell virological synapses. *Immunological reviews*, 251(1):113–124, 2013.
30. Alex Sigal and David Baltimore. As good as it gets? the problem of HIV persistence despite antiretroviral drugs. *Cell host & microbe*, 12(2):132–138, 2012.
31. Blandine Monel, Elodie Beaumont, Daniela Vendrame, Olivier Schwartz, Denys Brand, and Fabrizio Mammano. Hiv cell-to-cell transmission requires the production of infectious virus particles and does not proceed through env-mediated fusion pores. *Journal of virology*, 86(7):3924–3933, 2012.
32. Luis M Agosto, Pradeep D Uchil, and Walther Mothes. HIV cell-to-cell transmission: effects on pathogenesis and antiretroviral therapy. *Trends in microbiology*, 23(5):289–295, 2015.
33. Laurelle Jackson, Jessica Hunter, Sandile Cele, Isabella Markham Ferreira, Andrew C Young, Farina Karim, Rajhmun Madansein, Kaylesh J Dullabh, Chih-Yuan Chen, Noel J Buckels, Yashica Ganga, Khadija Khan, Mikael Boulle, Gila Lustig, Richard A Neher, and Alex Sigal. Incomplete inhibition of HIV infection results in more HIV infected lymph node cells by reducing cell death. *eLife*, 7:e30134, 2018.
34. Irene A Abela, Livia Berlinger, Merle Schanz, Lucy Reynell, Huldrych F Günthard, Peter Rusert, and Alexandra Trkola. Cell-cell transmission enables HIV-1 to evade inhibition by potent cd4bs directed antibodies. *PLoS pathogens*, 8(4):e1002634, 2012.
35. Christopher JA Duncan, James P Williams, Torben Schifflner, Kathleen Gärtner, Christina Ochsenbauer, John Kappes, Rebecca A Russell, John Frater, and Quentin J Sattentau. High-multiplicity HIV-1 infection and neutralizing antibody evasion mediated by the macrophage-t cell virological synapse. *Journal of virology*, 88(4):2025–2034, 2014.

- 302 36. Peng Zhong, Luis M Agosto, Anna Ilinskaya, Batsukh Dorjbal, Rosaline Truong, David Derse, Pradeep D Uchil, Gisela Heidecker, and Walther Mothes. Cell-to-cell transmission can overcome
303 multiple donor and target cell barriers imposed on cell-free HIV. *PLoS one*, 8(1):e53138, 2013.
- 304 37. Torben Schiffner, Quentin J Sattentau, and Christopher JA Duncan. Cell-to-cell spread of hiv-1 and evasion of neutralizing antibodies. *Vaccine*, 31(49):5789–5797, 2013.
- 305 38. Luis M Agosto, Melissa B Herring, Walther Mothes, and Andrew J Henderson. HIV-1-infected cd4+ t cells facilitate latent infection of resting cd4+ t cells through cell-cell contact. *Cell reports*, 24(8):
306 2088–2100, 2018.
- 307 39. Amy E Baxter, Rebecca A Russell, Christopher JA Duncan, Michael D Moore, Christian B Willberg, Jose L Pablos, Andrés Finzi, Daniel E Kaufmann, Christina Ochsenbauer, John C Kappes, Fedde
308 Groot, and Quentin J Sattentau. Macrophage infection via selective capture of HIV-1-infected cd4+ t cells. *Cell host & microbe*, 16(6):711–721, 2014.
- 309 40. Dror Kolodkin-Gal, Sandrine L Hulot, Birgit Koriath-Schmitz, Randi B Gombos, Yi Zheng, Joshua Owuor, Michelle A Lifton, Christian Ayeni, Robert M Najarian, Wendy W Yeh, et al. Efficiency of
310 cell-free and cell-associated virus in mucosal transmission of human immunodeficiency virus type 1 and simian immunodeficiency virus. *Journal of virology*, 87(24):13589–13597, 2013.
- 311 41. Marion Sourisseau, Nathalie Sol-Foulon, Françoise Porrot, Fabien Blanchet, and Olivier Schwartz. Inefficient human immunodeficiency virus replication in mobile lymphocytes. *Journal of virology*,
312 81(2):1000–1012, 2007.
- 313 42. Natalia L Komarova, Daniela Anghelina, Igor Voznesensky, Benjamin Trinité, David N Levy, and Dominik Wodarz. Relative contribution of free-virus and synaptic transmission to the spread of HIV-1
314 through target cell populations. *Biology letters*, 9(1):20121049, 2013.
- 315 43. Shingo Iwami, Junko S Takeuchi, Shinji Nakaoka, Fabrizio Mammano, François Clavel, Hisashi Inaba, Tomoko Kobayashi, Naoko Misawa, Kazuyuki Aihara, Yoshio Koyanagi, et al. Cell-to-cell
316 infection by hiv contributes over half of virus infection. *Elife*, 4:e08150, 2015.
- 317 44. Q. Sattentau. Avoiding the void: cell-to-cell spread of human viruses. *Nat Rev Microbiol*, 6(11):815–26, 2008. ISSN 1740-1534 (Electronic) 1740-1526 (Linking). . URL <https://www.ncbi.nlm.nih.gov/pubmed/18923409>.
- 318 45. Nicole LK Galloway, Gilad Doitsh, Kathryn M Monroe, Zhiyuan Yang, Isa Muñoz-Arias, David N Levy, and Warner C Greene. Cell-to-cell transmission of hiv-1 is required to trigger pyroptotic death
319 of lymphoid-tissue-derived cd4 t cells. *Cell reports*, 12(10):1555–1563, 2015.
- 320 46. Martin Nowak and Robert M May. *Virus dynamics: mathematical principles of immunology and virology: mathematical principles of immunology and virology*. Oxford University Press, UK, 2000.
- 321 47. Libin Rong, Michael A Gilchrist, Zhilan Feng, and Alan S Perelson. Modeling within-host hiv-1 dynamics and the evolution of drug resistance: trade-offs between viral enzyme function and drug
322 susceptibility. *Journal of Theoretical biology*, 247(4):804–818, 2007.
- 323 48. Gila Lustig, Sandile Cele, Farina Karim, Yashica Ganga, Khadija Khan, Bernadette Gosnell, Yunus Moosa, Rohen Harrichandparsad, Suzaan Marais, Ravindra K Gupta, Derache Anne, Jennifer
324 Giandhari, Tulio de Oliveira, Katya Govender, John Adamson, Vinod Patel, and Alex Sigal. The cns in the face of art contains t cell origin HIV which can lead to drug resistance. *bioRxiv*,
325 <https://doi.org/10.1101/588426>, 2019.
- 326 49. Peter L Anderson, Jennifer J Kiser, Edward M Gardner, Joseph E Rower, Amie Meditz, and Robert M Grant. Pharmacological considerations for tenofovir and emtricitabine to prevent HIV infection.
327 *Journal of Antimicrobial Chemotherapy*, 66(2):240–250, 2010.
- 328 50. Saskia ME Vrouwenraets, Ferdinand WNM Wit, Jacqueline van Tongeren, and Joep MA Lange. Efavirenz: a review. *Expert opinion on pharmacotherapy*, 8(6):851–871, 2007.
- 329 51. Stephen Taylor, Marta Boffito, Saye Khoo, Erasmus Smit, and David Back. Stopping antiretroviral therapy. *Aids*, 21(13):1673–1682, 2007.
- 330 52. H. J. Ribaud, D. W. Haas, C. Tierney, R. B. Kim, G. R. Wilkinson, R. M. Gulick, D. B. Clifford, C. Marzolini, C. V. Fletcher, K. T. Tashima, D. R. Kuritzkes, and E. P. Acosta. Pharmacogenetics of
331 plasma efavirenz exposure after treatment discontinuation: an Adult AIDS Clinical Trials Group Study. *Clin. Infect. Dis.*, 42(3):401–407, Feb 2006.
- 332 53. Jonathan Shuter. Forgiveness of non-adherence to HIV-1 antiretroviral therapy. *Journal of Antimicrobial Chemotherapy*, 61(4):769–773, 2008.
- 333 54. B. M. Best, P. P. Koopmans, S. L. Letendre, E. V. Capparelli, S. S. Rossi, D. B. Clifford, A. C. Collier, B. B. Gelman, G. Mbeo, J. A. McCutchan, D. M. Simpson, R. Haubrich, R. Ellis, and I. Grant.
334 Efavirenz concentrations in csf exceed ic50 for wild-type HIV. *J Antimicrob Chemother*, 66(2):354–7, 2011. ISSN 1460-2091 (Electronic) 0305-7453 (Linking). . URL <http://www.ncbi.nlm.nih.gov/pubmed/21098541>.
- 335 55. B Best, S Letendre, E Capparelli, R Ellis, S Rossi, P Koopmans, and I Grant. Efavirenz and emtricitabine concentrations consistently exceed wild-type ic50 in cerebrospinal fluid: Charter findings.
336 In *16th Conference on Retroviruses and Opportunistic Infections*, 2009.
- 337
338

339 Figure Captions

340 **Fig.1. Wild-type virus is predicted to be more rapidly supplanted by the drug resistant mutant with**
341 **cell-free infection relative to cell-to-cell spread.** A) Schematic. Orange cells are mutant infected, green are wild-type
342 infected, grey uninfected. Arrows represent infection attempts, with an "x" denoting an infection attempt blocked by drug. B)
343 Measurement of the replication ratio (R), defined as the number of infected cells at the end of 48 hours of infection (N_{out})
344 divided by input number of infected cells added directly or from which cell-free virus was harvested at infection start (N_{in}).
345 Infected cells are in the GFP positive gate. Left plots shows N_{out} per mL for wild-type and mutant infection when infection
346 was by cell-to-cell spread and N_{in} per mL was 1×10^4 . Right plots shows N_{out} per mL for wild-type and mutant infection
347 when infection was by cell-free virus and N_{in} per mL was 2×10^5 . C) Measured R values for wild-type and L100I mutant HIV
348 for infection by cell-free and cell-to-cell. D) Expected frequency of the drug resistant mutant with (blue line) and without (red
349 line) a single cycle of cell-free infection. Frequency was calculated as $F_i^{mt} = N_i^{mt} / (N_i^{mt} + N_i^{wt})$, where N_i^{mt} and N_i^{wt} are the
350 number of mutant and wild-type infected cells respectively at infection cycle i , and where $N_i = RN_{i-1}$. Inset shows the ratio
351 of wild-type to mutant R values for cell-free infection and cell-to-cell spread.

352 **Fig.2. Frequencies of L100I and K103N EFV resistance mutations rise more rapidly with a cell-free infection**
353 **step.** A) Schematic of the experimental procedure. Targets denote uninfected cells to which cell-free virus or infected cells are
354 added. B) Frequencies of the L100I EFV resistance mutation with a cell-free step (blue points) and without a cell-free step
355 (red points) in three independent experiments. C) Frequencies of the K103N EFV resistance mutation with and without a
356 cell-free step in the same three independent experiments as (B).

357 **Fig.3. HIV infection with a cell-free infection cycle evolves multidrug resistance.** Frequencies of drug resistant
358 mutations for infection with a cell-free infection cycle (blue) and without a cell-free infection cycle (red) for three independent
359 evolution experiments. light grey shading indicates the days at which the infection was carried out under EFV monotherapy
360 conditions (20nM EFV). Dark grey background shading indicates the days at which the infection was carried out in the face of
361 the two drugs (20nM EFV and 770nM FTC).

362 **Fig.4. Increasing drug concentration in coculture infection increases the rate of drug resistance evolution.** A)
363 L100I and B) K103N mutation frequencies for infection without a cell-free infection cycle passaged either at 20nM EFV (red)
364 or at 40nM EFV (orange). Mean and standard deviation from 3 independent experiments.

365 **Fig.5. Frequency of resistance mutations with a cell-free infection cycle under increased selective pressure.**
366 A) L100I and B) K103N mutation frequencies for infection with a cell-free step passaged either at 20nM EFV (dark blue) or at
367 40nM EFV (light blue). Mean and standard deviation from 3 independent experiments.

368 Supplementary Figure Captions

369 **SFig.1. Mutant frequencies measured at start of evolution experiments after two cycles of infection in the**
370 **absence of drug.** The mean frequency for L100I, K103N and M184I were $3 \times 10^{-2} \pm 4 \times 10^{-2}$, $2 \times 10^{-2} \pm 3 \times 10^{-2}$,
371 $2 \times 10^{-3} \pm 5 \times 10^{-3}$ respectively. The mutation frequency for M184V was below the detection threshold of 10^{-3} .

372 **SFig.2. Frequencies of single and linked multidrug resistant mutations.** A) Infection in the presence of a cell-free
373 step and B) absence of a cell-free step for 3 experiments. Light grey background shading indicates the days at which the
374 infection was carried out under 20nM EFV monotherapy. Dark grey background shading indicates the days at which the
375 infection in the face of 20nM EFV and 770nM FTC).

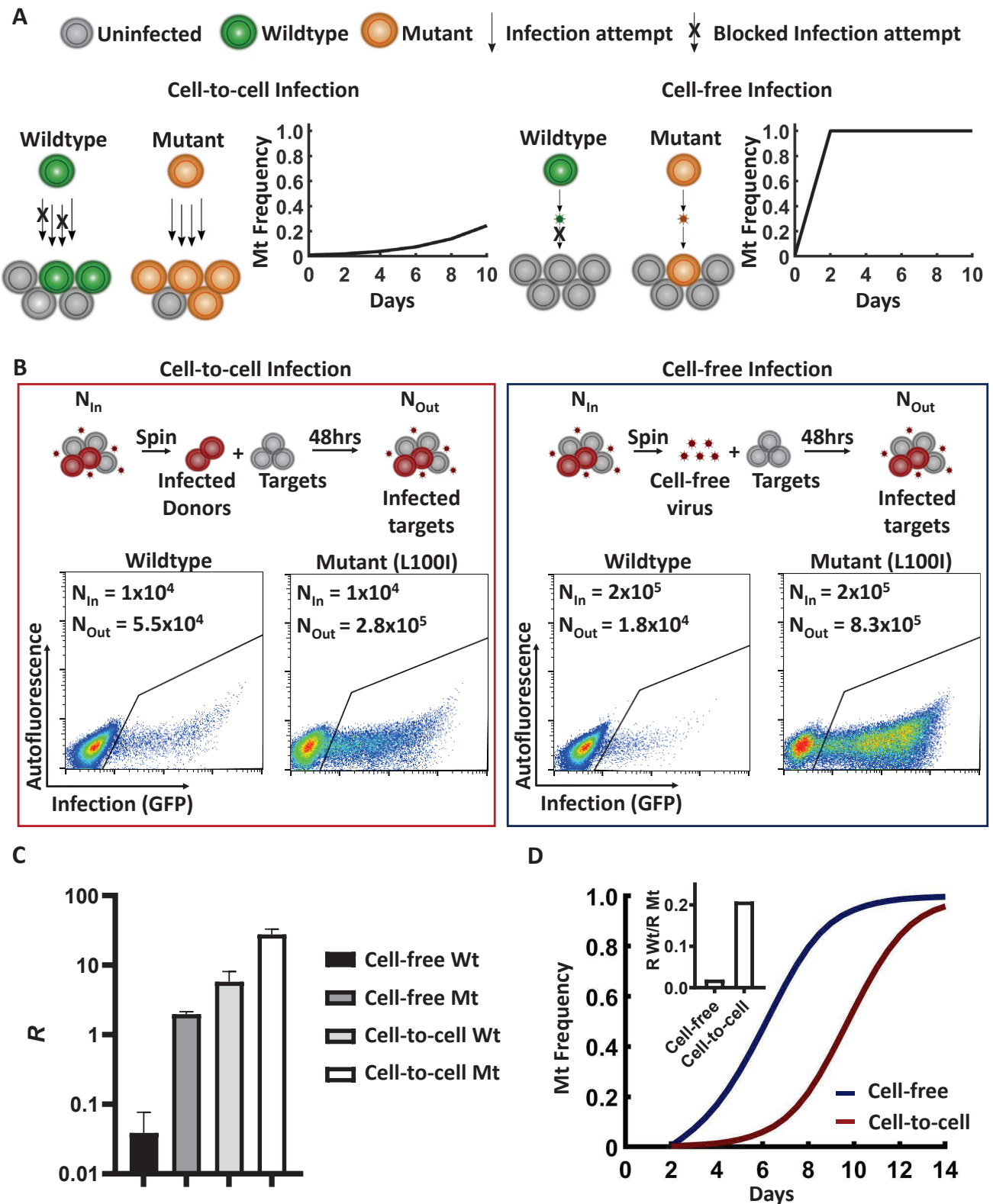


Fig. 1. Wild-type virus is predicted to be more rapidly supplanted by the drug resistant mutant with cell-free infection relative to cell-to-cell spread. A) Schematic. Orange cells are mutant infected, green are wild-type infected, grey uninfected. Arrows represent infection attempts, with an "x" denoting an infection attempt blocked by drug. B) Measurement of the replication ratio (R), defined as the number of infected cells at the end of 48 hours of infection (N_{out}) divided by input number of infected cells added directly or from which cell-free virus was harvested at infection start (N_{in}). The cellular and cell-free fractions were derived by spinning the sample and using the infected cells from the pellet (cell-to-cell, left plot) or the filtered supernatant of the same infected cells (cell-free, right plot) for infection. Infected cells are in the GFP positive gate. Left plots shows N_{out} per mL for wild-type and mutant infection when infection was by cell-to-cell spread and N_{in} per mL was 1×10^4 . Right plots shows N_{out} per mL for wild-type and mutant infection when infection was by cell-free virus and N_{in} per mL was 2×10^5 . C) Measured R values for wild-type and L100I mutant HIV for infection by cell-free and cell-to-cell. D) Expected frequency of the drug resistant mutant with (blue line) and without (red line) a single cycle of cell-free infection. Frequency was calculated as $F_i^{mt} = N_i^{mt} / (N_i^{mt} + N_i^{wt})$, where N_i^{mt} and N_i^{wt} are the number of mutant and wild-type infected cells respectively at infection cycle i , and where $N_i = R \cdot N_{i-1}$. Inset shows the ratio of wild-type to mutant R values for cell-free infection and cell-to-cell spread.

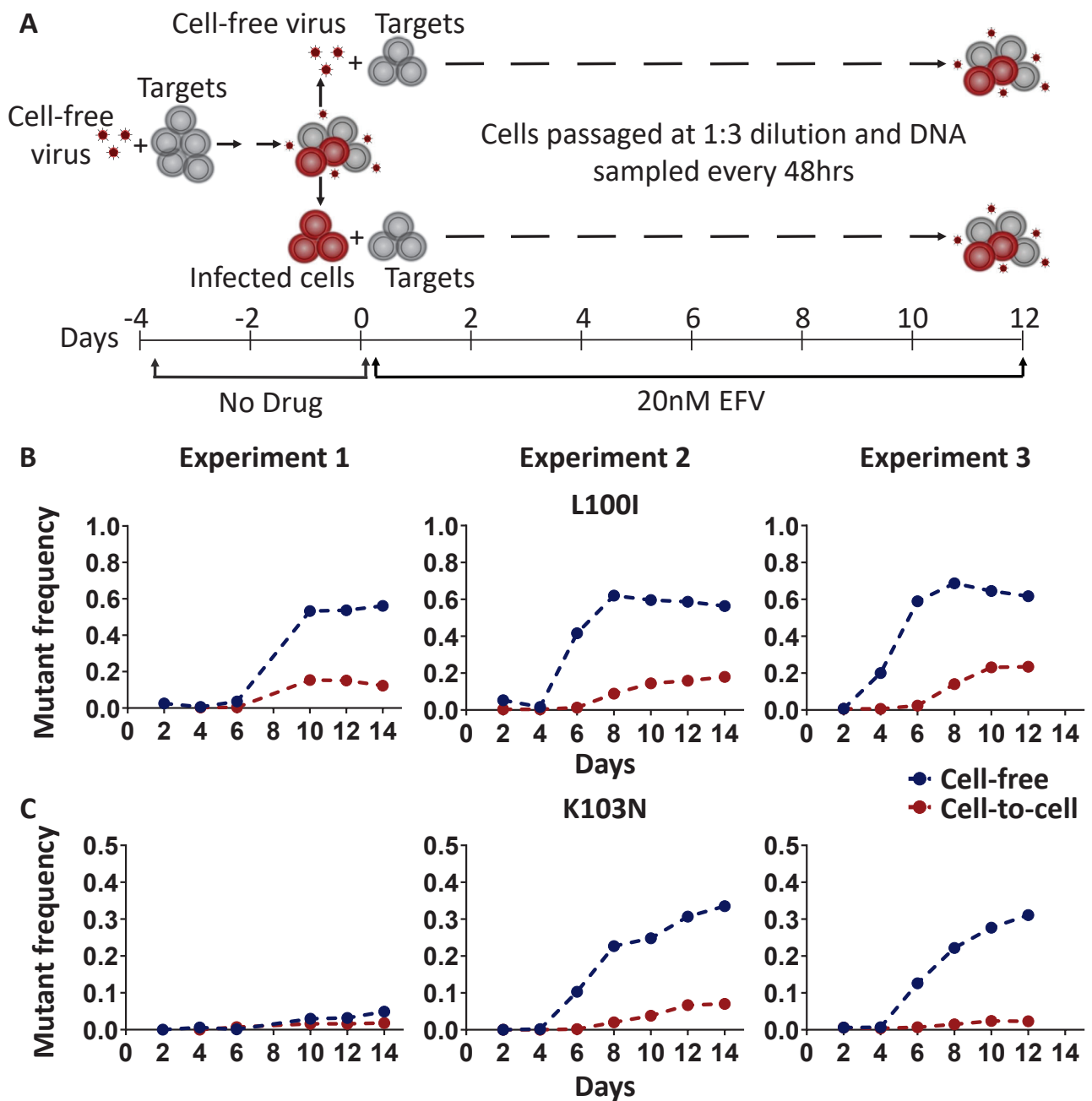


Fig. 2. Frequencies of L100I and K103N EFV resistance mutations rise more rapidly with a cell-free infection step. A) Schematic of the experimental procedure. Targets denote uninfected cells to which cell-free virus or infected cells are added. B) Frequencies of the L100I EFV resistance mutation with a cell-free step (blue points) and without a cell-free step (red points) in three independent experiments. C) Frequencies of the K103N EFV resistance mutation with and without a cell-free step in the same three independent experiments as (B).

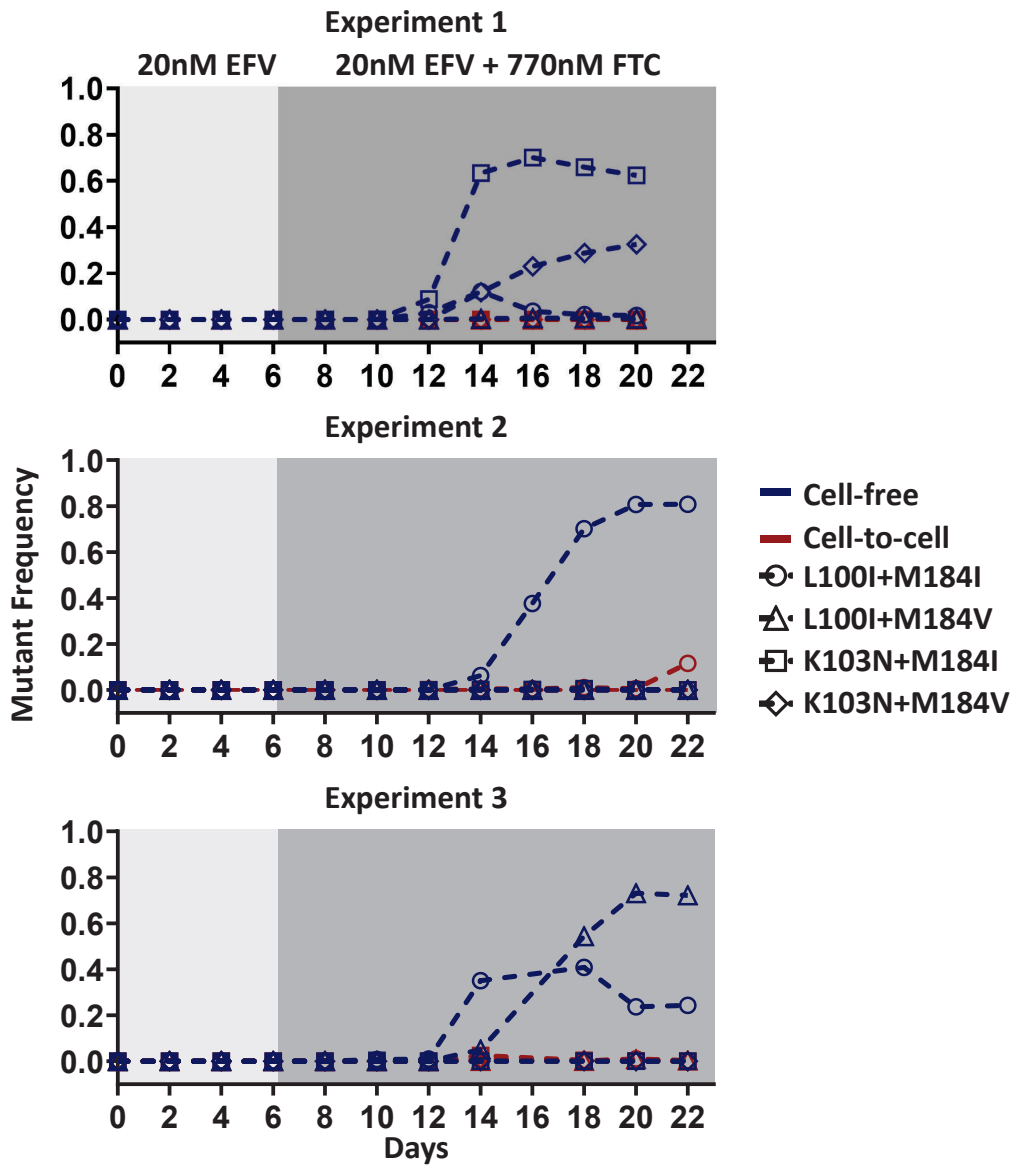


Fig. 3. HIV infection with a cell-free infection cycle evolves multidrug resistance. Frequencies of drug resistant mutations for infection with a cell-free infection cycle (blue) and without a cell-free infection cycle (red) for three independent evolution experiments. Light grey shading indicates the days at which the infection was carried out under EFV monotherapy conditions (20nM EFV). Dark grey background shading indicates the days at which the infection was carried out in the face of the two drugs (20nM EFV and 770nM FTC).

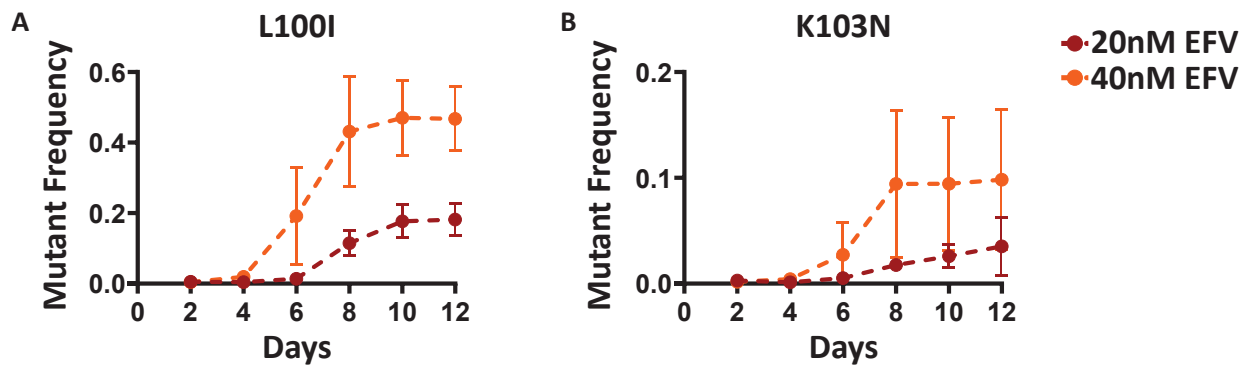


Fig. 4. Increasing drug concentration in coculture infection increases the rate of drug resistance evolution. A) L100I and B) K103N mutation frequencies for infection without a cell-free infection cycle passaged either at 20nM EFV (red) or at 40nM EFV (orange). Mean and standard deviation from 3 independent experiments.

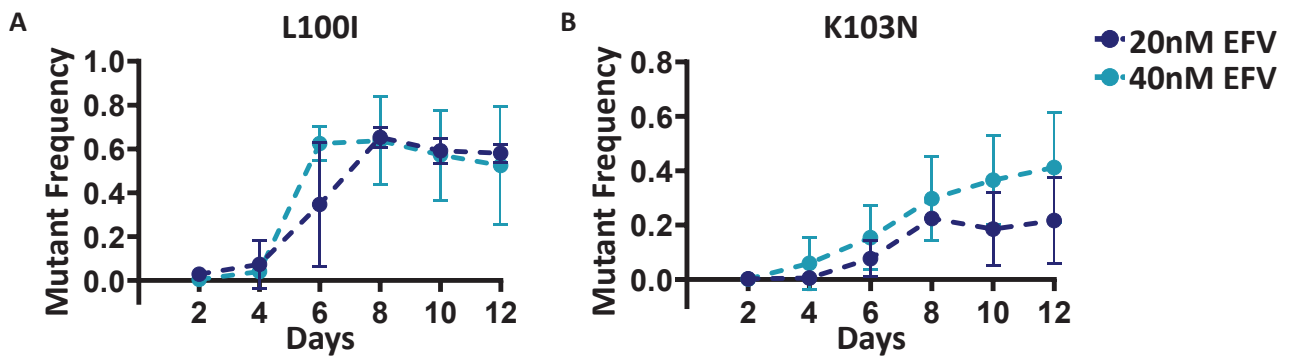
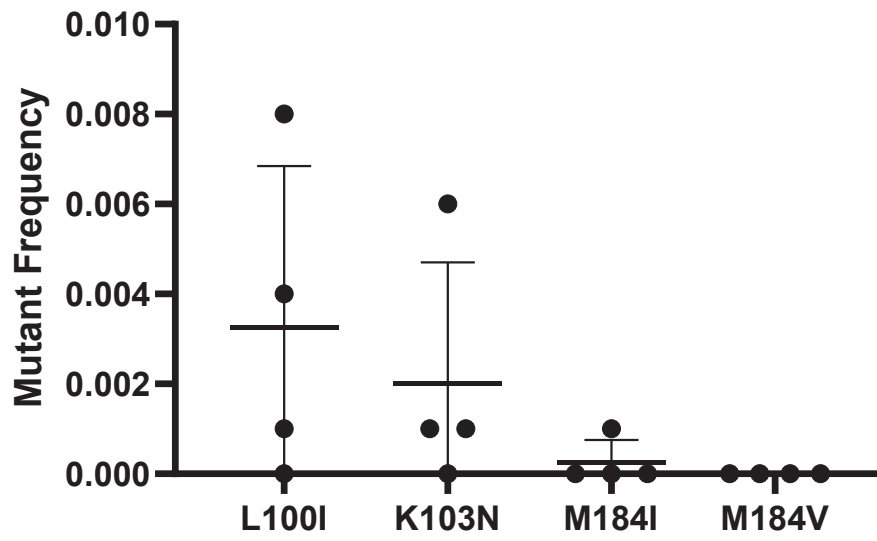
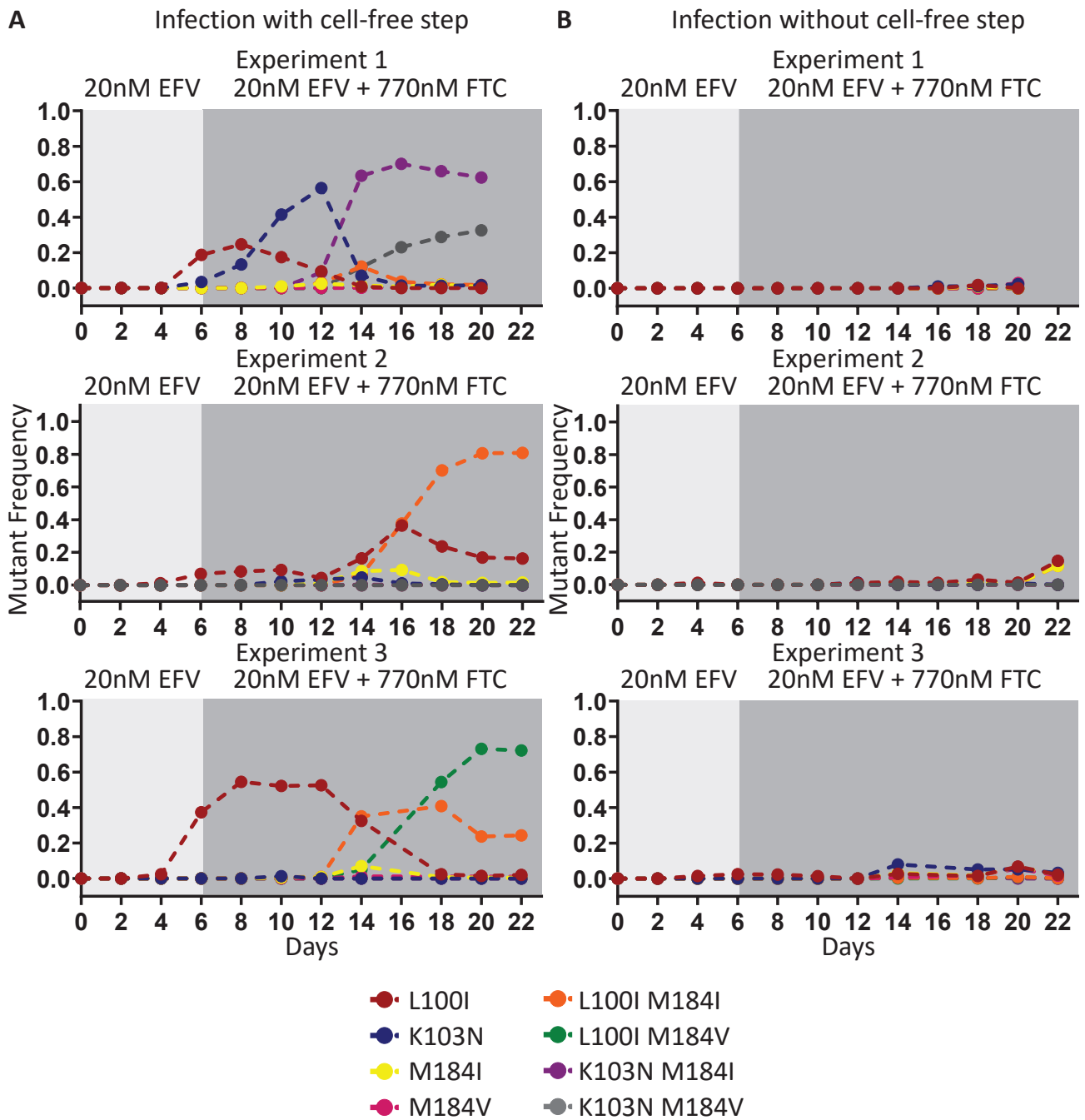


Fig. 5. Frequency of resistance mutations with a cell-free infection cycle under increased selective pressure. A) L100I and B) K103N mutation frequencies for infection with a cell-free step passaged either at 20nM EFV (dark blue) or at 40nM EFV (light blue). Mean and standard deviation from 3 independent experiments.



SFig. 1. Mutant frequencies measured at start of evolution experiments after two cycles of infection in the absence of drug. The mean frequency for L100I, K103N and M184I were $3 \times 10^{-2} \pm 4 \times 10^{-2}$, $2 \times 10^{-2} \pm 3 \times 10^{-2}$, $2 \times 10^{-3} \pm 5 \times 10^{-3}$ respectively. The mutation frequency for M184V was below the detection threshold of 10^{-3} .



SFig. 2. Frequencies of single and linked multidrug resistant mutations. A) Infection in the presence of a cell-free step and B) absence of a cell-free step for 3 experiments. Light grey background shading indicates the days at which the infection was carried out under 20nM EFV monotherapy. Dark grey background shading indicates the days at which the infection in the face of 20nM EFV and 770nM FTC).

CHAPTER 4:

Increased interferon response in HIV cell-to-cell spread

In chapters 1 and 2, I demonstrated that HIV infection modes determines infected cell survival as well as the rate of selection of drug resistant mutants. Given the differences observed between HIV infection modes in the previous two chapters, I then set out to determine whether differences could be detected at the transcriptional level in cells infected by either cell-free infection or cell-to-cell spread. My specific contributions to the following project are as follows: conceptualization of the project, experimental design, *in vitro* HIV infection of lymph node cells obtained from clinically indicated lung resections, sorting of cellular populations for RNA-seq by FACS, cDNA library preparation for sequencing, analysis of RNA-Seq data, curation of data into figures and writing of the manuscript.

Increased interferon response in HIV cell-to-cell spread

1 Jessica Hunter^{1,2}, Marko Vukovic^{3,4,5,6}, Carly G.K. Ziegler^{3,4,5,6}, Hylton E. Rodel^{1,7}, Yashica Ganga¹, Alex K. Shalek^{3,4,5,6},
2 Alex Sigal^{1,2,8*},

3 **1** Africa Health Research Institute, Durban 4001, South Africa.

4 **2** School of Laboratory Medicine and Medical Sciences, University of KwaZulu-Natal, Durban, South Africa.

5 **3** Ragon Institute of MGH, Harvard, and MIT, Cambridge, USA;

6 **4** Department of Chemistry, Institute for Medical Engineering and Sciences, MIT, Cambridge, USA

7 **5** Broad Institute of MIT and Harvard, Cambridge, USA

8 **6** Koch Institute for Integrative Cancer Research, MIT, Cambridge

9 **7** Division of Infection and Immunity, University College London, London, UK;

10 **8** Max Planck Institute for Infection Biology, Berlin 10117, Germany.

11 * alex.sigal@ahri.org

12 Abstract

13 HIV cell-to-cell spread is a highly efficient mode of infection that relies on cellular interactions to transmit virions between an
14 infected and uninfected cell. Cell-to-cell spread is expected to be an effective infection mode in environments such as lymph
15 nodes, where infectable cells are tightly packed and there are no strong shear flows to disturb cellular interactions. Here we
16 used RNA-Seq to investigate which genes are differentially regulated following ex vivo HIV infection of lymph node cells,
17 and whether there is specific differential regulation of host genes in cell-to-cell versus cell-free infection. We used HIV which
18 expresses YFP upon infection and sorted YFP positive cells from lymph nodes infected by either cell-free infection or cell-to-cell
19 spread. Using principle component analysis, we observed clustering of the cell-to-cell and cell-free infected lymph nodes by
20 their transcriptional profiles. Both cell-to-cell and cell-free HIV infection led to upregulation of genes in the inflammatory
21 response. A smaller gene set was differentially regulated in cell-to-cell versus cell-free infection. Cell-to-cell spread differentially
22 upregulated genes from the interferon α and γ pathways and downregulated genes in the Myc pathway involved in cell cycle
23 progression. Specific interferon upregulated genes in cell-to-cell spread versus cell-free infection included the antiviral response
24 genes IRF7, ISP15, IFIT1, IFIT2, IFIT3 and MX1. Therefore, cell-to-cell spread qualitatively differs from cell-free infection
25 in inducing a stronger innate antiviral response in lymph node cells, similar to the gene expression pattern of lymph node
26 infection in vivo. This may indicate that this infection mode may be predominant in the lymph node compartment which is
27 important for HIV replication and persistence.

28 Introduction

29 Cell-to-cell spread of HIV has been shown to efficiently transmit virus between cells through a variety of pathways which
30 reduce the probability that the virion is lost in the process of finding a cell to infect (1–3). While majority of the virions
31 are transmitted by cell-to-cell spread of HIV, a substantial proportion are transmitted by cell-free infection (4–6), which is
32 most sensitive to neutralizing antibodies (7–10) and antiretroviral drugs (1, 3, 11, 12) but may be important for transmission
33 between individuals (13). In addition, the higher sensitivity to inhibitors of cell-free infection may allow it to more rapidly
34 evolve resistance (14). Whether there are differences in terms of the cellular response to infection between cell-to-cell spread
35 and cell-free infection is still poorly understood. Such differences may be detected at the level of the transcriptomic response to
36 the infection.

37 A rapid host response to HIV infection is the innate response involving interferon (IFN), which attempts to control viral
38 replication and induces other immune pathways (15–17). It is not yet known whether this response hinders or facilitates HIV
39 disease progression (17). Another response to infection is cell cycle arrest (18–21). However, HIV has evolved the ability to
40 cross the nuclear membrane, bypassing the requirement of a dividing cell (22). Previous studies have investigated the gene
41 expression in CD4 T cells from HIV infected individuals, which have demonstrated increased expression in genes regulating
42 cell-cycle and type 1 interferon response in comparison to CD4 T cells from uninfected individuals (23–27). Furthermore,
43 interferon-stimulated genes are associated with high viral replication and disease progression (24, 26, 28). Elite controllers
44 and infected individuals on ART have reduced expression of genes relating to interferon pathways relative to viremic patients
45 (24, 26).

46 Lymphatic tissue is the site of substantial viral replication and pathology (29, 30) and is a likely site of the HIV reservoir.
47 Lymph node cells of HIV infected individuals not on ART show upregulation of genes involved in immune defenses, especially
48 those relating to the interferon response (27, 28, 31). Conditions within lymph nodes make it the ideal environment for HIV to
49 transmit by cell-to-cell spread (32). This is due to the large number of infectable cells (30, 33, 34) in close proximity to each
50 other (35–39) and the lack of flow within this anatomical site (5, 40, 41). Insufficient drug penetration in the lymph node may
51 also contribute to ongoing replication in this site (42, 43).

52 It has yet to be determined whether cells infected by cell-to-cell spread respond with a different transcriptional profile
 53 relative to cells infected by cell-free infection. Identifying genes uniquely expressed in cells infected by cell-to-cell spread could
 54 lead to the identification novel targets for therapies which target this more drug resistant mode of infection. In addition, a
 55 gene signature for cell-to-cell spread may indicate environments where this infection mode is prevalent. To investigate this,
 56 we sequenced the transcriptomes of lymph node CD4 T cell populations infected *ex vivo* by either cell-free infection or by
 57 cell-to-cell spread. We analysed the near whole transcriptome sequences for similarities as well as differences in gene expression
 58 between the populations infected by the two different modes of infection. In cells infected by either modes of infection, we
 59 observed an upregulation of genes involved in inflammatory pathways compared to uninfected populations. However, cell-to-cell
 60 infected populations exhibited an substantial increase in expression of interferon-stimulated genes (ISGs) which was specific to
 61 this infection mode.

62 Results

63 **HIV cell-to-cell spread induces a specific transcriptional response.** We examined whether cell-to-cell spread leads to differential
 64 gene expression (Figure 1A). We used RNA-Seq to quantify gene expression patterns in human lymph node cells either uninfected
 65 or infected *ex vivo* with HIV. HIV infection was either by cell-free transmission or by coculture with infected cells, through
 66 which infection is by a combination of cell-free infection and cell-to-cell spread (4, 5). We used cellularized primary human
 67 lymph node cells from three HIV-negative individuals undergoing indicated lung resections (STable 1). Lymph node cells were
 68 infected by the addition of either cell-free NL4-3YFP virus or by coculture with NL4-3YFP infected donor cells, incubated for
 69 36 hours, then sorted using flow cytometry (Figure 1B). We used a negative selection on CD8 T cells rather than staining
 70 directly for CD4 T cells because HIV downregulates CD4 upon infection (44). We differentiated the infected target cells from
 71 the infected donor cells in our coculture infections by staining the target cells with cell trace far red (CTFR). Cells infected
 72 with cell-free HIV underwent the same staining. We sorted populations of 1×10^3 cells each for the uninfected (Figure 1B top
 73 panel, blue gate), cell-free infected (Figure 1B middle panel, purple gate), and cell-to-cell infected (Figure 1B bottom panel,
 74 red gate) populations.

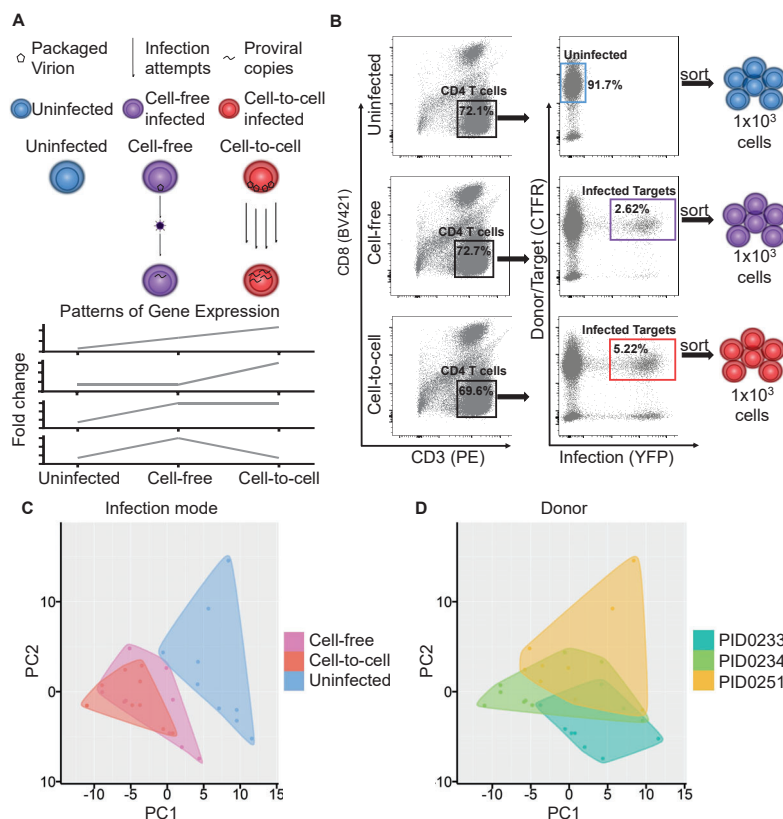


Fig. 1. Gating strategy and transcriptional patterns in HIV cell-to-cell spread versus cell-free infection. (A) Schematic of HIV infection attempts. Arrows represent infection attempts. Below are possible differences in expression patterns per gene. (B) Gating strategy for sorting of cell populations for RNA-Seq. The left panel depicts the selection of CD3+CD8- T cells. In the right panel, infected cells were identified based on YFP expression and targets were differentiated from donors based on CTFR staining. (C) Principle component analysis (PCA) of the top 100 most variable genes after rlog normalization in DESeq with clusters grouped based on infection conditions indicated by different colours. Blue indicates uninfected, purple cell-free infected, and red cell-to-cell spread infected. (D) PCA with clusters grouped based on lymph node donors. Yellow is PID0251, green is PID0234, and cyan PID0233.

75 We performed a differential expression analysis using DESeq. Principle component analysis (PCA) showed that when the
 76 populations were grouped based on infection conditions, the first principle component (PC1) was predominantly dependent
 77 on the response generated from the infection conditions (Figure 1C). When the populations were grouped based on donor,
 78 donor-to-donor variability was mostly responsible for the second principle component (PC2) (Figure 1D). There is clear
 79 separation of the uninfected cell populations from both infected cell populations with the greatest separation between the
 80 uninfected cluster and the infected by cell-to-cell spread cluster (Figure 1C). There is also a clustering of the cell-to-cell versus
 81 cell-free conditions, although the separation is less compared to uninfected cells.

82 **Differential gene set enrichment in cell-to-cell spread versus cell-free infection.** We performed a Gene Set Enrichment Analysis
 83 (GSEA) (45) to determine which sets of genes relating to specific biological functions were enriched in our infection conditions.
 84 We compared the genes expressed in our dataset against the genes contained in the hallmark gene sets (46). We examined the
 85 normalized enrichment scores (NES) for the gene sets with the greatest enrichment between the cell-to-cell and cell-free infected
 86 conditions, selected based on a p-value of < 0.1 . 17 gene sets met this condition (Figure 2A). The GSEA for the top 5 most
 87 enriched gene sets are shown in Supplementary Figure 1. Gene sets specifically enriched in the cell-to-cell condition relative
 88 to the cell-free included the interferon α response and interferon γ response (Figure 2A). Cell cycle regulation also showed
 89 differences in enrichment between the infection modes. The MYC Target V1 set of genes relating to cell-cycle progression was
 90 significantly downregulated in HIV cell-to-cell spread relative to the cell-free infection. This indicates that cell-to-cell spread
 91 differentially activates the interferon response and may induce stronger cell-cycle arrest by downregulating MYC responsive
 92 genes.

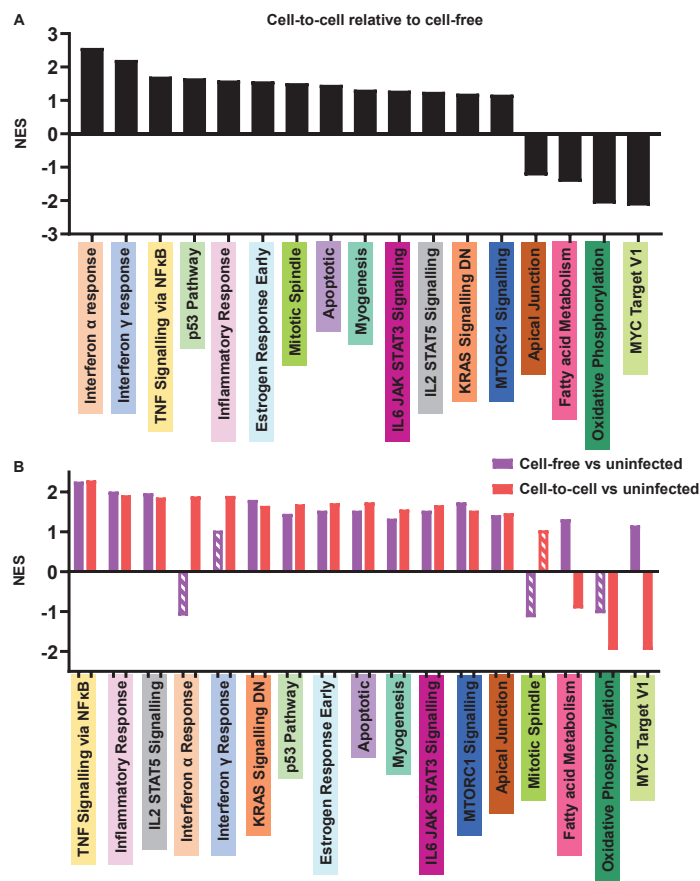


Fig. 2. Differentially regulated gene sets in cell-to-cell spread versus cell-free infection in lymph node cells. Normalized enrichment scores (NES) plotted for the 17 gene sets which were differentially regulated at a significance level of $p < 0.1$ in a comparison between cell-to-cell spread and cell-free infection. (A) NES of the gene sets for the cell-to-cell versus cell-free infection conditions. (B) NES of the cell-free (purple bars) and cell-to-cell (red bars) infection conditions relative to uninfected cells. Striped bars indicate gene sets for which the p-value was not significant.

93 To investigate the transcriptional regulation versus uninfected cells of the 17 genes chosen as the most differentially regulated
 94 between cell-to-cell and cell-free, we examined the NES relative to uninfected (Figure 2B). We observed that TNF signaling
 95 via NFkB followed by the inflammatory response were the most upregulated in both infection modes versus uninfected cells.
 96 In contrast, the interferon α response was upregulated in cell-to-cell spread but showed a trend of being downregulated in

97 cell-free infection relative to uninfected cells, and the interferon γ gene set was upregulated in cell-to-cell but not significantly
 98 upregulated in cell-free. Finally, the MYC Target V1 set of genes was upregulated with cell-free infection but downregulated
 99 with cell-to-cell spread. This indicates that some of the differentially regulated gene sets between cell-to-cell spread and cell-free
 100 infection can be regulated in the opposite directions, not merely upregulated or downregulated by both to different levels.

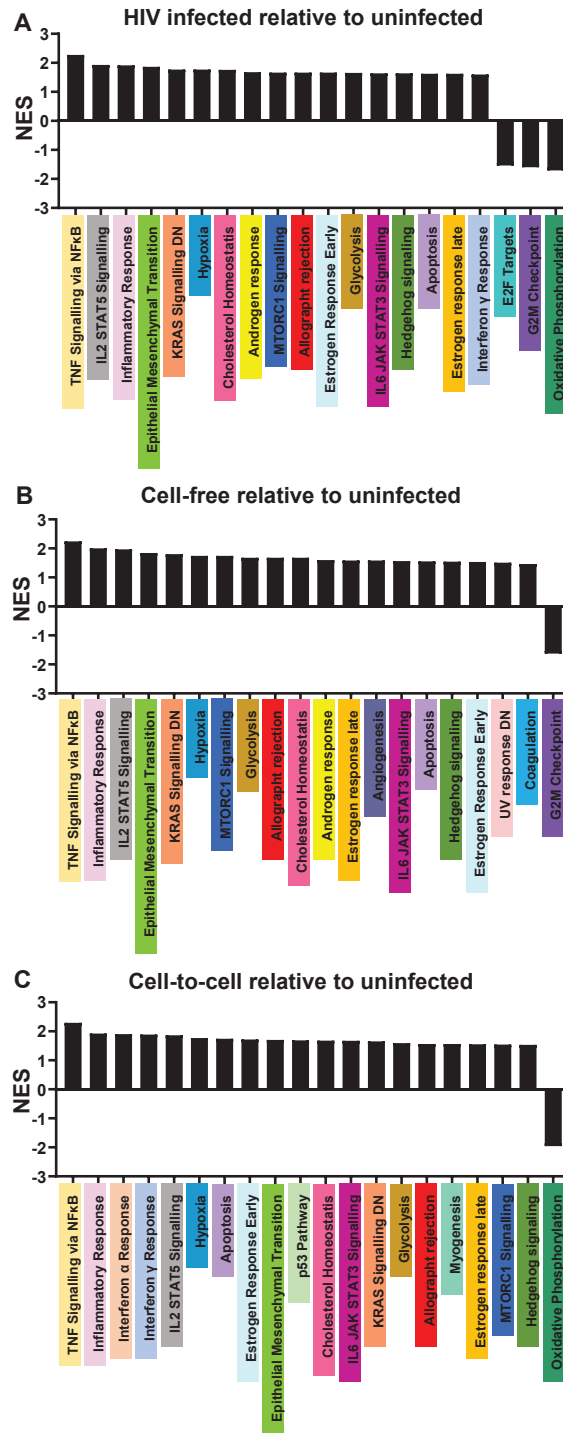


Fig. 3. Gene sets differentially regulated in HIV infected relative to uninfected lymph node cells. Normalized enrichment scores (NES) plotted for the top 20 most significant gene sets in a comparison between cells infected by both infection modes (A), cell-free infection (B), or cell-to-cell spread (C).

101 Next, we looked at the top enriched gene sets in HIV infection of lymph nodes without pre-selecting on the most differentially

expressed gene sets in cell-to-cell spread versus cell-free infection. We first combined both infection conditions and compared to uninfected (Figure 3A). Differentially regulated gene sets in the combined infection dataset included upregulation of TNF signaling via NFkB, IL2 STAT5 signalling, and the inflammatory response, all associated with the immune response (Figure 3A). In addition, gene sets not clearly associated with the immune response, including the epithelial to mesenchymal transition, cholesterol homeostasis, and the androgen/estrogen response, were upregulated. There was also differential regulation of gene sets involved in proliferation, growth arrest, and apoptosis.

When cell-to-cell and cell-free were compared to uninfected cells separately without pre-selecting on the most differentially expressed genes in cell-to-cell versus cell-free infection, additional sets were upregulated, including angiogenesis, UV response (possibly a response to DNA damage) and coagulation (Figure 3B-C). In the cell-free relative to uninfected comparison, the interferon α and γ responses do not appear in the most significantly enriched gene sets (Figure 3B). In the cell-to-cell relative to uninfected comparison, the interferon γ and the interferon α gene sets were upregulated, as well as the p53 pathway involved in growth arrest and apoptosis (Figure 3C).

Taken together, the main differences between cell-to-cell spread and cell-free infection in lymph node cells seems to relate to the interferon pathways, which are significantly upregulated in cell-to-cell spread but not significantly upregulated (interferon γ) and possibly downregulated (interferon α) in cell-free infection. In addition, there are differences in gene sets involved in cell-cycle progression, which may indicate greater growth arrest in cell-to-cell spread relative to cell-free infection.

Interferon induced genes upregulated in HIV cell-to-cell spread relative to cell-free infection. We compared gene expression for individual genes in the different infection conditions (Figure 4). Approximately 1.4×10^3 genes for the cell-free infected condition and 2.6×10^3 genes for the cell-to-cell infected condition were differentially expressed relative to uninfected condition (Figure 4A). When either infection condition was compared with uninfected cells, an upregulation of genes involved in inflammatory processes such as LTA and CD83 were observed (Figure 4B-C). The p53 regulatory gene, GSDME, was upregulated in the cell-free and cell-to-cell infected relative to the uninfected cells. LIME1, involved in B cell and T cell activation through B cell receptor and T cell receptor signalling, was downregulated by both infection modes.

When cell-to-cell spread was compared to cell-free infection, 47 genes were found to be differentially expressed with significant p values (Figure 4A). Consistent with the GSEA results, majority of the individual genes significantly upregulated in the cell-to-cell relative to the cell-free infection were interferon induced genes, this included all of the top 10 most significantly upregulated genes (Figure 4D). Examples which are involved in the antiviral response include MX1, IRF7, IFIT2, IFIT3 and ISG15.

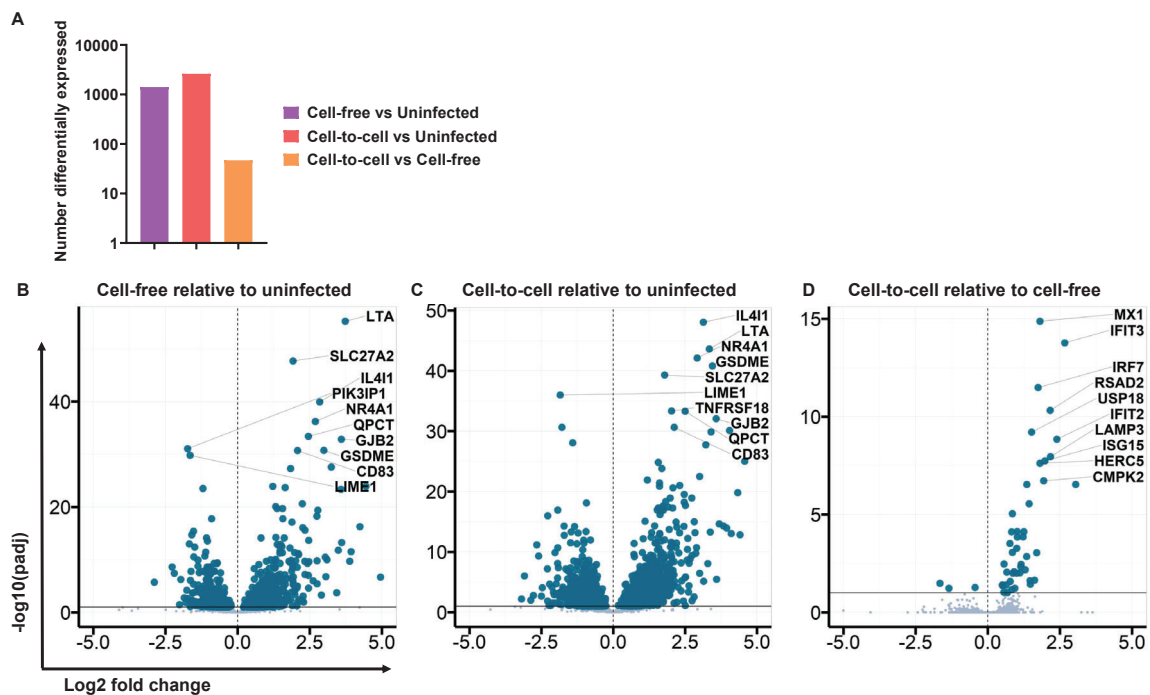


Fig. 4. Interferon induced genes upregulated in HIV cell-to-cell spread versus cell-free infection. (A) Number of differentially expressed genes for cell-free versus uninfected (purple bars), cell-to-cell versus uninfected (red bars) and cell-to-cell versus cell-free (orange bars). (B-D) Volcano plots of differentially expressed genes for cell-free relative to uninfected (B), cell-to-cell relative to uninfected (C), or cell-to-cell relative to cell-free (D). Log transformed fold-change is represented on the x-axis, with genes left of zero indicating downregulation whereas genes right of zero indicating upregulation. Significance is represented on the y-axis. Large circles represent genes differentially expressed with significant p-adjusted values (< 0.1) and small circles represent genes which are not significantly differentially regulated. The top 10 most significant differentially expressed genes are labelled on each plot.

130 Given the results of the GSEA and the differential gene expression analysis, we aimed to identify the genes which played the
 131 most significant role in the transcriptional response to HIV cell-to-cell spread (Figure 5). We cross-referenced the differentially
 132 expressed genes with the genes which had the highest variability in expression between the cell-to-cell and cell-free infection
 133 conditions. We then identified which of these genes were contained within the most enriched gene sets within our data set.

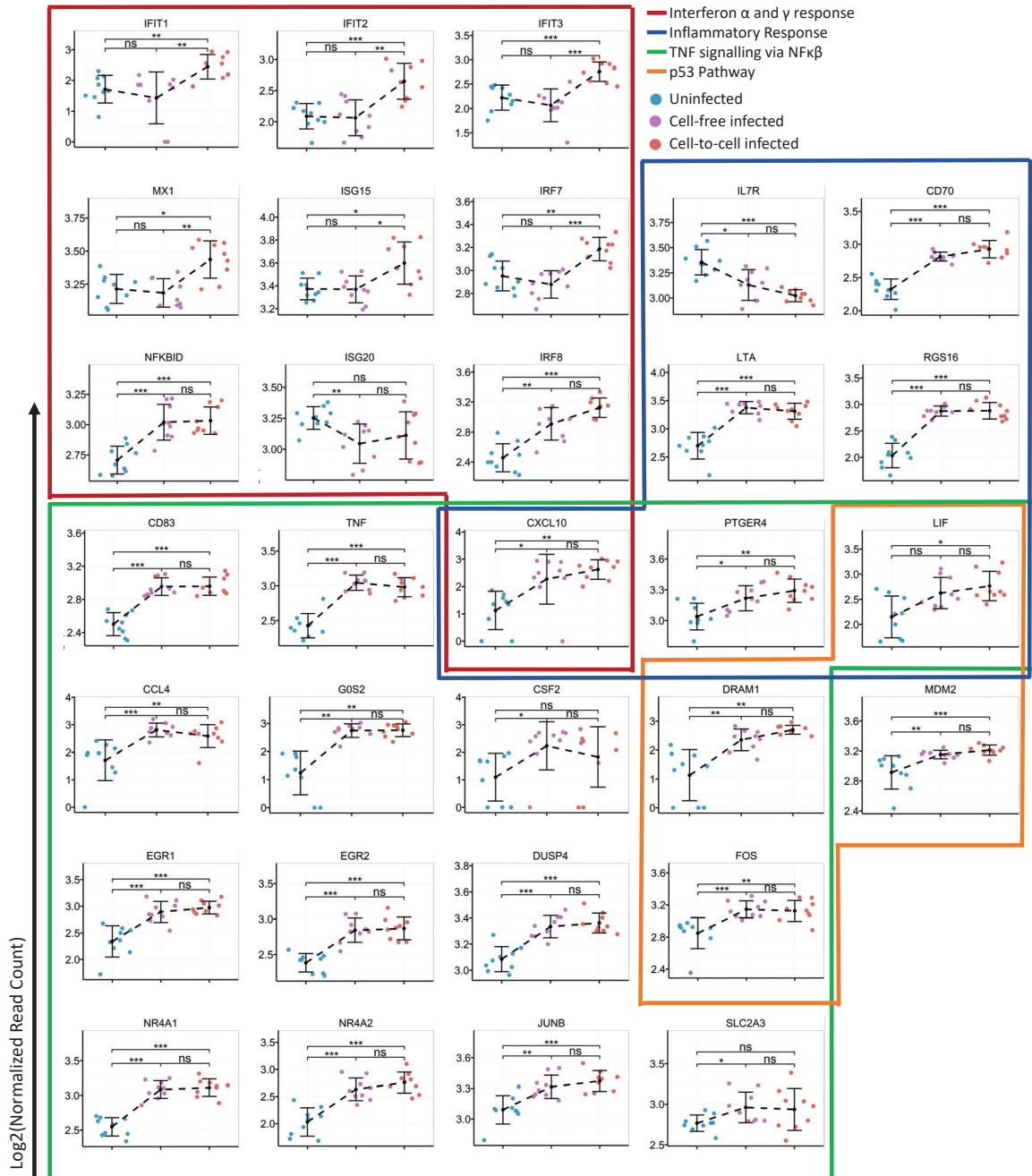


Fig. 5. Differentially expressed genes within the most enriched genes sets in HIV cell-to-cell spread. The normalized log₂ transformed read count of the individual genes is represented on the y-axis. The mean read count \pm std for each infection condition is black. Blue circles are uninfected lymph nodes, purple circles are cell-free infected lymph nodes, and red circles are cell-to-cell infected lymph nodes. Differentially expressed genes within the interferon alpha and gamma response gene sets are outlined in red, inflammatory response gene set outlined in blue, TNF signalling via NFkB gene set outlined in green, and p53 pathway gene set outlined in orange. p-values are * < 0.01; ** < 0.001; *** < 0.0001 as determined by Wilcoxon test with Bonferroni multiple comparison correction.

134 As indicated in both GSEA and the differential gene expression analysis, the upregulation of genes involved in the interferon
 135 pathways appears to differentiate the transcriptional response to HIV infection in cell-to-cell spread from cell-free infection
 136 (Figure 5, red outline). The level of expression of many of the identified interferon induced genes, including IFIT1, IFIT2, IFIT3,

137 MX1, ISG15 and IRF7, was significantly greater in HIV cell-to-cell spread relative to both cell-free infected and uninfected
138 cells (Figure 5, red outline). Relatively few genes (NFKBID, IRF8 and CXCL10) in the interferon gene sets showed significant
139 upregulation in the cell-free infected relative to uninfected cells and in these cases the cell-to-cell infected condition was likewise
140 upregulated. One of the identified genes in the interferon gene sets, ISG20, was downregulated in the cell-free infected condition
141 relative to the uninfected condition.

142 In contrast, with few exceptions, the genes which form part of the inflammatory response (Figure 5, blue outline), TNF
143 signalling via NFKB (Figure 5, green outline), and p53 pathway (Figure 5, orange outline), demonstrated significant upregulation
144 in both the cell-to-cell spread and cell-free infection relative to uninfected cells. This indicates that transcriptional regulation is
145 similar in response to HIV cell-to-cell spread versus cell-free infection with one striking exception detected by this analysis,
146 which was the interferon response. In this case, cell-free infection tended to upregulate few of the component genes, while
147 cell-to-cell spread robustly upregulated almost all of the genes.

148 Discussion

149 Using an analysis of the transcriptomic response in ex-vivo HIV infected human lymph nodes, we have shown that there are
150 multiple differentially regulated genes in HIV cell-to-cell spread versus cell-free infection. The major contributor to these
151 differences is differential regulation of the interferon response. The interferon response is not significantly upregulated in cell-free
152 infection, but is robustly upregulated when infection is by cell-to-cell spread. This is apparent in the Gene Set Enrichment
153 Analysis (GSEA), where the interferon γ and α gene sets were significantly upregulated in cell-to-cell spread but not in cell-free
154 infection. Genes differentially upregulated in cell-to-cell spread versus cell-free infection include the interferon stimulated genes
155 MX1, IFIT3, IRF7, and others. There were also similarities in the transcriptional response between the infection modes, but
156 they were in different pathways, including the TNF and the p53 growth arrest/apoptosis response. It is important to note that
157 while cell-to-cell and cell-free modes are different from each other, these differences are small when compared to the differences
158 of both infection modes when to uninfected cells. This can be seen in the GSEA results for a gene set such as TNF signaling
159 via NFKB which a high NES in the cell-to-cell infected condition relative to the cell-free infected condition (Figure 2A) but
160 when both infection modes are compared to the uninfected condition the NES seem very similar to each other (Figure 2B).

161 The interferon response has been previously shown to be associated with HIV infection. Gene expression in pre-ART CD4+
162 T cells from HIV infected individuals demonstrate significant upregulation of genes relating to type 1 interferons (interferon α
163 and β), cell cycle, apoptosis (23, 25–27). These host transcriptional responses may contribute to CD4+ T cell depletion during
164 HIV infection in non-ART suppressed individuals by disrupting CD4+ T cell differentiation. It was suggested that activated
165 CD4+ T cells may enter a hyperproliferative state induced by type I interferon, resulting in a greater number of short lived
166 effector cells and fewer long lived memory cells (23).

167 Additionally, the observed upregulation of interferon-stimulated genes (ISGs) was reported to positively correlate with
168 high viremia and disease progression (24, 26). Some of the ISGs associated with viremia include MX1, TAP1, IFI35, ISG15
169 and IFIT3 (26). There is an increase of ISG expression in CD4+ T cells from acute and chronically infected non-controllers
170 but not in elite controllers (24, 26). ISG expression of ART suppressed non-controllers with undetectable viral loads was
171 comparable to that of elite controllers (26, 47), further highlighting the positive correlation between viremia/disease progression
172 and the upregulation of interferon genes. Central memory CD4+ T cells in HIV infected individuals also showed an increase in
173 expression of interferon signalling and inflammatory genes (48). It has also been reported that genes involved in the interferon
174 response are upregulated in the lymph nodes of HIV infected individuals not on ART (28, 31).

175 Upregulation of the interferon pathway is involved in HIV mediated cell death. The ISG, IFI16 (49), is required to
176 sense abortive HIV infection and trigger caspase-1-mediated pyroptotic cell death (50). A further study by the same group
177 demonstrated that cell-to-cell spread was required to trigger caspase-1-mediated pyroptosis (51). IFI16 is also involved in
178 an interferon response positive feedback loop and increases the production of interferons (52). Previously, we have been
179 shown that cell death is increased in cells infected with multiple copies of HIV (12). Since ISGs are involved in sensing HIV
180 reverse transcripts and triggering cell death, multiple infection attempts, which occurs during cell-to-cell spread, may cause the
181 increased interferon response observed for the cell-to-cell infected cells relative to the cell-free infected cells in this study.

182 Given that the interferon response is prevalent in viremic individuals and results in cytotoxicity, our data showing that
183 cell-to-cell spread but not cell-free HIV infection upregulates the interferon response in lymph node cells may indicate that this
184 infection mode is responsible for the majority of the pathogenesis in HIV infection. Therefore, a better understanding of this
185 infection mode may offer a path to reduce HIV pathogenesis in therapeutic strategies.

186 Materials and Methods

187 **Ethical Statement.** Lymph nodes were obtained from participants undergoing indicated lung surgeries for diagnostic purposes
188 and/or complications of inflammatory lung disease. Informed consent was obtained from each participant, and the study
189 protocol approved by the University of KwaZulu-Natal Institutional Review Board (approval BE024/09).

190 **Viruses and lymph node cells.** The pNL4-3YFP molecular clone was a gift from D. Levy. Viral stocks of NL43 were produced
191 by transfection of HEK293 cells with the molecular clone plasmid using TransIT-LT1 (Mirus) transfection reagent. Supernatant
192 containing released virus was harvested two days post-transfection and filtered through a 0.45 micron filter (GVS). The
193 supernatant containing virus was stored in 0.5ml aliquots at -80°C. Lymph node cells were obtained by mechanical separation

194 of lymph nodes and frozen at 5×10^6 cells/ml in a solution of FBS and 10% DMSO with 2.5 $\mu\text{g/ml}$ Amphotericin B (Lonza).
195 Cells were stored in liquid nitrogen until use, then thawed and resuspended at 1×10^6 cells/ml in complete RPMI 1640 medium
196 supplemented with L-Glutamine, sodium pyruvate, HEPES, non-essential amino acids (Lonza), 10% heat-inactivated FBS
197 (Hyclone), and IL-2 at 5 ng/ml (PeproTech).

198 **Infection of lymph node cultures.** Thawed lymph node cells were activated with phytohemagglutinin at 10 $\mu\text{g/ml}$ (Sigma-Aldrich,
199 St Louis, MO) for 48 hours at 37°C. Infected donor cells, for the coculture infections, were generated by infection of 1^6 lymph
200 node cells with 2×10^8 viral copies of HIV NL4-3YFP and incubated for 48 hours at 37°C. Target cells for HIV infection by
201 cell-to-cell spread or cell-free infection were stained with cell trace far red (CTFR) (Life Technologies) as per the manufacturers
202 instructions. 1×10^6 stained target cells were then infected either by cell-free infection with the addition of supernatant
203 containing 1×10^8 viral copies or by coculture with 1×10^4 unstained infected donors. Infections were then incubated for 48
204 hours at 37°C.

205 **Antibody staining and cell sorting.** Infected and uninfected lymph node cultures were washed once with PBS and stained with
206 CD3-PE and CD8-BV421 (Biolegend) by incubating the cells with 0.5 μl of each antibody for 20 minutes at 4°C. Stained cells
207 were washed once more with PBS to remove excess antibodies. The stained cells were then resuspended in 500 μl of FACS
208 buffer (PBS with 10%FCS). BD FACSAria III flow cytometer was used to sort populations of uninfected(YFP-), cell-free
209 infected(YFP+) and cell-to-cell infected(YFP+) cells. In each population 1×10^3 of either uninfected or infected target(CTFR)
210 T cells (CD3+CD8-) were sorted into 300 μl lysis buffer (RLT with 1% 2-mercaptoethanol(BME)). Sorted populations were
211 snap frozen in a dry ice and 99 percent iso-propanol slurry. Samples were stored at -80°C until transported in liquid nitrogen
212 to the Shalek lab at Massachusetts Institute of Technology(MIT) in Boston.

213 **RNA-Seq.** cDNA libraries were prepared according to the protocol previously described by Trombetta *et al* (53). Briefly, frozen
214 samples were thawed and RNA was purified using RNeasy Plus Mini Kit (Qiagen). RNA was then cleaned using RNA-SPRI
215 beads (Beckman Coulter). cDNA was then generated by reverse transcription of the RNA. Next, the cDNA was amplified
216 by PCR and normalized. The libraries were barcoded by PCR with index primers and pooled. A final DNA-SPRI bead
217 (Beckman Coulter) clean-up of the pooled libraries was performed. The prepared cDNA libraries were then sequenced on
218 an Illumina NextSeq instrument. Sequenced transcriptomes were aligned to the GRCh38 reference genome and read count
219 libraries generated by RSEM software package.

220 **Transcriptomics data analysis.** DESeq2 was used to analyse the read count libraries in the R programming platform. The basic
221 work flow that was followed has been described in the paper by Love *et al* (54) (see also: <http://bioconductor.org/packages/release/bioc/vignettes/DESeq2/inst/doc/DESeq2.html>). Principle component analysis (PCA) was run to check for clustering of samples
222 by condition. The top 100 most variable genes yielded the greatest separation of the clustered conditions. Genes with less than
223 10 reads total across the samples were removed. Differential expression analysis in DESeq2 was used to identify differentially
224 regulated genes between the conditions. DESeq2 uses Bejamini-Hochberg procedure to ascribe significance, generating adjusted
225 p values for the differentially regulated genes. Volcano plots were generated by plotting the adjusted p values against the fold
226 change in expression. Genes with adjusted p values less than 0.1 were considered significant and are represented with larger
227 circles. Gene set enrichment analysis (GSEA) was used to compare our expression data set to the hallmark gene sets. This
228 gene set database was selected because it aims to summarize the most relevant biological processes. Gene sets with the greatest
229 difference between the modes of infection were identified by comparing the infected by cell-to-cell condition to the infected by
230 cell-free condition. Gene sets enriched with a nominal p value less than 0.1 were considered significant and the NES of these
231 gene sets were plotted for each of our comparisons. We identified individual genes of interest by cross-referencing the genes
232 with highest variability in our data set with the genes contained within the most enriched genes sets in the cell-to-cell condition.
233 The read counts for the single genes was plotted for each condition. Wilcoxon test with Bonferroni multiple comparison
234 correction was used to determine statistical significance of the change in expression between the conditions.
235

236 Acknowledgments

237 This work was supported by National Institute of Allergy and Infectious Diseases, National Institutes of Health Grant
238 1R01AI138546. JH is supported by a fellowship from the South African National Research Foundation.

239 References

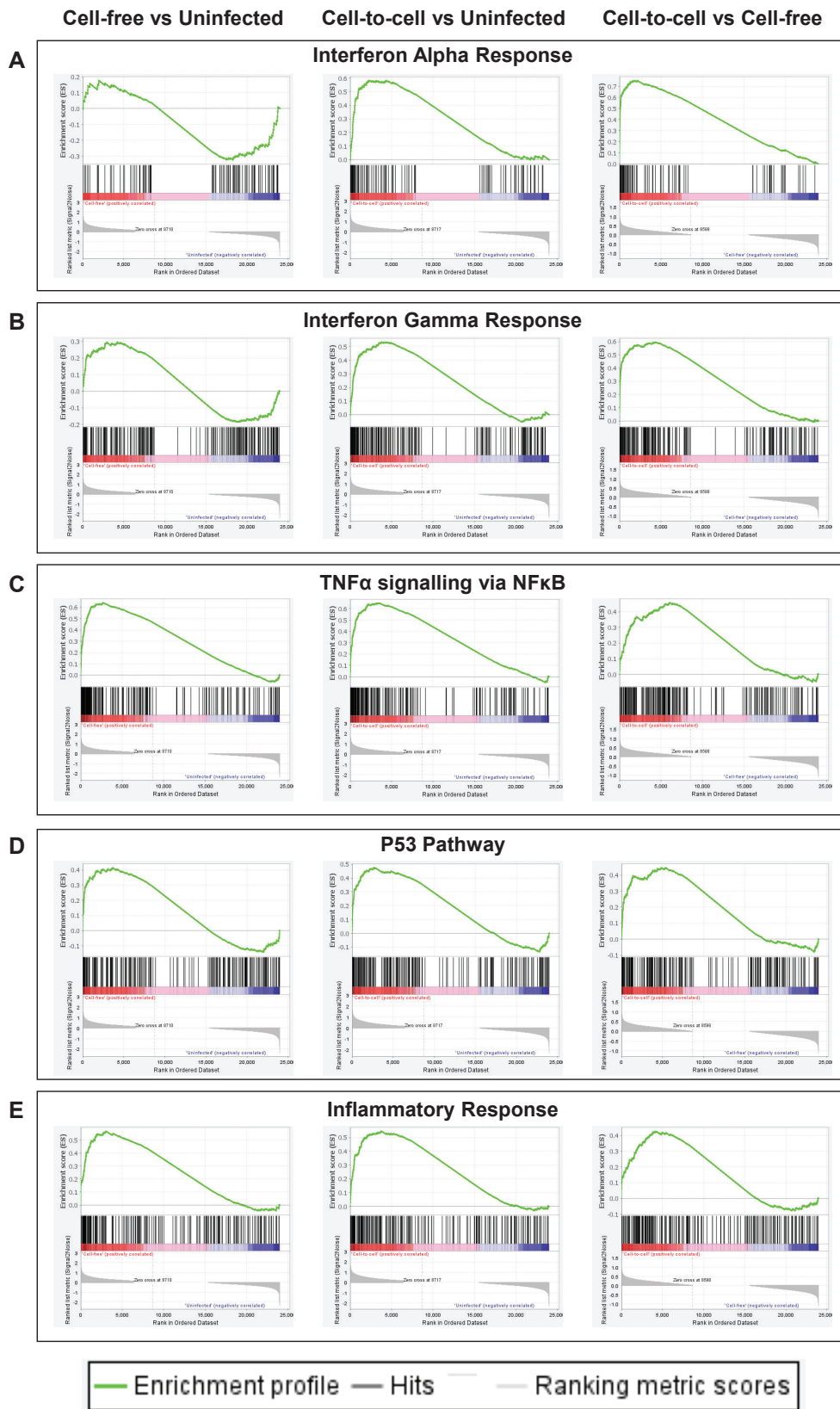
- 240 1. Alex Sigal, Jocelyn T Kim, Alejandro B Balazs, Erez Dekel, Avi Mayo, Ron Milo, and David Baltimore. Cell-to-cell spread of HIV permits ongoing replication despite antiretroviral therapy. *Nature*,
241 477(7362):95, 2011.
- 242 2. Ping Chen, Wolfgang Hübner, Matthew A Spinelli, and Benjamin K Chen. Predominant mode of human immunodeficiency virus transfer between t cells is mediated by sustained env-dependent
243 neutralization-resistant virological synapses. *Journal of virology*, 81(22):12582–12595, 2007.
- 244 3. Christopher JA Duncan, Rebecca A Russell, and Quentin J Sattentau. High multiplicity HIV-1 cell-to-cell transmission from macrophages to cd4+ t cells limits antiretroviral efficacy. *AIDS (London, England)*, 27(14):2201, 2013.
- 245 4. Shingo Iwami, Junko S Takeuchi, Shinji Nakaoka, Fabrizio Mammano, François Clavel, Hisashi Inaba, Tomoko Kobayashi, Naoko Misawa, Kazuyuki Aihara, Yoshio Koyanagi, et al. Cell-to-cell
246 infection by hiv contributes over half of virus infection. *Elife*, 4:e08150, 2015.
- 247 5. Marion Sourisseau, Nathalie Sol-Foulon, Françoise Porrot, Fabien Blanchet, and Olivier Schwartz. Inefficient human immunodeficiency virus replication in mobile lymphocytes. *Journal of virology*,
248 81(2):1000–1012, 2007.
- 249 6. Natalia L Komarova, Daniela Anghelina, Igor Voznesensky, Benjamin Trinité, David N Levy, and Dominik Wodarz. Relative contribution of free-virus and synaptic transmission to the spread of HIV-1
250 through target cell populations. *Biology letters*, 9(1):20121049, 2013.
- 251

- 252 7. Irene A Abela, Livia Berlinger, Merle Schanz, Lucy Reynell, Huldrych F Günthard, Peter Rusert, and Alexandra Trkola. Cell-cell transmission enables HIV-1 to evade inhibition by potent cd4bs
253 directed antibodies. *PLoS pathogens*, 8(4):e1002634, 2012.
- 254 8. Christopher JA Duncan, James P Williams, Torben Schiffner, Kathleen Gärtner, Christina Ochsenbauer, John Kappes, Rebecca A Russell, John Frater, and Quentin J Sattentau. High-multiplicity
255 HIV-1 infection and neutralizing antibody evasion mediated by the macrophage-t cell virological synapse. *Journal of virology*, 88(4):2025–2034, 2014.
- 256 9. Peng Zhong, Luis M Agosto, Anna Ilinskaya, Batsukh Dorjbal, Rosaline Truong, David Derse, Pradeep D Uchil, Gisela Heidecker, and Walther Mothes. Cell-to-cell transmission can overcome
257 multiple donor and target cell barriers imposed on cell-free HIV. *PLoS one*, 8(1):e53138, 2013.
- 258 10. Torben Schiffner, Quentin J Sattentau, and Christopher JA Duncan. Cell-to-cell spread of hiv-1 and evasion of neutralizing antibodies. *Vaccine*, 31(49):5789–5797, 2013.
- 259 11. Luis M Agosto, Pradeep D Uchil, and Walther Mothes. HIV cell-to-cell transmission: effects on pathogenesis and antiretroviral therapy. *Trends in microbiology*, 23(5):289–295, 2015.
- 260 12. Laurelle Jackson, Jessica Hunter, Sandile Cele, Isabella Markham Ferreira, Andrew C Young, Farina Karim, Rajhmun Madansein, Kaylesh J Dullabh, Chih-Yuan Chen, Noel J Buckels, Yashica
261 Ganga, Khadija Khan, Mikael Boule, Gila Lustig, Richard A Neher, and Alex Sigal. Incomplete inhibition of HIV infection results in more HIV infected lymph node cells by reducing cell death. *eLife*,
262 7:e30134, 2018.
- 263 13. Q. Sattentau. Avoiding the void: cell-to-cell spread of human viruses. *Nat Rev Microbiol*, 6(11):815–26, 2008. ISSN 1740-1534 (Electronic) 1740-1526 (Linking). . URL <https://www.ncbi.nlm.nih.gov/pubmed/18923409>.
- 264 14. Jessica Hunter, Sandile Cele, Laurelle Jackson, Jennifer Giandhari, Tulio de Oliveira, Gila Lustig, and Alex Sigal. HIV cell-to-cell spread slows evolution of drug resistance. *bioRxiv*, 2020.
- 265 15. K Gibbert, JF Schlaak, D Yang, and U Dittmer. Ifn- α subtypes: distinct biological activities in anti-viral therapy. *British journal of pharmacology*, 168(5):1048–1058, 2013.
- 266 16. Andrea R Stacey, Philip J Norris, Li Qin, Elizabeth A Haygreen, Elizabeth Taylor, John Heitman, Mila Lebedeva, Allan DeCamp, Dongfeng Li, Douglas Grove, et al. Induction of a striking systemic
267 cytokine cascade prior to peak viremia in acute human immunodeficiency virus type 1 infection, in contrast to more modest and delayed responses in acute hepatitis b and c virus infections. *Journal*
268 *of virology*, 83(8):3719–3733, 2009.
- 269 17. Netanya S Utay and Daniel C Douek. Interferons and hiv infection: the good, the bad, and the ugly. *Pathogens & immunity*, 1(1):107, 2016.
- 270 18. Betty Poon, Kathie Grovit-Ferbas, Sheila A Stewart, and Irvin SY Chen. Cell cycle arrest by vpr in hiv-1 virions and insensitivity to antiretroviral agents. *Science*, 281(5374):266–269, 1998.
- 271 19. Keiko Sakai, Joseph Dimas, and Michael J Lenardo. The vif and vpr accessory proteins independently cause hiv-1-induced t cell cytopathicity and cell cycle arrest. *Proceedings of the National*
272 *Academy of Sciences*, 103(9):3369–3374, 2006.
- 273 20. Jianglin He, Sunny Choe, Robert Walker, Paola Di Marzio, David O Morgan, and Nathaniel R Landau. Human immunodeficiency virus type 1 viral protein r (vpr) arrests cells in the g2 phase of the
274 cell cycle by inhibiting p34cdc2 activity. *Journal of virology*, 69(11):6705–6711, 1995.
- 275 21. JB Jowett, Vicente Planelles, Betty Poon, Neil P Shah, Meng-Liang Chen, and IS Chen. The human immunodeficiency virus type 1 vpr gene arrests infected t cells in the g2+ m phase of the cell
276 cycle. *Journal of virology*, 69(10):6304–6313, 1995.
- 277 22. Véronique Zennou, Caroline Petit, Denise Guetard, Ulf Nerhass, Luc Montagnier, and Pierre Charneau. HIV-1 genome nuclear import is mediated by a central dna flap. *Cell*, 101(2):173–185,
278 2000.
- 279 23. Ahmad R Sedaghat, Jennifer German, Tanya M Teslovich, Joseph Cofrancesco, Chunfa C Jie, C Conover Talbot, and Robert F Siliciano. Chronic cd4+ t-cell activation and depletion in human
280 immunodeficiency virus type 1 infection: type i interferon-mediated disruption of t-cell dynamics. *Journal of virology*, 82(4):1870–1883, 2008.
- 281 24. Martin D Hycza, Colin Kovacs, Mona Loufy, Roberta Halpenny, Lawrence Heisler, Stuart Yang, Olivia Wilkins, Mario Ostrowski, and Sandy D Der. Distinct transcriptional profiles in ex vivo cd4+
282 and cd8+ t cells are established early in human immunodeficiency virus type 1 infection and are characterized by a chronic interferon response as well as extensive transcriptional changes in cd8+
283 t cells. *Journal of virology*, 81(7):3477–3486, 2007.
- 284 25. Chaoyu Xu, Baochun Ye, Zongping Han, Mingxing Huang, and Yuja Zhu. Comparison of transcriptional profiles between cd4+ and cd8+ t cells in hiv type 1-infected patients. *AIDS research and*
285 *human retroviruses*, 30(2):134–141, 2014.
- 286 26. Margalida Rotger, Kristen K Dang, Jacques Fellay, Erin L Heinzen, Sheng Feng, Patrick Descombes, Kevin V Shianna, Dongliang Ge, Huldrych F Günthard, David B Goldstein, et al. Genome-wide
287 mrna expression correlates of viral control in cd4+ t-cells from hiv-1-infected individuals. *PLoS Pathog*, 6(2):e1000781, 2010.
- 288 27. Melinda Judge, Erica Parker, Denise Naniche, and Peter Le Souëf. Gene expression: the key to understanding hiv-1 infection? *Microbiology and Molecular Biology Reviews*, 84(2), 2020.
- 289 28. Anthony J Smith, Qingsheng Li, Stephen W Wietrefe, Timothy W Schacker, Cavan S Reilly, and Ashley T Haase. Host genes associated with hiv-1 replication in lymphatic tissue. *The Journal of*
290 *Immunology*, 185(9):5417–5424, 2010.
- 291 29. Giuseppe Pantaleo, Cecilia Graziosi, James F Demarest, Luca Butini, Maria Montroni, Cecil H Fox, Jan M Orenstein, Donald P Kotler, and Anthony S Fauci. HIV infection is active and progressive
292 in lymphoid tissue during the clinically latent stage of disease. *Nature*, 362(6418):355–358, 1993.
- 293 30. Janet Embretson, Mary Zupancic, Jorge L Ribas, Alien Burke, Paul Racz, Klara Tenner-Racz, and Ashley T Haase. Massive covert infection of helper t lymphocytes and macrophages by hiv during
294 the incubation period of aids. *Nature*, 362(6418):359–362, 1993.
- 295 31. Qingsheng Li, Anthony J Smith, Timothy W Schacker, John V Carlis, Lijie Duan, Cavan S Reilly, and Ashley T Haase. Microarray analysis of lymphatic tissue reveals stage-specific, gene expression
296 signatures in hiv-1 infection. *The Journal of Immunology*, 183(3):1975–1982, 2009.
- 297 32. Thomas T Murooka, Maud Deruaz, Francesco Marangoni, Vladimir D Vrbanac, Edward Seung, Ulrich H Von Andrian, Andrew M Tager, Andrew D Luster, and Thorsten R Mempel. HIV-infected t
298 cells are migratory vehicles for viral dissemination. *Nature*, 490(7419):283–287, 2012.
- 299 33. Klara Tenner-Racz, Hans-Jürgen Stellbrink, Jan Van Lunzen, Claus Schneider, Jan-Peter Jacobs, Birgit Raschdorff, Gudrun Großschuppff, Ralph M Steinman, and Paul Racz. The unenlarged lymph
300 nodes of hiv-1-infected, asymptomatic patients with high cd4 t cell counts are sites for virus replication and cd4 t cell proliferation: the impact of highly active antiretroviral therapy. *The Journal of*
301 *experimental medicine*, 187(6):949–959, 1998.
- 302 34. Claire Deleage, Stephen W Wietrefe, Gregory Del Prete, David R Morcock, Xing Pei Hao, Michael Piatak Jr, Julian Bess, Jodi L Anderson, Katherine E Perkey, Cavan Reilly, et al. Defining hiv and
303 siv reservoirs in lymphoid tissues. *Pathogens & immunity*, 1(1):68, 2016.
- 304 35. Clare Jolly, Kirk Kashafi, Michael Hollinshead, and Quentin J Sattentau. HIV-1 cell to cell transfer across an env-induced, actin-dependent synapse. *Journal of Experimental Medicine*, 199(2):
305 283–293, 2004.
- 306 36. Wolfgang Hübner, Gregory P Mc Nerney, Ping Chen, Benjamin M Dale, Ronald E Gordon, Frank YS Chuang, Xiao-Dong Li, David M Asmuth, Thomas Huser, and Benjamin K Chen. Quantitative 3d
307 video microscopy of HIV transfer across t cell virological synapses. *Science*, 323(5922):1743–1747, 2009.
- 308 37. Benjamin M Dale, Gregory P Mc Nerney, Deanna L Thompson, Wolfgang Hubner, Kevin De Los Reyes, Frank YS Chuang, Thomas Huser, and Benjamin K Chen. Cell-to-cell transfer of hiv-1 via
309 virological synapses leads to endosomal virion maturation that activates viral membrane fusion. *Cell host & microbe*, 10(6):551–562, 2011.
- 310 38. Fedde Groot, Sonja Welsch, and Quentin J Sattentau. Efficient hiv-1 transmission from macrophages to t cells across transient virological synapses. *Blood, The Journal of the American Society of*
311 *Hematology*, 111(9):4660–4663, 2008.
- 312 39. Amy E Baxter, Rebecca A Russell, Christopher JA Duncan, Michael D Moore, Christian B Willberg, Jose L Pablos, Andrés Finzi, Daniel E Kaufmann, Christina Ochsenbauer, John C Kappes, Fedde
313 Groot, and Quentin J Sattentau. Macrophage infection via selective capture of HIV-1-infected cd4+ t cells. *Cell host & microbe*, 16(6):711–721, 2014.
- 314 40. Philippe Bousso and Ellen A Robey. Dynamic behavior of t cells and thymocytes in lymphoid organs as revealed by two-photon microscopy. *Immunity*, 21(3):349–355, 2004.
- 315 41. Susanna Celli, Zacarias Garcia, and Philippe Bousso. Cd4 t cells integrate signals delivered during successive dc encounters in vivo. *The Journal of experimental medicine*, 202(9):1271–1278,
316 2005.
- 317 42. C. V. Fletcher, K. Staskus, S. W. Wietrefe, M. Rothenberger, C. Reilly, J. G. Chipman, G. J. Beilman, A. Khoruts, A. Thorkelson, T. E. Schmidt, J. Anderson, K. Perkey, M. Stevenson, A. S. Perelson,
318 D. C. Douek, A. T. Haase, and T. W. Schacker. Persistent HIV-1 replication is associated with lower antiretroviral drug concentrations in lymphatic tissues. *Proc Natl Acad Sci U S A*, 111(6):2307–12,
319 2014. ISSN 1091-6490 (Electronic) 0027-8424 (Linking). . URL <https://www.ncbi.nlm.nih.gov/pubmed/24469825>.
- 320 43. R. Lorenzo-Redondo, H. R. Fryer, T. Bedford, E. Y. Kim, J. Archer, S. L. Kosakovsky Pond, Y. S. Chung, S. Penugonda, J. G. Chipman, C. V. Fletcher, T. W. Schacker, M. H. Malim, A. Rambaut,
321 A. T. Haase, A. R. McLean, and S. M. Wolinsky. Persistent HIV-1 replication maintains the tissue reservoir during therapy. *Nature*, 530(7588):51–6, 2016. ISSN 1476-4687 (Electronic) 0028-0836
322 (Linking). URL <http://www.ncbi.nlm.nih.gov/pubmed/26814962>.
- 323 44. Benjamin K Chen, Rajesh T Gandhi, and David Baltimore. Cd4 down-modulation during infection of human t cells with human immunodeficiency virus type 1 involves independent activities of vpu,
324 env, and nef. *Journal of virology*, 70(9):6044–6053, 1996.
- 325 45. Aravind Subramanian, Pablo Tamayo, Vamsi K Mootha, Sayan Mukherjee, Benjamin L Ebert, Michael A Gillette, Amanda Paulovich, Scott L Pomeroy, Todd R Golub, Eric S Lander, et al. Gene set
326 enrichment analysis: a knowledge-based approach for interpreting genome-wide expression profiles. *Proceedings of the National Academy of Sciences*, 102(43):15545–15550, 2005.
- 327 46. Arthur Liberzon, Chet Birger, Helga Thorvaldsdóttir, Mahmoud Ghandi, Jill P Mesirov, and Pablo Tamayo. The molecular signatures database hallmark gene set collection. *Cell systems*, 1(6):
328 417–425, 2015.
- 329 47. Francois Vigneault, Matthew Woods, Maria J Buzon, Chun Li, Florencia Pereyra, Seth D Crosby, Jennifer Rychert, George Church, Javier Martinez-Picado, Eric S Rosenberg, et al. Transcriptional
330 profiling of cd4 t cells identifies distinct subgroups of hiv-1 elite controllers. *Journal of virology*, 85(6):3015–3019, 2011.
- 331 48. Gustavo Olvera-García, Tania Aguilar-García, Fany Gutiérrez-Jasso, Iván Imaz-Rosshandler, Claudia Rangel-Escareño, Lorena Orozco, Irma Aguilar-Delfín, Joel A Vázquez-Pérez, Joaquín Zúñiga,
332 Santiago Pérez-Patrigón, et al. A transcriptome-based model of central memory cd4 t cell death in hiv infection. *BMC genomics*, 17(1):1–14, 2016.
- 333 49. Michelle J Dawson and Joseph A Trapani. The interferon inducible autoantigen, ifi 16: localization to the nucleolus and identification of a dna-binding domain. *Biochemical and biophysical research*
334 *communications*, 214(1):152–162, 1995.
- 335

- 336 50. Kathryn M Monroe, Zhiyuan Yang, Jeffrey R Johnson, Xin Geng, Gilad Doitsh, Nevan J Krogan, and Warner C Greene. Ifi16 dna sensor is required for death of lymphoid cd4 t cells abortively
337 infected with hiv. *Science*, 343(6169):428–432, 2014.
- 338 51. Nicole LK Galloway, Gilad Doitsh, Kathryn M Monroe, Zhiyuan Yang, Isa Muñoz-Arias, David N Levy, and Warner C Greene. Cell-to-cell transmission of hiv-1 is required to trigger pyroptotic death
339 of lymphoid-tissue-derived cd4 t cells. *Cell reports*, 12(10):1555–1563, 2015.
- 340 52. Mikayla R Thompson, Shruti Sharma, Maninjay Atianand, Søren B Jensen, Susan Carpenter, David M Knipe, Katherine A Fitzgerald, and Evelyn A Kurt-Jones. Interferon γ -inducible protein (ifi)
341 16 transcriptionally regulates type i interferons and other interferon-stimulated genes and controls the interferon response to both dna and rna viruses. *Journal of Biological Chemistry*, 289(34):
342 23568–23581, 2014.
- 343 53. John J Trombetta, David Gennert, Diana Lu, Rahul Satija, Alex K Shalek, and Aviv Regev. Preparation of single-cell rna-seq libraries for next generation sequencing. *Current protocols in molecular*
344 *biology*, 107(1):4–22, 2014.
- 345 54. Michael I Love, Wolfgang Huber, and Simon Anders. Moderated estimation of fold change and dispersion for rna-seq data with deseq2. *Genome biology*, 15(12):550, 2014.

Participant ID	Sex	Age (Years)	LN Location
0233	M	37	Right Lateral/Peribronchial
0234	M	45	Right Lateral
0251	M	22	Left Lateral/Mediastinal

SFig. 1. Participant information for the lymph node cells used to infect in vitro to determine whether there are differences in transcriptional responses from different infection modes



Sfig. 2. GSEA reports for our three condition comparisons for the top 5 most enriched gene sets in cell-to-cell infected relative to the cell-free infected. The top green graph indicates the enrichment profile in the gene set for a given comparison. The section with the red and blue bar indicates where the genes in that gene set appear in the ranked list of genes. Black lines indicates a positive hit for a gene present in gene set which was also present in our data set. Grey graphs indicates the score attributed to a given gene at that position in the ranked list. A) Interferon alpha response B) Interferon gamma response C) TNF α signalling via NF κ B D) P53 pathway E) Inflammatory response

828 **GENERAL DISCUSSION:**

829

830 HIV transmits both cell-free infection and cell-to-cell spread, yet the consequences of the virus infecting
831 both modes is unclear. In this thesis, I demonstrate that transmitting by both modes of infection is
832 advantageous for HIV in a dynamic environment. The infection modes, led to different outcomes in 1)
833 infected cell survival at suboptimal drug levels, 2) drug resistance evolution and, 3) the host
834 transcriptional response to HIV infection. Here, I confirm that HIV cell-to-cell spread is less sensitive
835 to ARVs. Furthermore, I demonstrate that under suboptimal drug suppression, cell-to-cell spread
836 increases the number of live infected cells. I also demonstrate, that while cell-to-cell spread replicates
837 in the face of drug, the selection of drug resistance occurs more rapidly with cell-free infection. Lastly,
838 I show that infection by the different modes leads to differences at the transcriptional level.

839 In chapter 2, it was demonstrated that infected cell survival at intermediate drug strengths results
840 predictably in two different outcomes depending on infection mode. When cell-free infection (which
841 mostly results in a single infection per cell) is partially inhibited, the number of live infected cells is
842 reduced. This is a numerical consequence of decreasing the number of infections per cell from one to
843 zero. In contrast, when cell-to-cell spread, which results in multiple infection attempts per cell, is
844 partially inhibited the number of live infected cells increases. If every infection attempt increases the
845 probability of cell death, then the reduction, but not elimination, of all HIV infections per cell by
846 intermediate drug concentration would increase the probability of HIV's survival. Thus, the increase in
847 live infected cells observed for cell-to-cell spread was as a result of reduced cell death which correlated
848 with fewer viral DNA copies per cell. This infection mode-dependent outcome was demonstrated in
849 both cell lines (*in vitro*) and primary lymph node cells (*in vitro*). The results presented here explain why
850 previous studies showed that cell death upon HIV infection is associated with copies of reverse
851 transcribed HIV. Such studies demonstrated HIV induces cell death, through double stranded DNA
852 breaks generated by integration attempts [1] or via interferon- γ - inducible protein 16 (IFI16) sensing of
853 abortive reverse transcripts following non-productive infection of resting T cells [2, 3]. The HIV
854 reservoir relies on long term survival of infected cells. Therefore, these findings may have important
855 implications relating to the establishment of a the HIV reservoir in sites where viral replication is not
856 fully suppressed by drug [4].

857 The experimental design in this chapter allowed us to determine whether cell-to-cell spread increases
858 cell death by using inhibition of cell-to-cell spread or cell-free infection by antiretroviral therapy. The
859 results clearly demonstrate that partial inhibition of cell-to-cell spread leads to approximately 2-fold
860 increase in live infected cells.

861 In chapter 3, it was demonstrated that infection mode determines the rate of drug resistance selection.
862 Infection with a cell-free step resulted in more rapid selection of drug resistance relative to infection by

863 cell-to-cell spread. The slower rate of drug resistance selection observed in cell-to-cell spread indicates
864 that selective pressure applied to this efficient infection mode is decreased. This permits the continued
865 transmission of drug sensitive wildtype virus despite the presence of drug, resulting in a more gradual
866 replacement with a drug resistant mutant. Applying a stronger selective pressure to cell-to-cell spread,
867 by the addition of higher drug concentration, increased the rate of drug resistance evolution similar to
868 infection with a cell-free step. These observations may indicate why it is advantageous for HIV to
869 transmit by cell-free infection in addition to cell-to-cell spread, despite the greater efficacy of the latter
870 infection mode.

871 For the evolution of drug resistance, a critical parameter is the strength of selection. This is true of the
872 drug concentration in the experiments presented here. If drug levels are too low, the wild-type strain
873 has higher fitness and selection acts against resistant strains. If drug levels are higher, then the resistant
874 strain has higher fitness and is selected for. However, if drug levels are too high, then even the resistant
875 strain is suppressed. Cell-to-cell infection alters the effective drug concentration seen by the virus. This
876 can potentially shift the balance from selection of the drug sensitive virus to selection of the drug
877 resistant virus.

878 An important assumption made in the experimental design and analysis is the presence of a
879 quasispecies on which the selective pressure provided by the antiretroviral drugs will work. While the
880 mutation rate of HIV, combined with the estimated intra-host population size of the virus, makes the
881 presence of the single mutants very likely, if the mutants are absent we expect precisely the opposite
882 effect of cell-free infection as what we described: clearance of the drug sensitive population will lead
883 to the inability of the virus to acquire new drug resistance mutations as this requires a replicating viral
884 population.

885 Drug resistance may not offer any overall growth advantage compared to the cell-to-cell condition in
886 the presence of a low concentration of EFV alone as replication of the virus can take place by cell-to-
887 cell spread without the drug resistance. However, the selection of a drug resistance mutant may have
888 consequences if the selection pressure changes, as it provides a basis for additional mutations.

889 The capacity for HIV to select more fit genotypes rapidly may play an important role when evolving
890 resistance to multiple drugs contained in ART regimes. In chapter 3, it was demonstrated that when a
891 second drug was introduced after a short period of monotherapy, infections with a cell-free step evolved
892 resistance to both drugs more easily. It has been proposed that instances of monotherapy allows HIV to
893 accumulate drug resistance mutations in a stepwise fashion [5, 6]. Monotherapy may occur following
894 treatment interruptions due to differing half-lives of the drugs found in ART regimes [7]. If HIV evolves
895 more rapidly by cell-free infection relative to cell-to-cell spread, cell-free infection may allow for the
896 evolution of drug resistance to a single drug during a brief window of monotherapy. If subsequently the

897 other drugs in the ART regime are reintroduced, the now partially resistant virus would only need to
898 evolve resistance to the additional drugs for the virus to be multidrug resistant. Understanding the role
899 of both modes of infection in the evolution of drug resistance may be important to minimize virologic
900 failure in patients receiving ART.

901 Evolution of drug resistance is promoted in environments in which part of the population is in sub-
902 environment where mutations are likely and another part of the population in a sub-environment where
903 the selection pressure is strong. Furthermore, there is flow between these environments of the evolving
904 virus. With a dual infection mode, sub-environments are not required since their function is performed
905 by infection modes with different selection pressures.

906 "Evolvability" associated with a cycle of cell-free infection may not be the only reason cell-free
907 infection is present. It is also less cytotoxic and triggers a weaker interferon response, as demonstrated
908 in chapter 4. What the contribution of each factor is, is yet unclear. The goal of this work was to map
909 the factors which may play a role. ART here was used as an experimental lever and was effective at
910 mapping the conditions at which cell-free infection had an advantage. Furthermore, cell-free infection
911 is unlikely to work in the absence of cell-to-cell spread in cellular infection, and in evolution it was only
912 considered in combination with cycles of cell-to-cell spread.

913 The results of Chapter 2 demonstrate the possibility that cell-free, under a defined set of conditions, can
914 contribute to more rapid evolution, additional studies are required to examine whether this possibility
915 occurs under the circumstances of clinical infection. However, such studies may require inhibitors of
916 cell-to-cell spread, which are currently not available as such studies may require inhibitors of cell-to-
917 cell spread, which are currently not available.

918 Together the studies presented in chapter 2 and 3, indicate that infection by both modes may present a
919 strategy of effective persistence in the context of spatial or temporal drug heterogeneity in the body [6].
920 As demonstrated in chapter 3, the cell-free infection mode promotes rapid drug resistance evolution.
921 Should a drug resistant mutant evolve by cell-free infection in a site with low drug concentrations, it
922 may then have the capacity to replicate in a compartment with higher drug levels or where additional
923 drugs are present. At this step, the more drug insensitive cell-to-cell spread may assist with the
924 transmission within this new site. In chapter 2, infection by cell-to-cell spread with the K103N EFV
925 resistant mutant virus shifted the peak of live infected cells to higher drug concentrations (~100nM
926 EFV). This drug concentration is comparable to that which has been reported in the lymph nodes of
927 ART treated individuals [4]. Conjointly, the works presented in these chapters indicate how together
928 both modes of infection may work hand in hand in HIV evolution and spread in the face of suboptimal
929 ART.

930 Given the infection mode-dependent outcomes observed in chapter 2 and 3, lastly, it was investigated
931 whether differences between the infection modes could be detected at the level of the transcriptional
932 response. In chapter 4, cell-to-cell spread was demonstrated to result in differential gene regulation
933 relative to cell-free infection. Upregulation of many inflammatory genes were observed in cells infected
934 with HIV by both modes of infection. However, infection by cell-to-cell spread resulted in the
935 upregulation of interferon-stimulated genes (ISGs) which was specific to this mode of infection. The
936 conclusion that the interferon response is differentially upregulated in cell-to-cell spread versus cell-
937 free infection is supported by the fold-change in expression and the level of significance of individual
938 genes (Chapter 4, Figure 4), and by upregulated gene sets (Chapter 4, Figure 5).

939 The two analysis techniques used in this chapter, differential gene expression analysis and Gene Set
940 Enrichment Analysis (GSEA), differ in their approach to analysing gene expression data. Differential
941 gene expression analysis describes individual genes whereas GSEA is a method which describes gene
942 sets. Gene sets are groups of genes that share biological function. Investigating the overall enrichment
943 of a gene set can be more informative than investigating individual genes as often the change in
944 expression of an individual gene may be stochastically lost or gained and so may not accurately inform
945 on biological function.

946 Interestingly, previous studies have reported upregulation of ISGs in the lymph nodes of HIV infected
947 individuals [8, 9]. Lymph nodes are an important site of the HIV reservoir and cell-to-cell spread is
948 thought to contribute substantially to viral replication within the lymph nodes. This is because of the
949 ideal conditions within this compartment for cell-to-cell spread, such as many infectable cells [10, 11]
950 which are closely packed together [12-16] with limited lymphatic flow to disturb cellular interactions
951 [17, 18]. The results presented in this chapter may confirm that cell-to-cell spread is the predominant
952 mode of infection within the lymph node compartment.

953 The upregulation of ISGs specific to cell-to-cell spread, observed in chapter 4, may further demonstrate
954 higher cytotoxicity associated with this infection mode, as observed in chapter 2. A study by Monroe
955 et al., reported that IFI16 was required to sense abortive HIV infections and trigger caspase-1-mediated
956 pyroptotic cell death [2]. A further study by this group demonstrated that cell-to-cell spread, and not
957 cell-free infection, could trigger the caspase-1-mediated pyroptosis [3]. While IFI16 is an ISG itself
958 [19], it is also required for production of interferons and an ISGs response to viral infection [20].
959 Increased expression of genes relating to the interferon response has been shown to correlate with
960 increased viremia and disease progression [21, 22]. Given the association of the interferon response
961 with cytotoxicity and disease progression, the results presented in chapter 4, showing upregulation of
962 the interferon response in cell-to-cell spread but not in cell-free infection may indicate that this infection
963 mode is responsible for majority of the pathogenesis in HIV infection.

964 Altogether, the results presented here demonstrate that differences in cell survival, viral evolution, and
965 host transcriptome are contingent upon mode of infection.

966

967

968

969

970

971

972

973

974

975

976

977

978

979

980

981

982

983

984

985

986

987

988

989

990

991

992

993

994 **FUTURE RESEARCH:**

995

996 Key future research to improve and validate the current results presented are as follows:

997 Given the results presented in chapter 3, which demonstrated more rapid evolution of drug resistance
998 by cell-free infection compared to cell-to-cell spread at 20nM and 40nM EFV, it may be of interest to
999 predict how evolution by the two infection modes may occur at higher drug concentrations. Higher drug
1000 concentrations may be more clinically relevant. Using measured replication ratios of cell-to-cell spread
1001 and cell-free infection at higher drug concentrations, I propose a model predicting the evolution of drug
1002 resistance at these higher drug concentrations. Furthermore, I plan to examine mass spectrometry
1003 measurements of ARV levels from longitudinal plasma samples from ART treated patients. This
1004 analysis will demonstrate the clinical relevance of the model presented in this chapter, by showing that
1005 similar drug levels are observed in ART treated patients as what I used in the evolution experiments
1006 and in the model.

1007 Following the identification of genes of interest by the transcriptomic analysis in chapter 4, I propose
1008 to validate the gene products of these genes of interest using ELISA and flow cytometry. I also plan to
1009 align the sequencing data to the HIV genome to assess the regulation of viral genes in response to HIV
1010 infection by different modes. Should cell-to-cell spread lead to multiple HIV infections per cell we
1011 might expect higher expression of viral genes relative to cell-free infection. The levels of viral genes
1012 expressed by the different infection modes may correlate with the observed patterns of host gene
1013 expression.

1014 **CONCLUSION:**

1015 The results presented in this thesis demonstrate that modes of HIV infection play a role in determining
1016 factors such as cell survival, selection of drug resistance mutations, and host transcriptome response
1017 to infection. Having two outcomes from infection modes gives HIV a higher chance of survival in a
1018 changing environment. For any cure strategy to be successful it should therefore address the role of
1019 both modes of infection in HIV's pathogenesis.

1020 **REFERENCES:**

- 1021 1. Cooper, A., et al., *HIV-1 causes CD4 cell death through DNA-dependent protein kinase during*
 1022 *viral integration*. *Nature*, 2013. **498**(7454): p. 376.
- 1023 2. Monroe, K.M., et al., *IFI16 DNA sensor is required for death of lymphoid CD4 T cells*
 1024 *abortively infected with HIV*. *Science*, 2014. **343**(6169): p. 428-432.
- 1025 3. Doitsh, G., et al., *Cell death by pyroptosis drives CD4 T-cell depletion in HIV-1 infection*.
 1026 *Nature*, 2014. **505**(7484): p. 509-514.
- 1027 4. Fletcher, C.V., et al., *Persistent HIV-1 replication is associated with lower antiretroviral drug*
 1028 *concentrations in lymphatic tissues*. *Proceedings of the National Academy of Sciences*, 2014.
 1029 **111**(6): p. 2307-2312.
- 1030 5. Moreno-Gamez, S., et al., *Imperfect drug penetration leads to spatial monotherapy and rapid*
 1031 *evolution of multidrug resistance*. *Proceedings of the National Academy of Sciences*, 2015.
 1032 **112**(22): p. E2874-E2883.
- 1033 6. Feder, A., K. Harper, and P.S. Pennings, *Challenging conventional wisdom on the evolution of*
 1034 *resistance to multi-drug HIV treatment: Lessons from data and modeling*. *bioRxiv*, 2019: p.
 1035 807560.
- 1036 7. Taylor, S., et al., *Stopping antiretroviral therapy*. *Aids*, 2007. **21**(13): p. 1673-1682.
- 1037 8. Li, Q., et al., *Microarray analysis of lymphatic tissue reveals stage-specific, gene expression*
 1038 *signatures in HIV-1 infection*. *The Journal of Immunology*, 2009. **183**(3): p. 1975-1982.
- 1039 9. Smith, A.J., et al., *Host genes associated with HIV-1 replication in lymphatic tissue*. *The*
 1040 *Journal of Immunology*, 2010. **185**(9): p. 5417-5424.
- 1041 10. Embretson, J., et al., *Massive covert infection of helper T lymphocytes and macrophages by*
 1042 *HIV during the incubation period of AIDS*. *Nature*, 1993. **362**(6418): p. 359-362.
- 1043 11. Pantaleo, G., et al., *HIV infection is active and progressive in lymphoid tissue during the*
 1044 *clinically latent stage of disease*. *Nature*, 1993. **362**(6418): p. 355-358.
- 1045 12. Jolly, C., et al., *HIV-1 cell to cell transfer across an Env-induced, actin-dependent synapse*.
 1046 *Journal of Experimental Medicine*, 2004. **199**(2): p. 283-293.
- 1047 13. Groot, F., S. Welsch, and Q.J. Sattentau, *Efficient HIV-1 transmission from macrophages to T*
 1048 *cells across transient virological synapses*. *Blood, The Journal of the American Society of*
 1049 *Hematology*, 2008. **111**(9): p. 4660-4663.
- 1050 14. Hübner, W., et al., *Quantitative 3D video microscopy of HIV transfer across T cell virological*
 1051 *synapses*. *Science*, 2009. **323**(5922): p. 1743-1747.
- 1052 15. Dale, B.M., et al., *Cell-to-cell transfer of HIV-1 via virological synapses leads to endosomal*
 1053 *virion maturation that activates viral membrane fusion*. *Cell host & microbe*, 2011. **10**(6): p.
 1054 551-562.
- 1055 16. Baxter, A.E., et al., *Macrophage infection via selective capture of HIV-1-infected CD4+ T cells*.
 1056 *Cell host & microbe*, 2014. **16**(6): p. 711-721.
- 1057 17. Sourisseau, M., et al., *Inefficient human immunodeficiency virus replication in mobile*
 1058 *lymphocytes*. *Journal of virology*, 2007. **81**(2): p. 1000-1012.
- 1059 18. Bousso, P. and E.A. Robey, *Dynamic behavior of T cells and thymocytes in lymphoid organs as*
 1060 *revealed by two-photon microscopy*. *Immunity*, 2004. **21**(3): p. 349-355.
- 1061 19. Dawson, M.J. and J.A. Trapani, *The interferon inducible autoantigen, Ifi 16: localization to the*
 1062 *nucleolus and identification of a DNA-binding domain*. *Biochemical and biophysical research*
 1063 *communications*, 1995. **214**(1): p. 152-162.
- 1064 20. Thompson, M.R., et al., *Interferon γ -inducible protein (IFI) 16 transcriptionally regulates type*
 1065 *i interferons and other interferon-stimulated genes and controls the interferon response to*
 1066 *both DNA and RNA viruses*. *Journal of Biological Chemistry*, 2014. **289**(34): p. 23568-23581.
- 1067 21. Hycza, M.D., et al., *Distinct transcriptional profiles in ex vivo CD4+ and CD8+ T cells are*
 1068 *established early in human immunodeficiency virus type 1 infection and are characterized by*

- 1069 *a chronic interferon response as well as extensive transcriptional changes in CD8+ T cells.*
1070 *Journal of virology*, 2007. **81**(7): p. 3477-3486.
- 1071 22. Rotger, M., et al., *Genome-wide mRNA expression correlates of viral control in CD4+ T-cells*
1072 *from HIV-1-infected individuals.* *PLoS Pathog*, 2010. **6**(2): p. e1000781.